CHARLES UNIVERSITY IN PRAGUE
FACULTY OF PHARMACY IN HRADEC KRÁLOVÉ
Department of Biochemical Sciences

# STUDIES ON CARBONYL REDUCTASES 1 AND 3 VARIANTS WITH EMPHASIS ON S-NITROSOGLUTATHIONE AS SUBSTRATE AND INACTIVATOR

# STUDIUM MUTACÍ KARBONYLREDUKTASY 1 A 3 S DŮRAZEM NA S-NITROSOGLUTATHION JAKO SUBSTRÁT A INAKTIVÁTOR

Diploma thesis

Supervisors:
**Dr. Claudia Staab**
**Dr. Hans-Jörg Martin**
Christian-Albrechts-University in Kiel
Faculty of Medicine
Department of Toxicology and Pharmacology for Natural Scientists

**Prof. Ing. Vladimír Wsól, Ph.D.**
Charles University in Prague
Faculty of Pharmacy in Hradec Králové
Department of Biochemical Sciences

2010 TEREZA HARTMANOVÁ

# DECLARATION

I declare that this thesis is my original author's work which I have worked out independently. All literature and other sources, from which I have gathered information during its preparation, are listed in the bibliography and are properly cited in the work.

Location, date

Signature

# ABSTRACT

Charles University in Prague
Faculty of Pharmacy in Hradec Králové
Department of Biochemical Sciences

Candidate: Tereza Hartmanová
Supervisor: Dr. Claudia Staab, Dr. Hans-Jörg Martin, Prof. Ing. Vladimír Wsól, Ph.D.
Title of the diploma thesis: Studies on carbonyl reductases 1 and 3 variants with emphasis on S-nitrosoglutathione as substrate and inactivator

Human CBR1 and CBR3 (carbonyl reductases 1 and 3) are monomeric, NADPH-dependent enzymes belonging to the short chain dehydrogenase/reductase superfamily. Although they are highly similar at the amino acid level (72 % identity) the enzymes exhibit considerable differences in substrate specificity. The CBR1 substrate spectrum is well described, including a variety of compounds *e.g.* the endogenous indol isatin, S-nitrosoglutathione (GSNO), prostaglandins, quinones, and many carbonyl group bearing xenobiotics. In contrast, CBR3 shows a distinct and much narrower range of substrates and its role is still not fully clarified. Nevertheless, the dissimilar substrate spectra strongly indicate that CBR1 and CBR3 play different metabolic roles.

In the present study, the catalytic properties of CBR1 towards the latest CBR1 substrate described, GSNO, were investigated. CBR3 was assessed for potential GSNO-reducing activity, but no *in vitro* activity was observed. Thus, to assess the residues and mechanism responsible for the CBR1 properties, a certain number of amino acid residues of CBR3 were replaced to correspond to CBR1. The variants were created using splicing by overlap extension, cloned into the pET-28b(+) vector, overexpressed in *E. coli* and purified via Ni-affinity chromatography. We found out that GSNO was an acceptable substrate for several CBR3 variants, interestingly all of them comprising the change in sequence at positions 236-244, that also influenced catalytic properties with isatin and 9,10-phenantrenequinone. In CBR1, together with all variants with catalytic activity determined, inactivation starting at a GSNO concentration of about 100 μM was detected. Further investigations, including reactivation of CBR1 by treatment with dithiothreitol suggested cysteine S-glutathionylation as the underlying mechanism.

# ABSTRAKT

Universita Karlova v Praze
Farmaceutická fakulta v Hradci Králové
Katedra biochemických věd

Kandidát: Tereza Hartmanová
Školitel: Dr. Claudia Staab, Dr. Hans-Jörg Martin, Prof. Ing. Vladimír Wsól, Ph.D.
Název diplomové práce: Studium mutací karbonylreduktasy 1 a 3 s důrazem na S-nitrosoglutathion jako substrát a inaktivátor

Lidské CBR1 a CBR3 (karbonylreduktasa 1 a 3) jsou monomerní, na NADPH závislé enzymy patřící do nadrodiny dehydrogenas/reduktas s krátkým řetězcem. Přestože na aminokyselinové úrovni si jsou oba enzymy velmi podobné (72 % shoda), v substrátové specifitě vykazují značné rozdíly. Substráty CBR1 jsou velmi dobře popsány. Zahrnují řadu látek jako endogenní indol isatin, S-nitrosoglutathion (GSNO), prostaglandiny, chinony a mnoho xenobiotik, které obsahují karbonylovou skupinu. Na rozdíl od CBR1 je výčet substrátů CBR3 mnohem menší a různorodý a role CBR3 stále není plně objasněna. Přesto tyto odlišnosti v substrátové specifitě naznačují rozdílné metabolické role.

V této práci byly studovány katalytické vlastnosti CBR1 a jejího posledního popsaného substrátu, GSNO. Možné domněnky, že CBR3 by mohla také redukovat GSNO nebyly *in vitro* potvrzeny. Proto, k odhadnutí aminokyselin a mechanismů zodpovědných za vlastnosti CBR1, byly určité aminokyseliny v sekvenci CBR3 změněny tak, aby odpovídaly sekvenci CBR1. Mutanty byly vytvořeny pomocí splice overlap extension metody, naklonovány do vektoru pET28, namnoženy v *E. coli* a purifikovány pomocí Ni-afinitní chromatografie. Bylo zjištěno, že GSNO je přijatelným substrátem pro několik CBR3 mutantů. Zajímavé bylo, že všechny z nich obsahovaly mutace na pozicích 236-244, které také ovlivňují katalytické vlastnosti vůči isatinu a 9,10-phenantrochinonu. CBR1 společně se všemi mutanty vykazujícími aktivitu vůči GSNO byly GSNO inaktivovány. Inaktivace začínala zhruba při 100 μM koncentraci GSNO. Následující výzkum zahrnující reaktivaci CBR1 pomocí inkubace s dithiothreitolem nasvědčuje, že inaktivačním mechanismem je S-glutathionylace cysteinů.

# CONTENTS

# 1 INTRODUCTION

Maintaining the body´s balance in chemical composition is a constant, dynamic process, which is regulated continuously. The majority of catalytic reactions that assure this equilibrium are mediated by enzymes. Almost all processes in a biological cell require enzymes to occur. Enzymes are largely specific for their substrates, *i.e.* every enzyme only speeds up one reaction or a small set of reactions from many options. Hence, the set of enzymes expressed in a particular cell determines the occurring metabolic pathways.

Nowadays, the human body has to deal with a number of foreign substances which are not natural, *i.e.* are not part of the normal constitution of the human body and often have harmful effects. These compounds, the so-termed xenobiotics, are found in food, air and medication. The most common xenobiotics are drugs or environmental pollutants. The process that describes how the human body excretes these substances is called biotransformation and consists of a set of metabolic pathways which collectively alter the chemical structure of xenobiotics. These pathways, which are considered to be of ancient origin, often act to protect from damaging effects of xenobiotics and can be found in all major groups of organisms.

As a tight control of enzyme activity is necessary for keeping stable conditions inside the body, every single change of an enzyme can cause a genetic disease. The major role of enzymes is demonstrated by the fact that just one single damaged enzyme out of the thousands can cause a lethal illness. In addition, increased expression levels of certain enzymes can contribute to disease and then, enzyme inhibition can be used for treatment *e.g.* in the case of high blood pressure or diabetes. Research is also being conducted on malfunctioning enzymes linked to blood disorders *e.g.* anaemia. Furthermore, geneticists have discovered that in some hereditary diseases total absence of some enzyme is the cause of the defect. Some of these enzyme-deficiency disorders can be treated by the supply of the enzyme. In summary, the biochemical characterization of enzymes is of great interest as enzymes play essential roles in normal human physiology as well as contribute to pathophysiology if they are damaged or their levels altered.

# 2 THEORETICAL PART

## 2.1 Redox reactions in metabolism

Redox (reduction-oxidation) reactions play a major role in all biotransformational phases of xenobiotic metabolism. The way a compound passes through the body is described by metabolic processes called absorption, distribution, metabolism and excretion. All these reactions are divided into three main phases of metabolism. Nonsynthetic phase I reactions may include oxidation, reduction or hydrolysis. Oxidation means the enzymatic addition of oxygen or disposal of hydrogen from a lipophilic compound, making it more polar and thus more water-soluble. Many phase I enzymes are located in the ER membrane. The predominant enzymes of ER oxidative metabolism are the monooxygenases. There are two major types of microsomal monooxygenases: the cytochrome P450 (cyt P450) system and the flavin-containing monooxygenases. The cytochrome P450 system is involved in the oxidative metabolism of many endogenous substances, as well as the detoxification of a wide variety of xenobiotics. Flavin-containing monooxygenases catalyse the oxidation of substances (primarily xenobiotics) bearing functional groups containing nitrogen, sulphur or phosphorus.

Reductive phase I reactions have also been described and may be of great pharmacological importance. For the most part, reductive routes in phase I are accomplished by members of the aldo-keto reductases (AKR) and short-chain dehydrogenases/reductases (SDR) superfamilies and the quinone reductases (QR), the subgroup of the MDR (medium-chain dehydrogenase/reductase) superfamily. These families are known to constitute important phase I enzymes (Oppermann and Maser 2000).

In phase II, the polar functional groups of phase I derivatives are conjugated with carboxyl (-COOH), hydroxyl (-OH), amino ($NH_2$), and sulfhydryl (-SH) groups found in sulfonates, glutathione, glucuronic acid or amino acids. The enzymes that initiate this activation are called transferases. The conjugated products are often inactive in comparison to the corresponding phase I metabolites. Additionally, the phase II product can be further modified and metabolised in phase III for transport out of the cell.

A non-physiological condition related to redox state is oxidative stress. Normally, a reducing environment is present in the cells. However, when cells are not able to metabolically cope with the production of peroxides, free radicals and other reactive oxygen species (ROS), unnatural oxidative redox conditions arise. Many enzyme groups are involved in the metabolism of ROS. Among the best studied implicated enzymes are superoxide dismutase, catalase and glutathione peroxidase and researchers are intensively studying other enzyme families involved.

## 2.2 Carbonyl reduction

Although the endogenous carbonyl metabolism is well described, the roles of carbonyl-reducing enzymes in xenobiotic metabolism are still not well elucidated (Rosemond and Walsh 2004). Unarguably, carbonyl reduction plays a major role in the phase I metabolism of carbonyl substances. This role consists in an inactivation or detoxication of the reactive aldehyde or ketone moiety through reduction to a hydroxyl group (Hoffmann and Maser 2007). The reaction products are less lipophilic than the parent compounds and therefore easier to conjugate and excrete (Testa and Kramer 2007).

The chemical carbonyl function (aldehyde or ketone group) frequently occurs in endogenous compounds such as hormones, mediators, cofactors, neurotransmitter precursors and lipid aldehydes derived from oxidative stress and their metabolites. Reactive, oxidative stress-related, carbonyl compounds (RCCs) are formed during lipid peroxidation and sugar glycoxidation. RCCs are the cause of the carbonyl stress, which results in the formation of adducts and protein cross-links leading to malfunctioning protein function and damages in all tissues (Negre-Salvayre, Coatrieux et al. 2008). The RCCs include substances such as acrolein, 4-hydroxynonenal and malondialdehyde. Furthermore, the carbonyl group is widely spread in xenobiotics such as alimentary products, medications, or environmental pollutants. In endogenous substances the carbonyl group is often a determining factor for the biological activity, *e.g.* the 3-keto group in steroid hormones (Oppermann 2007).

Carbonyl reducing enzymes (CRs) are found both in mammalian and non-mammalian organisms. Non-mammals using CRs are plants, bacteria, yeast, fish and insects. Among mammals with determined CRs metabolic activity following species were identified: rabbit, hamster, mouse, monkey, chicken, pig, dog and cattle.

Human carbonyl-reducing enzymes occur in many different kinds of tissue, such as liver, lung, heart, kidney, brain, ovary and adrenal gland. Carbonyl reduction is performed by enzymes belonging to two main superfamilies *i.e.* the short-chain dehydrogenases/reductases family (SDR) and the aldo-keto reductases (AKRs). Enzymes from both superfamilies can catalyse the reduction of xenobiotic carbonyl compounds and endogenous steroids.

## 2.3 Carbonyl reducing enzymes

### 2.3.1 The aldo-keto reductase superfamily

The aldo-keto reductase (AKR) superfamily comprises at present 160 known enzymes of monomeric, mostly NADPH-dependent, oxidoreductases with a length of about 320 amino acids, that bind their cofactor without a Rossmann-fold motif (Jez, Bennett et al. 1997). AKRs are involved in biosynthesis, intermediary metabolism, and detoxication. Steroids, glucose, glycosylation end-products, lipid peroxidation products and environmental pollutants belong to the AKR substrates.

All AKRs possess a double domain protein with a βαβ fold characteristic of nucleotide binding proteins (Schade, Early et al. 1990). The AKRs contain a parallel β8/α8-barrel motif. The substrate-binding site is located in a large, deep elliptical pocket at the C-terminal end of the β barrel with a bound NADPH in an extended conformation (Wilson, Bohren et al. 1992). The lipophilic nature of the pocket prefers aromatic and apolar substrates over polar ones. The active site of the AKR members contains a highly conserved tetrade of the amino acids Tyr, His, Asp and Lys. Based on sequence comparisons, the AKR superfamily has been subdivided into 15 families, namely AKR 1-15 (Barski, Tipparaju et al. 2008). Further information about the AKR superfamily can be found at Dr. T. Penning's web site http://www.med.upenn.edu/akr.

### 2.3.2 The short-chain dehydrogenase/reductase superfamily

The enzymes belonging to the short-chain dehydrogenase/reductase (SDR) superfamily form another large carbonyl reducing superfamily with no structural similarities to AKRs. SDRs represent one of the oldest protein superfamilies and are widespread in both procaryotic and eucaryotic organisms. At present, at least 70

characterised, highly different, human enzymes of this family are known (Bray, Marsden et al. 2009). To the main substrates metabolised by SDRs belong prostaglandins, steroids, sugars and aromatic hydrocarbons. The superfamily is made up of enzymes averaging 250-350 amino acids in length (Hoffmann and Maser 2007). Most of the SDRs are known to be NAD- or NADP- dependent oxidoreductases. The sequence identity between SDR family members ranges typically between 15-30 % in pairwise comparisons (Kallberg, Oppermann et al. 2002); nevertheless, they share common structural properties.

First, the SDR superfamily was divided into two major families, "classical" and "extended". The "classical" SDRs have about 250 amino acid residues in length, while the "extended" family members have an additional 100-residue domain in the C terminal region (Jörnvall, Persson et al. 1995). The classical SDRs have a relatively small α-helical substrate binding site. The extended SDRs have a larger substrate binding site, including a two-stranded parallel β-sheet and an α-helix bundle containing three helices. Beyond that, the two families have different glycine-motifs in the cofactor binding part.

Later, the SDR superfamily was clustered into six families, namely the “intermediate” , “divergent” , “complex” (Persson, Kallberg et al. 2003) and “atypical“ families, in addition to the established “classical” and “extended” families (Figure 1).

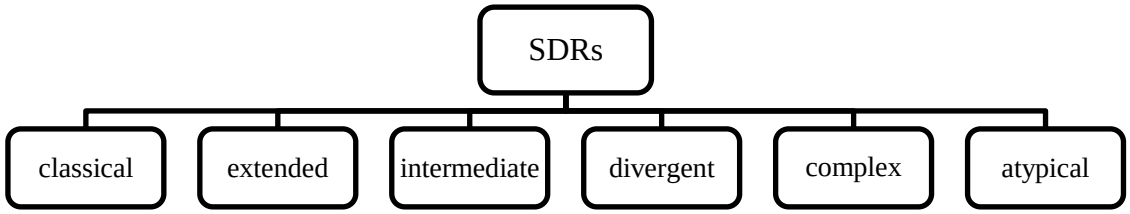


Figure 1: Classification of SDRs

The Rossmann fold, a common dinucleotide binding motif composed of βαβ units is the most important unifying feature of SDRs (Duax, Ghosh et al. 2000) additionally to its presence in long-chain dehydrogenases/reductases and medium-chain dehydrogenases/reductases (Kavanagh, Jörnvall et al. 2008). In SDRs, the catalytic site typically includes a highly conserved amino acid triad composed of the amino acids Ser, Tyr and Lys, even though variations on this motif also exist. Generally, it is the most common nucleotide cofactor binding domain. Furthermore, SDR proteins have a

structurally conserved N-terminal region with a glycine-rich pattern (TGxxxGxG), which contributes to NAD(H) or NADP(H) cofactor binding (Jörnvall, Persson et al. 1995; Tanaka, Nonaka et al. 1996) and a structurally variable C-terminal region, consisting of several α-helices, that binds the substrate. During the reaction, a fixed binding order is kept: the cofactor binds in the first place, subsequently followed by the substrate (Grimm, Maser et al. 2000). This fixed binding order is called sequential ordered bi-bi mechanism or bi-bi reaction.

### 2.3.3 New nomenclature of SDRs

Because SDRs form one of the largest enzyme superfamilies with more than 46.000 members found in the Uniprot and Refseq sequence databases and the number of newly described SDRs is still increasing, the establishment of a systematic nomenclature was needed. Therefore, a new nomenclature system has been established by Persson, Kallberg et al. 2009. In the new nomenclature scheme, each SDR family has been given a number. At present, there are 48 human SDR families detected. The numbering begins with the SDR families found in human with lowest numbers, followed by families from mammals or other eukaryotic members. Next, SDR families with members present both in bacteria and archaea and last, SDR families present just in bacteria were numbered. All SDR families are listed on the SDR web page http://www.sdr-enzymes.org.

The family number is followed by a letter signifying the SDR type, namely "classical" (C), "extended" (E), "intermediate" (I), "divergent" (D), "complex" (X) and "atypical" (A) SDRs. All these types differ in properties of the specific sequence patterns at the coenzyme binding and active site (for more information about the specific features of different types of SDRs see reference Kavanagh, Jörnvall et al. 2008.) The last distinguishing letter in the nomenclature scheme is the number at the end giving to each member of SDR family a specific individual denotation (see Figure 2). This system makes the nomenclature hierarchical, but still clearly informative. Using the new nomenclature CBR1 is reported as SDR21C1, CBR3 as SDR21C2 (Persson, Kallberg et al. 2009). Nevertheless, in this thesis we stick to the "old" nomenclature as the "new" nomenclature is still not fully implemented.

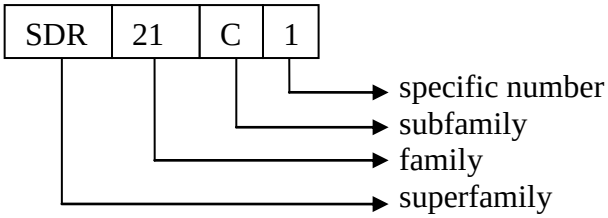


Figure 2: New nomenclature system of SDRs (CBR1 in this case)

### 2.3.4 Carbonyl reductases of the SDR superfamily

Several members of the SDR superfamily have been shown to reduce endogenous and xenobiotic carbonyl compounds *in vitro*. Among human CBRs, the best studied member is carbonyl reductase 1 (CBR1) (Oppermann 2007), followed by the much less known carbonyl reductase 3 (CBR3). Carbonyl reductases belong to the "classical" SDR family.

A special case is the enzyme called carbonyl reductase 4 (CBR4) with less than 30 % similarity and different substrate specifity in comparison to the other two CBRs. Further, CBR4 differs in terms of subcellular localization and subunit structure (Endo, Matsunaga et al. 2008). Here, the old nomenclature is clearly misleading and according to the new nomenclature CBR4 is numbered as SDR45C1 (Persson, Kallberg et al. 2009). This classification is strongly different from SDR21C1 (CBR1) and SDR21C2 (CBR3) and points out that they are not related apart from the SDR features.

### 2.3.5 Carbonyl reductase 1 (CBR1)

CBR1 was first isolated from human brain in 1973 by Ris and von Wartburg (Ris and von Wartburg 1973). CBR1 is a low molecular weight, monomeric, cytosolic, NADPH-dependent enzyme of the SDR superfamily with broad substrate specificity for many endogenous and xenobiotic carbonyl compounds. It is mapped to chromosome 21 at 21q22.12 and composed of 277 amino acids. The best known substrates include endogenous prostaglandins, steroids and other aliphatic aldehydes and ketones (Forrest and Gonzalez 2000). Regarding xenobiotics, CBR1 reduces *p*-quinones, anthracyclines, ketoaldehydes, aromatic aldehydes and NNK (4-(methylnitrosamino)-1-(3-pyridyl)-1-butanone), the carcinogenic nitrosamine of tobacco smoke (Atalla and Maser 2001; Finckh, Atalla et al. 2001).

Immunohistochemical staining showed presence of CBR1 in all organs assessed (Wirth and Wermuth 1985; Wirth and Wermuth 1992), but the various level of staining indicated a heterogeneous distribution in the body. Strong staining was found in liver, epidermis, stomach, small intestine, kidney, CNS, pituitary gland, smooth muscle fibres, blood vessels and cardiac muscle. Poor staining was located in connective tissue and CNS. Weak or no staining was observed in cerebellum, oral cavity, oesophagus, seminal vesicle, epididymis, *vas deferens*, prostate gland, glomerular capsule, thyroid gland, pancreas, ovary and skeletal muscle fibres (Forrest and Gonzalez 2000).

In general, CBR1 catalyses the following reaction:

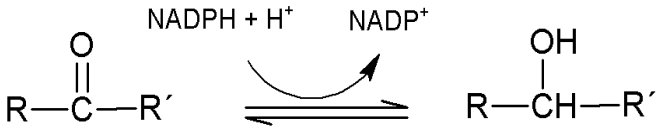


Figure 3: General reaction catalysed by CBR1

As mentioned above, CBR1 metabolises a broad spectrum of substrates. The first reports about CBR1 indicated that CBR1, also named 9-ketoreductase or 15-hydroxyprostaglandin dehydrogenase, was involved in prostaglandin and steroid metabolism. But later Wermuth found out that quinones based on the polycyclic aromatic structure, were much better substrates (Wermuth, Platts et al. 1986), with ubiquinone-1, menadione, and 9,10-phenanthrenequinone representing the best ones (Forrest and Gonzalez 2000). In prostaglandin metabolism, CBR1 inactivates PGE2 by conversion to PGF2α. The glutathione (GSH) adduct of PGA1 is also reduced by CBR1, in contrast to free PGA1, which is not metabolised at all (Wermuth 1981). However, the velocity of PGE1 and PGE2 reduction was approximate 50 times lower than the velocity of menadione reduction. Nevertheless, according to Kelner, CBR1 may play an *in vivo* role in prostaglandin metabolism (Kelner, Estes et al. 1997).

Ketoaldehydes *(e.g.* phenylglyoxal), aromatic aldehydes containing an electrophilic substituent (*e.g.* 4-nitrobenzaldehyde), and the biogenic aldehydes, indoleacetaldehyde and 4-hydroxyphenylacetaldehyde, were also readily metabolised although fairly high concentrations were required (Wermuth 1981). The lowest Michaelis constants and the highest maximal velocities were measured for ubiquinone and menadione (Wermuth 1981) and menadione is often used as a model substrate.

Quinones are converted to semiquinone radicals in a one-electron reduction or to hydroquinones in a two-electron reduction. Hydroquinones can be further conjugated in phase II and excreted (Oppermann 2007). This mechanism is involved in detoxication of endogenous substances and xenobiotics. On the other hand CBR1 plays a role in toxication *e.g.* the conversion of the anthracycline-based chemotherapeutical drugs daunorubicin and doxorubicin, resulting in cardiotoxicity.

Further reductase activity, comparable to menadione values, was found with the endogenous indole substrate isatin (indole-2,3-dione) (Usami, Kitahara et al. 2001; El-Hawari, Favia et al. 2009). Previously, no endogenous substrates had shown so high activity values and isatin has become the best known endogenous substrate for CBR1 (Usami, Kitahara et al. 2001). Isatin is an endogenous oxidised indole with a wide spectrum of behavioural and metabolic effects. Isatin and its derivatives form the base of many natural substances. Its output is increased during stress. Antagonism of atrial natriuretic peptide function and a role in NO signalling are the best described functions of isatin (Medvedev, Buneeva et al. 2007).

CBR1 plays a protective role in oxidative stress, tumour metastasis, neurodegeneration and apoptosis (Ismail, Al-Mulla et al. 2000; Botella, Ulschmid et al. 2004). Although no clear evidence explains which substrate is responsible for those effects, a study showed, that, *in vitro*, CBR1 inactivates the lipid aldehyde 4-oxo-2-nonenal (Carbone, Doorn et al. 2004), which is formed during oxidative stress. This supports the idea that CBR1 is involved in the oxidative stress response and elimination of reactive oxygen species (Pilka, Niesen et al. 2009).

### 2.3.6 CBR1 and S-nitrosoglutathione reduction

The fact that the glutathione adduct of PGA1 is reduced by CBR1 (free PGA1 is not) suggested the presence of a GSH-binding pocket close to the catalytic site. Bateman, Rauh et al. (2008) identified the GSH-binding site in the cleft of the enzyme site with the GSH-Cys oriented towards the nicotinamide moiety of the cofactor. Interactions between GSH and CBR1 are mediated along the entire GSH tripeptide structure. CBR1 contains five cysteine residues (positions 26, 122, 150, 226 and 227). To identify the reactive cysteine residue and investigate its possible role in GSH binding, each cysteine residue of human CBR1 was substituted with alanine by site-directed mutagenesis. Only the mutant Cys227Ala influenced the activity and this

position was suggested as the reactive residue involved in glutathione binding. The Cys227Ala mutant revealed 10 to 15-fold reduced $k_{cat}$ values in comparison to CBR1 wild type and the other four mutants, although addition of chloride rescued the activity of the enzyme (Tinguely and Wermuth 1999). The Cys227Ser mutation caused a similar decrease in activity as in the case of the Cys227Ala mutant, except that NaCl did not rescue the activity (Tinguely and Wermuth 1999). This was explained by the fact that the position 227 in the Cys227Ala mutant is occupied by a chloride ion (Bateman, Rauh et al. 2008).

S-nitrosoglutathione (GSNO), a nitrogen-containing GSH adduct, has recently been identified as an endogenous substrate with kinetic parameters comparable to the isatin and menadione values. Human CBR1 appears specific for this S-nitrosothiol, because the reduction of S-nitrosocysteine is not catalysed by CBR1. Before that report, CBR1 had only been known to reduce carbonyl groups to alcohol. The reduction of GSNO represents a different mechanism of reduction, where an NO bond is reduced. Furthermore, it was demonstrated that CBR1-dependent GSNO reduction occurs in A549 lung adenocarcinoma cell lysates. These findings indicated that CBR1 may play a role in the regulation of tissue levels of GSNO (Bateman, Rauh et al. 2008).

### 2.3.7 Carbonyl reductase 3 (CBR3)

CBR3 was discovered by Wanatabe, Sugawara et al. (1998) during the mapping of chromosome 21. The CBR3 gene location is 62 kb downstream from the original CBR1 gene on human chromosome 21q22.2. It is composed of 277 amino acids. The physiological role of CBR3 is still not fully clarified. CBR3 has been classified as a monomeric, cytosolic, NADPH-dependent oxidoreductase (Hoffmann and Maser 2007). The highest tissue distribution was detected in ovary, pancreas and intestine. Sex-specific expression was observed. Compared to ovary, lower concentrations were determined in prostate and testis (Miura, Nishinaka et al. 2008).

The CBR3 substrate spectrum is much narrower compared to CBR1. 1,2-naphthoquinone belongs to the best substrates for CBR3 and, interestingly, an overall preference of CBR3 for *o*-quinones is apparent (Pilka, Niesen et al. 2009). Although menadione has originally been reported as a CBR3 substrate (Lakhman, Ghosh et al. 2005), later studies revealed no CBR3 activity towards menadione (Miura, Nishinaka et

al. 2008; El-Hawari, Favia et al. 2009; Pilka, Niesen et al. 2009). To the non-quinone substrates of CBR3 belong oracin and isatin (Pilka, Niesen et al. 2009).

### 2.3.8 CBR1 versus CBR3

CBR1 and CBR3 show 72 % identity and 85 % similarity at the amino acid level (for sequence alignment see Figure 4). This level of identity is relatively high, compared to 15-30 % identity in other SDRs (Miura, Nishinaka et al. 2008). Both enzymes are composed of 277 amino acids and their genes are located close to each other on chromosome 21. In SDR classification, the CBRs belong to the "classical" SDR type with 140Ser-194Tyr-198Lys as a catalytic conserved triad (Jörnvall, Persson et al. 1995) and Gly-x-x-x-Gly-x-Gly motif as a glycine rich part of the Rossmann fold (Kallberg, Oppermann et al. 2002), with glycines at positions 12, 16, and 18. The catalytic triad is critically important for the enzyme function and seems to fix the position of cofactor and βαβ-folding (Hoffmann and Maser 2007).

CBR1 and CBR3 were explored under identical conditions with 111 different carbonyl substrates such as polyols, eicosanoids, steroids and xenobiotic carbonyl compounds, known as substrates for various types of carbonyl reductases (Matsunaga, Shintani et al. 2006; Pilka, Niesen et al. 2009). For CBR1, significant activity was found in 43 out of 111 substances, with quinones forming the largest fraction. In contrast, CBR3 reduced a very limited number of substrates with significantly decreased activity compared to CBR1. As mentioned above, the best substrate for CBR3 in this study was 1,2-naphthoquinone and a preference of CBR3 for *o*-quinones was evident. Another difference in substrate specificity was given by no activity of CBR3 towards eicosanoids or aliphatic carbonyls (Pilka, Niesen et al. 2009).

The 3D structure of both enzymes is similar. The main distinguishing feature is the conformation of the substrate binding loop. CBR1 shows a more closed and lipophilic active site, while the loop in CBR3 is more "open" and hydrophilic (El-Hawari, Favia et al. 2009; Pilka, Niesen et al. 2009). Despite high sequence similarities, the active site differs in shape and surface properties. Critical residues for substrate recognition were identified by Pilka, Niesen et al. 2009. Due to the thiomethyl group of Met142, a narrower substrate binding cleft was found in CBR1. In CBR3, this residue is replaced by Gln142. Three main critical positions for substrate recognition were suggested, namely position 230 (Trp in CBR1, Pro in CBR3), position 236 (Ala in

CBR1, Asp in CBR3) and position 142 (Met in CBR1, Gln in CBR3) (Pilka, Niesen et al. 2009). Moreover, there are only two amino acids in the CBR1 and CBR3 alignment which are encoded by triplets where all three bases differ completely. Trp230 is one of those two (El-Hawari, Favia et al. 2009) and was considered to be one of the important residues for catalysis. In the amino acid sequences of CBR1 among humans, rats, Chinese hamsters, and mice, the 230 tryptophan residue is highly conserved while in the human CBR3 the rigid amino acid proline occupies that position instead (Miura, Itoh et al. 2009). But in conclusion, Miura et al. 2009 presented the substitution of Pro230 for Trp230 in hCBR3 as having no apparent impact on their enzymatic activities and suggested that limited catalytic effect of carbonyl reductase activity of CBR3 in comparison to CBR1 is a common feature among animal species. In contrast, data from other studies indicate critical roles for Trp230 and Pro230 in surface properties of CBR1 and CBR3, respectively, in activity towards *p*-quinones (El-Hawari, Favia et al. 2009; Pilka, Niesen et al. 2009).

Additionally, in a sequence alignment of CBR1 and CBR3, nine amino acids at the C-terminal low-identity region, close to the catalytic cleft at positions 236-244, reveal low sequence similarity. In a mutant of CBR3, where these positions 236-244 were substituted with the corresponding CBR1 sequence, activity towards isatin was detected, although it was hardly comparable to the activity of CBR1 wild type. Other poorly conserved parts were found in the C-terminal region, near the catalytic Ser139. Together 10 mutants were generated and examined for isatin and 9,10-phenantrenequinone activity (El-Hawari, Favia et al. 2009). Interestingly, the change in CBR3 corresponding to CBR1 sequence at positions 230 and 236-244 resulted in significantly higher catalytic efficiency with isatin and 9,10-phenantrenequinone in comparison to the CBR3 wild type and other constructs without these mutations (El-Hawari, Favia et al. 2009).

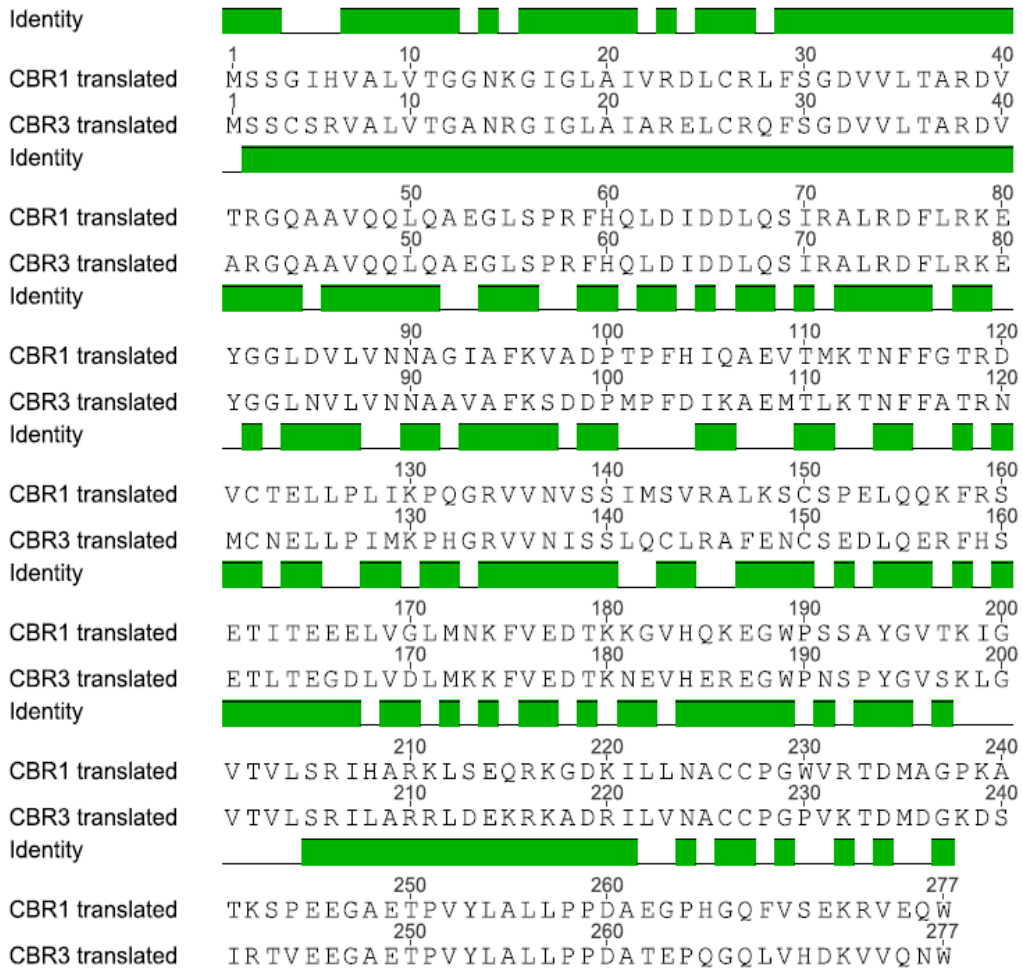


Figure 4: Geneious alignment of CBR1 and CBR3

## 2.4 NO metabolism focused on the role of GSNO

### 2.4.1 Nitric oxide (NO)

NO plays an important role in the nervous, immune and cardiovascular systems as a regulator and mediator of multiple processes. Besides mediating normal functions, NO has been implicated in pathophysiological states as hypertension, stroke, and neurodegenerative diseases. Nitric oxide is a short-lived, highly reactive and highly diffusible molecule (with a half-life of a few seconds) and synthesised by a group of NADPH-dependent enzymes called nitric oxide synthases (NOSs) from Arg and $O_2$. Potentially, NO is also generated by the reduction of $NO_x$ species that are derived from exogenous and endogenous sources (Hess, Matsumoto et al. 2005).

Three isoforms of NOS are known, namely neuronal NOS (NOS1 or nNOS), endothelial NOS (NOS3 or eNOS) and inducible NOS (NOS2 or iNOS). The names are derived from the activity (iNOS) or tissue from where they have been first described (nNOS, eNOS). Irrespective of their names, all three isoforms can be found in a variety of tissues and cell types. nNOS and eNOS expression is constitutive, while iNOS requires a stimulus to induce the expression. The generated nitric oxide interacts with the haem group of guanylate cyclase and activates the formation of cGMP, a second messenger with a major role in a number of physiological processes including homeostasis, platelet aggregation, smooth muscle tone, and bone growth (Smolenski, Burkhardt et al. 1998; Francis and Corbin 1999; Sausbier, Schubert et al. 2000).

### 2.4.2 Protein S-nitrosylation

The effects of NO are mediated by a number of mechanisms, but S-nitrosylation, the reaction of NO with cysteine thiol groups in proteins, has emerged as one of the most important ones. S-nitrosylation is a physiologically important post-translational modification controlled by mechanisms that include both the removal and the addition of the NO group from a Cys residue (Hess, Matsumoto et al. 2005). These mechanisms affect a number of proteins implicated in a variety of cellular processes. Both endogenous and exogenous NO react with the sulphur atom from cysteine in proteins to form relatively long-lived, naturally occurring S-nitrosothiols (SNOs) (Stamler, Jaraki et al. 1992; Gaston, Singel et al. 2006). Although NOSs unarguably play a central role in S-nitrosylation (Jaffrey, Erdjument-Bromage et al. 2001), it becomes increasingly recognised that additional metalloproteins might promote cellular S-nitrosylation (Benhar, Forrester et al. 2008).

S-nitrosylation can either increase or inhibit enzyme activity. The functional consequences of protein S-nitrosylation depend on the protein that is affected. S-nitrosylation has been shown to inhibit enzyme activity in cases such as the caspases, whereas in other proteins, such as matrix metalloproteinases, S-nitrosylation increases the activity of the enzymes.

Several studies have been published on the detection of potential S-nitrosylation sites. Perez-Mato, Castro et al. considered that the basic and acidic amino acids, enclosing the target cysteine, may affect and help to specify the position of the protein S-nitrosylation (Perez-Mato, Castro et al. 1999). The acid-base motif comprises

flanking acidic (Asp, Glu) and basic (Arg, His, Lys) residues (Stamler, Toone et al. 1997). However, this influence is still controversial as recently another study has suggested that the acid-base motif is not responsible for the S-nitrosylation and emphasised the role of more distant charged residues (Marino and Gladyshev 2009). Another factor, which can influence the specific site of S-nitrosylation, is protein allostery caused by ions ($Ca^{2+}$, $Mg^{2+}$, $H^{+}$) and $O_2$-based modifications (Hess, Matsumoto et al. 2005).

### 2.4.3 Protein denitrosylation

The removal of an NO group, known as denitrosylation, is still not well characterised. SNOs are mostly labile compounds and non-enzymatic S-NO bond degradation may be caused by light, heat, reducing compounds, nucleophilic agents or metal ions resulting in radicals or ions (Benhar, Forrester et al. 2009). There are two main cellular physiological denitrosylating enzyme systems: the thioredoxin (Trx) system (Benhar, Forrester et al. 2008) and the S-nitrosoglutathione reductase (GSNOR) system (Liu, Hausladen et al. 2001). GSNOR is originally known as class III alcohol dehydrogenase or glutathione-dependent formaldehyde dehydrogenase. According to the latest recommended nomenclature for the alcohol dehydrogenase family, GSNOR is termed alcohol dehydrogenase 3 (ADH3) (Duester, Farres et al. 1999; Staab, Hellgren et al. 2008). For more details about GSNOR see the GSNO chapter (2.4.4.).

The thioredoxin system comprises the Trx protein, TrxR (thioredoxin reductase) and NADPH. Thioredoxin is a protein with a redox-active disulphide in the conserved sequence -Cys-Gly-Pro-Cys- which is essential for its function. Caspase 3 was used to determine the Trx system denitrosylating effect. Inhibition of the Trx system increased the amount of S-nitrosylated caspase 3 and subsequently, the Trx system was established as a denitrosylase for a broad spectrum of proteins (Benhar, Forrester et al. 2008). Recent efforts to define the process of denitrosylation presumed a mixed-disulphide product between substrate and Trx or alternatively, the transfer of the NO group (Stoyanovsky, Tyurina et al. 2005; Benhar, Forrester et al. 2009). GSNO is also known as a substrate of the Trx reducing system (Nikitovic and Holmgren 1996).

### 2.4.4 S-nitrosoglutathione (GSNO)

GSNO (see Figure 5) is the key low-mass SNO in biological systems (Stamler, Jaraki et al. 1992). It was first identified in human airways (Gaston, Reilly et al. 1993). In physiological synthesis, activated NO intermediates react with glutathione (GSH) to form GSNO (Hogg, Singh et al. 1996).

$$2{\bullet}NO + O_2 \rightarrow 2\ {\bullet}NO_2$$
$${\bullet}NO + {\bullet}NO_2 \rightarrow N_2O_3$$
$$GSH + N_2O_3 \rightarrow GSNO + HNO_2$$

As a minor product GSNO is also formed in the oxidation of GSH by peroxynitrite (Moro, Darley-Usmar et al. 1994; van der Vliet, Hoen et al. 1998). Physiological levels of GSNO range between 1-10 μM (Gaston, Carver et al. 2003). GSNO is considered as an NO donor which releases NO under physiological conditions and serves as a reservoir and carrier for NO *in vivo* (Stamler, Jaraki et al. 1992; Lindermayr, Saalbach et al. 2005).

SNO homeostasis *in vivo* is ensured by synthesis of NO and decomposition of GSNO, the latter predominantly accomplished by GSNOR (Rusterucci, Espunya et al. 2007). GSNOR is a specific NADH-dependent GSNO reductase (Liu, Hausladen et al. 2001), although it is involved in formaldehyde metabolism as well (Benhar, Forrester et al. 2009). It has been revealed that the control of intracellular levels of both GSNO and S-nitrosylated proteins largely depends on GSNOR which helps to protect cells from nitrosative stress. GSNOR knockout mice have increased cellular amounts of both SNOs and GSNO (Liu, Hausladen et al. 2001; Liu, Yan et al. 2004). There appears to exist a transnitrosylation equilibrium between S-nitrosoglutathione GSNO and other SNOs (Gaston, Reilly et al. 1993).

More enzymes with denitrosylase activity have been reported. For instance xanthine oxidase (XO) is a flavoprotein enzyme containing iron and molybdenum and playing an important role in the catabolism of purines. XO facilitates the oxidation of hypoxanthine to xanthine and further of xanthine to uric acid. In the presence of purine or pteridine substrates, XO induces S-nitrosoglutathione (GSNO) decomposition (Trujillo, Alvarez et al. 1998)). The reduction of GSNO leads to the formation of GSH and •NO accompanied by peroxynitrite formation (Trujillo, Alvarez et al. 1998):

$$GSNO + \cdot O_2^- + H^+ \rightarrow GSH + \bullet NO + O_2$$

$$O_2^- + \bullet NO \rightarrow ONOO^-$$

The enzyme family of glutathione peroxidases (GPs) can be split up into two groups, selenium-independent and selenium-dependent enzymes. The selenium dependent GP group can decompose $H_2O_2$ (Kinnula, Crapo et al. 1995) by the glutathione redox cycle (Chance, Sies et al. 1979) which is responsible for capturing alkyl hydroperoxides. Selenium-dependent glutathione peroxidase 1 was found to catalyse the decomposition of GSNO in both presence and absence of different thiols to liberate NO (Hou, Guo et al. 1996).

Superoxide dismutase (SOD) is the enzyme catalysing the dismutation of superoxide into hydrogen peroxide and oxygen and thus serves a key antioxidant role. Three SODs are distinguished by different metal content. The copper-containing enzymes have been shown to catalyse •NO release from GSNO (Singh, Hogg et al. 1999).

Protein disulphide isomerase (PDI) is an abundant protein found in the lumen of the endoplasmic reticulum of eukaryotic cells. The major role of PDI is the formation and rearrangement of disulphide bonds in proteins. PDI contains two segments with homology to thioredoxin and belongs to the Trx superfamily. PDI was found to break GSNO bonds (Sliskovic, Raturi et al. 2005).

Carbonyl reductase1 (CBR1) efficiently reduces GSNO. This reduction is discussed in the "CBR1 and S-nitrosoglutathione reduction" chapter.

SNOs are usually very unstable in aqueous solution, *i.e.* S-nitrosocysteine has a half-life of less than 2 min, but surprisingly, GSNO undergoes decomposition over hours (Singh, Wishnok et al. 1996). The decomposition of GSNO does not occur spontaneously, presence of additional agents such as light, metal ions, heat, thiols or reducing agents is needed. Thiols can decay GSNO by two mechanisms. First, the faster mechanism is reversible transnitrosylation,

$$RSH + GSNO \leftrightarrow RSNO + GSH$$

whereas the second is S-thiolation, the reduction of GSNO by a thiol to generate a nitroxyl anion and a mixed disulphide (Zeng, Spencer et al. 2001). An example of the

second mechanism is decomposition of GSNO by GSH, an important determinant of the intracellular redox state (Schmidt, Grey et al. 1996).

$$GS^- + GSNO \rightarrow GSSG + NO^-$$

A non-thiol GSNO reducing agent is ascorbic acid (Kashiba-Iwatsuki, Yamaguchi et al. 1996), which is specific for S-NO cleavage.

GSNO plays an important and dual role in apoptosis, where it can serve either as inducer or inhibitor (Sandau and Brune 1996). Particularly, the neuroprotective effect of GSNO against oxidative stress has been shown (Inoue, Akaike et al. 1999). Another role of GSNO is inhibition of platelet activation and vasodilation (de Belder, MacAllister et al. 1994). Moreover, S-nitrosothiols are strong endogenous bronchodilators depleted in asthmatic airway lining fluid (Wu, Romieu et al. 2007).

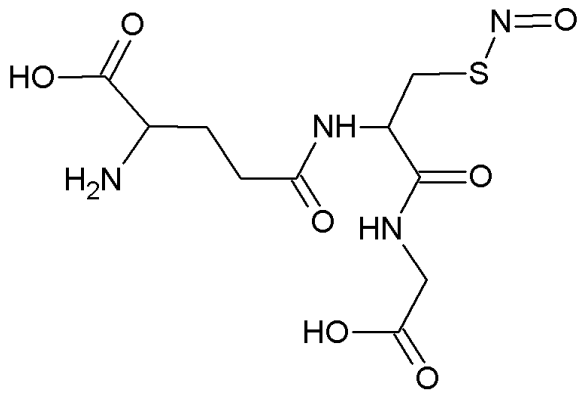


Figure 5: Structure of GSNO

### 2.4.5 S-glutathionylation

S-glutathionylation is another type of modification of the highly reactive Cys residues in proteins occurring both at physiological and non-physiological conditions. It implies the reversible formation of a disulphide bond between glutathione and a Cys thiol of the target protein (Thomas, Poland et al. 1995; Cotgreave and Gerdes 1998). GSH is a tripeptide, present in mammalian cells at concentrations that range between 1 and 10 mM (Tietze 1969) and containing a reactive cysteine thiol, which maintains

proteins in their reduced state. Moreover, it protects cell from oxidative stress and plays an important role in post-translational regulations of protein functions (Castellano, Ruocco et al. 2008). In presence of oxidative agents, two molecules of GSH can interact and form glutathione disulphide (GSSG).

It is suggested that S-glutathionylation may occur either by reaction of the reduced protein cysteine with glutathione disulphide (GSSG), or, alternatively, independent of GSSG formation by the reaction of an oxidatively activated protein thiol with GSH (Klatt and Lamas 2000). Not all cysteines in one protein can be S-glutathionylated; the reaction requires specific Cys orientation and is enhanced by basic neighbouring residues. Increased GSSG levels have been presumed as the leading mechanism for S-glutathionylation (Martinez-Ruiz and Lamas 2007) and occur in diseases related to oxidative stress (Giustarini, Milzani et al. 2005) such as cardiovascular, lung and neurodegenerative diseases or cancer (Mieyal, Gallogly et al. 2008). But GSSG is not the only S-glutathionylating agent. The reaction between GSNO and protein sulphydryls can also cause S-glutathionylation (as well as S-nitrosylation).

The mechanism of GSNO-mediated glutathionylation includes the homolytic cleavage of the S-NO bond producing •NO and thiyl (GS•) radicals (Mohr, Hallak et al. 1999). The thiyl radical can cause the formation of protein disulphides (protein-SSG). The homolytic cleavage of GSNO can be facilitated if the cysteine thiol in the target protein is activated by proximity to a basic amino acid, *e.g.* histidine. The activated thiol is a strong nucleophile while not activated thiols are less nucleophilic and their potential to destroy an S-NO bond is not powerful enough. They rather prefer to be S-nitrosylated. Therefore the nucleophilicity of cysteine residues is responsible for the GSNO type of modification (Mohr, Hallak et al. 1999).

# 3 AIM OF THE THESIS

- to prepare the desired mutants of CBR3 with selected changes incorporated in the sequence
- to clone these mutants together with CBR1 and CBR3 wild types into the plasmid vector pET-28b(+)
- to overexpress CBR1, CBR3 and the mutants into proteins and purify these proteins
- to study the effect of GSNO on CBR1, CBR3 and all overexpressed mutants and determine kinetic properties

# 4 MATERIAL

## 4.1 Chemicals

| | |
|---|---|
| Acetic acid | Sigma, Steinheim (Germany) |
| Acetone | Merck, Darmstadt (Germany) |
| Agar | Sigma, Steinheim (Germany) |
| Agarose Biozym Plague Genetic Pure | Biozym, Hessisch-Oldendorf (Germany) |
| Agarose NEEO Ultra Qualität | Carl Roth, Karlsruhe (Germany) |
| Ampicillin | AGS, Heidelberg (Germany) |
| Ascorbic acid | Merck, Darmstadt (Germany) |
| Bovine serum albumin | Behringwerke, Marburg (Germany) |
| Bradford reagent | Sigma-Aldrich, München (Germany) |
| Calcium chloride dihydrate | Merck, Darmstadt (Germany) |
| Coomassie | Serva, Heidelberg (Germany) |
| Copper (II) chloride 97 % | Sigma-Aldrich, München (Germany) |
| Dipotassium hydrogen phosphate dihydrate | Merck, Darmstadt (Germany) |
| Dithiothreitol | Sigma, Steinheim (Germany) |
| dNTPs | Promega, Madison (USA) |
| DTPA | Sigma-Aldrich, München (Germany) |
| EDTA | Sigma, Steinheim (Germany) |
| Ethanol | Carl Roth, Karlsruhe (Germany) |
| Glutathione | Sigma-Aldrich, München (Germany) |
| Glycerol 87 % | Carl Roth, Karlsruhe (Germany) |
| Hydrochloric acid | Merck, Darmstadt (Germany) |
| Imidazole | Merck, Darmstadt (Germany) |
| IPTG | Peqlab Biotechnologie, Erlangen (Germany) |
| Isopropyl alcohol | Merck, Darmstadt (Germany) |
| Kanamycin | Alexis-Biochemicals, Lörrach (Germany) |
| LB Broth | Miller Fisher Scientific, Schwerte (Germany) |

| | |
|---|---|
| Lysozym | Sigma-Aldrich, München (Germany) |
| $MgCl_2$ | Fermentas, St. Leon-Rot (Germany) |
| N-1-naphthylethylenediamine | Sigma-Aldrich, München (Germany) |
| NADPH | Carl Roth, Karlsruhe (Germany) |
| PIPES | Sigma-Aldrich, München (Germany) |
| Potassium dihydrogenphosphate | Merck, Darmstadt (Germany) |
| Sodium dihydrogenphosphate monohydrate | Promega, Mannheim (Germany) |
| Sodium hydroxide | Merck, Darmstadt (Germany) |
| Sodium chloride | Baker, Griesheim (Germany) |
| Sodium nitrite | Merck, Darmstadt (Germany) |
| Sulphanilamide | Sigma-Aldrich, München (Germany) |
| Tris Base | Sigma, Steinheim (Germany) |

## 4.2 Enzymes

| | |
|---|---|
| *Kpn*I | NEB, Frankfurt a. M. (Germany) |
| T4 DNA Ligase | NEB, Frankfurt a. M. (Germany) |
| T4 DNA Polymerase | Fermentas, St. Leon-Rot (Germany) |
| *Xho*I | NEB, Frankfurt a. M. (Germany) |
| TEV protease | Zoologisches Institut - Strukturbiologie Zentrum für Biochemie und Molekularbiologie Christian-Albrechts-Universitaet zu Kiel |
| *Taq* Polymerase | QIAGEN, Hilden (Germany) |

## 4.3 Bacterial strains

| | |
|---|---|
| *E.coli* HB101 strain | Amersham Biosciences, Freiburg (Germany) |
| *E. coli* BL21 (DE3) strain | Novagen, Merck, Darmstadt (Germany) |
| *E. coli* Origami strain | Novagen, Merck, Darmstadt (Germany) |

## 4.4 Oligonucleotides

| | |
|---|---|
| All PCR primers | MWG, Ebersberg (Germany) |

## 4.5 Plasmids

| | |
|---|---|
| pET-28b(+) | Novagen, Merck, Darmstadt (Germany) |

## 4.6 Kits

| | |
|---|---|
| Illustra TempliPhi 100 Amplification Kit | GE Healthcare, Buckinghamshire (UK) |
| QIAEX II Gel Extraction Kit | QIAGEN, Hilden (Germany) |
| QIAGEN Plasmid Midi Kit | QIAGEN, Hilden (Germany) |
| QIAquick Gel Extraction Kit | QIAGEN, Hilden (Germany) |
| QIAexpress Kit | QIAGEN, Hilden (Germany) |

## 4.7 Consumables

| | |
|---|---|
| 96-well microtest plates | Sarstedt, Nürnbrecht (Germany) |
| Amicon® Ultra-4 centrifugal filter device | Millipore, Billerica (USA) |
| Eppendorfs | Sarstedt, Nürnbrecht (Germany) |
| PD-10 Desalting columns | Amersham Biosciences Freiburg (Germany) |
| Disposable cuvettes | Sarstedt, Nümbrecht (Germany) |
| Pipette tips (every range of volume) | Sarstedt, Nümbrecht (Germany) |
| Ready Bis-Tris gels (gradient 4-12 %) | Invitrogen, Karlsruhe (Germany) |
| Sterile filter | Millipore, Billerica (USA) |
| Petri dishes | Sarstedt, Nümbrecht (Germany) |
| Multiply PCR cups 0.2 ml | Sarstedt, Nürnbrecht (Germany) |
| Multiply-µStrip of 8 tubes 0.2 ml | Sarstedt, Nürnbrecht (Germany) |

## 4.8 Markers and stains

| | |
|---|---|
| 6× Loading Dye Solution | Fermentas, St. Leon-Rot (Germany) |
| Gene Ruler 100 bp DNA Ladder Plus | Fermentas, St. Leon-Rot (Germany) |

| | |
|---|---|
| Protein Molecular Weight Marker | Fermentas, St. Leon-Rot (Germany) |
| SYBR Safe DNA Gel Stain | Invitrogen, Karlsruhe (Germany) |

## 4.9 Equipment

| | | |
|---|---|---|
| Analytical balance | R1605 | Sartorius, Göttingen (Germany) |
| Autoclave | Systec tuttnauer 2540EL | Systec, Wettenberg (Germany) |
| Centrifuges | Biofuge pico<br>Biofuge fresco<br>Biofuge 15R<br>Megafuge 11R | Heraeus, Hanau (Germany) |
| | J2-HS | Beckman, Krefeld (Germany) |
| Electrophoresis power supply | Power pack 300 | Bio-Rad Laboratories, München (Germany) |
| | Power Pack 35/60 | Phase, Lübeck (Germany) |
| Gel documentation system | Image Master VDS + FUJIFILM Imaging System FTI-500 | Pharmacia Biotech, Freiburg (Germany) |
| | Gel IX Imager | Intas, Göttingen (Germany) |
| | NU-72 | Benda, Weisloch (Germany) |
| Gel electrophoresis | 40-1214<br>40-0911 | PEQLAB Biotechnologie, Erlangen (Germany) |
| Heating blocks | Thermomixer 5436 | Eppendorf, Hamburg (Germany) |
| | Thermoblock TB2 | Biometra, Göttingen (Germany) |
| Incubator | B6030 | Heraeus, Hanau (Germany) |
| Incubator | TH 15, KS 15 | Edmund Bühler, Hechingen (Germany) |
| Microplate reader | | Tecan, Männedorf (Switzerland) |
| Multipipette | Multipipette Plus | Eppendorf, Hamburg (Germany) |

| | | |
|---|---|---|
| Nickel affinity chromatography | Äkta-Purifier | GE Healthcare, New Jersey (USA) |
| 1 ml Ni-NTA columns | | GE Healthcare, New Jersey (USA) |
| PCR Thermocycler | T-Gradient<br>T- profesional | Biometra, Göttingen (Germany) |
| pH meter | pH 535 Multical | WTW, Weilheim (Germany) |
| Pipettes | 1-10 µl<br>2-20 µl<br>20-200 µl<br>100-1000 µl | Eppendorf, Hamburg (Germany)<br>Gilson, Middleton (USA) |
| Precision balance | BP3100S | Sartorius, Göttingen (Germany) |
| Rocking platform | VWR | VWR International, Darmstadt (Germany) |
| SDS PAGE | XCell SureLock | Invitrogen, Karlsruhe (Germany) |
| Sonicator | Sonoplus UW2200 | Bandelin, Berlin (Germany) |
| Spectrophotometer | GeneQuant II | Pharmacia Biotech, Freiburg (Germany) |
| Vacuum concentrator | SPD121P SpeedVac | Thermo, Egelsbach (Germany) |
| Ultracentrifuge | TGA-65 | Kontron Analytical, (Schwitzerland) |
| Vortex | VF2 | Ika, Staufen (Germany) |

## 4.10 Software

| | |
|---|---|
| ACD/ChemSketch | Advanced Chemistry Development, Toronto (Canada) |
| Cary WinUV | Varian, Palo Alto (USA) |
| EndNote | Thomson Reuters, New York (USA) |
| FinchTV | Geospiza, Seattle (USA) |
| Gel IX Imager | Intas, Göttingen (Grmany) |
| Geneious | Biomatters, Auclkand (New Zealand) |
| GraphPad Prism | GraphPad Software, La Jolla (USA) |
| PyMOL | open source foundation |
| XFluor | Tecan, Männedorf (Switzerland) |

# 5 METHODS

## 5.1 Mutagenesis and cloning

### 5.1.1 Polymerase chain reaction (PCR)

PCR is a technique to amplify a piece of DNA generating thousands to millions of copies of the original sequence of the DNA molecule. PCR is based on the ability of a thermostable DNA polymerase to replicate a new strand of DNA complementary to the offered DNA template strand. In fact, any piece of DNA can be amplified into millions of identical copies as is shown in Figure 6. The method was established in 1984 by Kary Mullis who was awarded the Nobel Prize in Chemistry in 1993 for this work. PCR relies on thermal cycling, consisting of repeated heating and cooling cycles. Three major steps are involved in one PCR cycle. Each step, denaturation, annealing, and extension takes place at a different temperature. The first step, denaturation of the DNA, involves heating to 95°C, which dissociates the target DNA into two strands. In the second step, primers containing sequences complementary to the target region bind to the single strand generated in the previous PCR step. This annealing is proceeding at about 54°C. In the third step at about 72°C a thermostable DNA polymerase which can sustain high temperature moves along the DNA, reading its code and synthesising a copy. The general composition of PCR mixtures as used in this work is given in Table 1.

PCR requires the following conditions:

- $MgCl_2$ necessary for DNA polymerase activity, provided at a concentration of 0.5 to 2.5 mM
- buffer providing a suitable chemical environment for DNA polymerase
- dNTPs at a concentration of 20 to 200 μM, the structural elements from which the DNA polymerase synthesises a new DNA strand
- two primers (forward and reverse) at a concentration of 0.1 to 0.5 μM
- thermostable DNA Polymerase
- target DNA to be amplified at an amount smaller than 1 μg
- monovalent cations

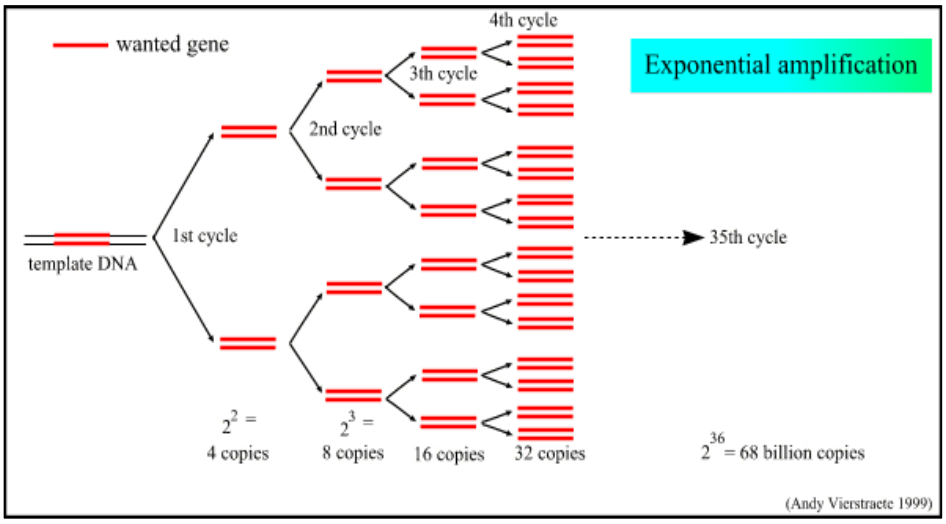


Figure 6: The exponential amplification of the gene in PCR (http://users.ugent.be)

Table 1: General composition of 20 µl and 50 µl PCR reaction mixture used in this work

| component | volume |
|---|---|
| *Taq* polymerase (5 U/µl) | 0.4 µl |
| template | 1 µl |
| dNTPs (10 mM each) | 0.4 µl |
| forward primer (100 pmol/µl) | 0.4 µl |
| reverse primer (100 pmol/µl) | 0.4 µl |
| *Taq* polymerase buffer | 2 µl |
| $MgCl_2$ (15 mM) | 1.5 µl |
| water | 13.9 µl |
| total volume | 20 µl |

| component | volume |
|---|---|
| *Taq* polymerase (5 U/µl) | 1 µl |
| template | 1 µl |
| dNTPs (10 mM each) | 1 µl |
| forward primer (100 pmol/µl) | 1 µl |
| reverse primer (100 pmol/µl) | 1 µl |
| *Taq* polymerase buffer | 5 µl |
| $MgCl_2$ (15 mM) | 4 µl |
| water | 36 µl |
| total volume | 50 µl |

The PCR temperature cycles are usually repeated 20-40 times. A variety of parameters influence the conditions such as the temperatures used and the length of each cycle kept during PCR. The PCR condition determinanting factors: the enzyme used for DNA amplification, the concentration of $Mg^{2+}$ ions and dNTPs in the reaction and the melting temperature of the primers. Thermo cycler conditions which were used for all assays are indicated in Table 2. The denaturation, annealing and extension step was repeated 30 times.

Table 2: Thermo cycler conditions during PCRs repeated 30 times

| step | duration | temperature | |
|---|---|---|---|
| initial denaturation | 1 min | 95°C | |
| denaturation | 1 min | 95°C | repeated 30x |
| annealing | 1 min /kb | 55°C | |
| extension | 1 min | 72°C | |
| final extension | 10 min | 72°C | |

### 5.1.2 Mutagenesis by splicing by overlap extension (SOE)

Gene splicing by overlap extension (SOE) is a sequence-independent technique used for site-directed mutagenesis and recombination of DNA molecules. The idea is based on adding or changing sequences at the end of a PCR product, so the product can serve as a new primer for a subsequent overlap-extension reaction, which enables insertion of mutations at specific positions in a sequence (Ho, Hunt et al. 1989; Horton 1995).

Two fragments of the target sequence are amplified in two separate PCR reactions as outlined in Figure 7. For each reaction one primer outside the region to be mutated and one mutagenic primer are used, the latter carrying the desired change in sequence. The two created intermediate PCR fragments comprise complementary ends formed by the mutagenic primers and can create a new DNA template by overlapping in a subsequent PCR to yield the recombinant product. During this extension the two outside primers are used to initiate the synthesis of the new fused product (Ho, Hunt et al. 1989; Horton 1997). In principle, to introduce mutations by SOE, the position of the mutation has no limitation and can be introduced anywhere along the targeted DNA (Vallejo, Pogulis et al. 1994).

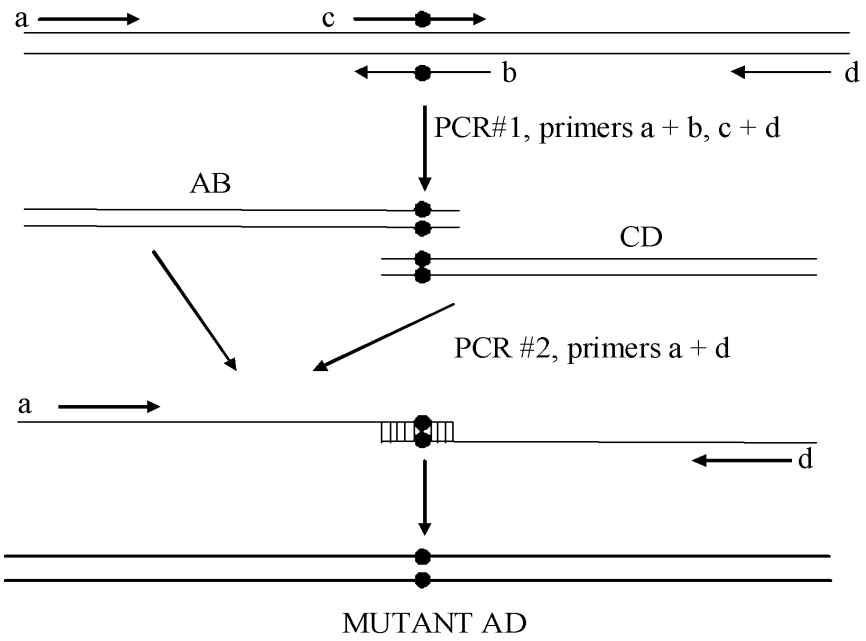


Figure 7: Mutagenesis by overlap extension
By PCR two segments of a DNA are amplified and then fused together in a subsequent reaction. Two specially designed mutagenic primers (b, c) enables to introduce the mutation forming complementary terminal regions of the intermediate PCR products. These regions can be fused by an overlap extension in a subsequent reaction. The amplification of the fused recombinant mutant is carried out by the use of the two outside primers (a, d) (Vallejo, Pogulis et al. 1994).

Several positions both in CBR1 and CBR3 were decided to be investigated. Some DNA fragments, already with incorporated mutated positions, were received from Yasser El-Hawari. The complete list of sequence mutations is given below in Table 6. In this thesis, efforts were made to replace positions Cys226 and Cys227 in CBR1 and Cys143 in CBR3 by Ser resulting in the mutants CBR1 Cys226Ser, CBR1 Cys227Ser and CBR3 Cys143Ser. In the first step 6 PCR reactions were run. Master Mix was prepared from double distilled water, *Taq* polymeras*e* buffer, $MgCl_2$, reverse and forward primers (see Table 3), dNTPs and *Taq* Polymerase, a thermostable DNA polymerase isolated from the bacterium *Thermus aquaticus*. As a template CBR1 and CBR3 already incorporated in pET-28b(+) vector were used. PCR products were analysed via agarose gel electrophoresis.

Table 3: Sequences of primers used for mutagenesis
In yellow are restriction sites for *Kpn*I, in red *Xho*I and in blue triplets coding changed amino acids

| PCR reaction number | position to be changed | primer | sequence of the primer |
|---|---|---|---|
| 1 | CBR1 Cys226Ser | forward | CTGTATCTGCAGGGTACCCCCGGGATGTCGTCCGGC |
| | | reverse | CACCCACCCTGGGCAGGAGGCATTCAGGAGGA |
| 2 | | forward | TCCTCCTGAATGCCTCCTGCCCAGGGTGGGTG |
| | | reverse | GACGACCTCGAGTCACCACTGTTCAAC |
| 3 | CBR1 Cys227Ser | forward | CTGTATCTGCAGGGTACCCCCGGGATGTCGTCCGGC |
| | | reverse | TCTCACCCACCCTGGGGAGCAGGCATTCAGGAG |
| 4 | | forward | CTCCTGAATGCCTGCTCCCCAGGGTGGGTGAGA |
| | | reverse | GACGACCTCGAGTCACCACTGTTCAAC |
| 5 | CBR3 Cys143Ser | forward | ATGATGGGTACCATGTCGTCCTGCAGCCGCGT |
| | | reverse | TTCAAAAGCCCTTAAAGACTGCAAACTACTGAT |
| 6 | | forward | ATCAGTAGTTTGCAGTCTTTAAGGGCTTTTGAA |
| | | reverse | GACGACCTCGAGTTACCAGTTTTGCACAAC |

### 5.1.3 Agarose gel electrophoresis

Agarose gel electrophoresis is a method to separate DNA fragments according to their sizes and to visualize them. As DNA is negatively charged, in an electric field it moves through the gel matrix towards the positive pole. The gel matrix slows the DNA molecules down and smaller molecules migrate faster than larger molecules. Depending on the fragment size, 0.75 % to 2.0 % agarose gels are usually used. The DNA is visualized on a UV trans-illuminator by staining with a fluorescent dye. In the preparative approaches, *i.e.* when a band was to be excised and extracted from the gel for further procedures the wavelength 366 nm instead of 312 nm was used for visualization. This wavelength assures no damage of the DNA during UV-exposure.

For separation an agarose concentration of 1 % (w/v) in 1 x TAE buffer (see Table 5) was used. To visualise the sample DNA SYBR®Safe, a stain for nucleic acids, was added according to the manufacturer's instruction. Before loading the gel with the PCR samples, each sample was mixed with 6 x Loading Dye Solution causing higher

density of the samples so that they sink to the bottom of the well. 10 µl of GeneRuler 100 bp Plus was used to check the size of the PCR products.

The appropriate DNA bands were excised from the gel and centrifuged through glass wool at 8.000 rpm for 10 min to remove the agarose. A flow through volume of 1 µl was used as a template for the following PCR reaction (see Table 4). The three new constructs were purified via a preparative 1 % agarose gel electrophoresis and the Qiagen gel extraction kit.

Table 4: Subsequent PCR reactions resulting in desired mutants
Restriction sites for *Kpn*I are displayed in yellow, *Xho*I in red.

| **PCR reaction number** | **position to be changed** | **template (number of PCR reaction)** | **primer** | **sequence of the primer** |
|---|---|---|---|---|
| 7 | CBR1 Cys226Ser | 1, 2 | forward | CTGTATCTGCAGGGTACCCCCGGGATGTCGTCCGGC |
| | | | reverse | GACGACCTCGAGTCACCACTGTTCAAC |
| 8 | CBR1 Cys227Ser | 3, 4 | forward | CTGTATCTGCAGGGTACCCCCGGGATGTCGTCCGGC |
| | | | reverse | GACGACCTCGAGTCACCACTGTTCAAC |
| 9 | CBR3 Cys143Ser | 5, 6 | forward | ATGATGGGTACCATGTCGTCCTGCAGCCGCGT |
| | | | reverse | GACGACCTCGAGTTACCAGTTTTGCACAAC |

Table 5: Composition of 40 x TAE buffer, pH 8.0

| **component** | **concentration** | **amount** |
|---|---|---|
| Tris | 40.0 mM | 121 g |
| 100 % acetic acid | 40.0 mM | 28.6 ml |
| 0,5 M $Na_2EDTA$ | 1.0 mM | 1 ml |
| $H_2O$ | | *ad* 500 ml |

### 5.1.4 Gel extraction and purification of DNA

The QIAquick Gel Extraction Kit Protocol using a microcentrifuge was followed for DNA preparation. All centrifugation steps were carried out at 13.000 rpm at room temperature. DNA fragments were excised from the preparative agarose gel, weighed and three volumes of Buffer QG were added to one volume of gel. To dissolve the gel, the gel pieces were incubated at 50°C for 10 min. Next, one volume of isopropanol was added. To bind the DNA, the samples were applied to the QIAquick column and centrifuged for 1 min. To dispose of all agarose traces 0.5 ml of Buffer QG was added to the column and centrifuged again for 1 min. The columns were washed with 0.75 ml of Buffer PE and centrifuged twice for one min to remove all residual ethanol. DNA was eluted with 40 µl of Buffer EB. All buffer compositions are described in the manufacturer´s instructions.

### 5.1.5 Measuring DNA concentration

Concentration and quality of a sample of DNA were measured by the GeneQuant II UV spectrophotometer. The aromatic rings of the bases in DNA absorb UV light with an absorption maximum at 260 nm. Proteins absorb ultraviolet light at 280 nm, largely due to the aromatic tryptophan ring. If there is a protein contaminant, there is additional OD280 which decreases the OD ratio between 260 and 280 nm. Clean DNA has an OD260/OD280-ratio between 1.8 and 2.0. A smaller value indicates a contamination.

### 5.1.6 Digestion of DNA fragments and pET-28b(+) vector

Restriction endonucleases are enzymes found in bacteria that cleave the sugar-phosphate backbone of DNA at specific recognition nucleotide sequences termed restriction sites. Several hundred different restriction endonucleases have been isolated. Besides the fragments which were constructed in this thesis, additional constructs together with CBR3 wild type (CBR3wt) fragment were kindly provided by Yasser El-Hawari in the form of undigested PCR products or already incorporated in the vector pET-15b(+). CBR1 already incorporated in a modified version of the pET-28b(+) vector

(see appendix) was kindly provided by Claudia Staab. For the complete list and form of inserted mutations see Table 6.

PCR fragments with desired mutations, CBR3wt and pET-28b(+) were double digested by restriction endonucleases *Kpn*I and *Xho*I (New England Biolabs, NEB). The reaction mixture (see Table 7) of a total volume of 20 µl was prepared and incubated for 60 min at 37°C in a heat block. As restriction endonucleases are supplied in 50 % glycerol, the addition of restriction enzymes should not exceed 10 % of the total volume to avoid star activity (alteration of the specificity of restriction enzyme) caused by glycerol. The purification of the fragments is required to avoid possible interferences of reaction compounds with subsequent reactions.

Table 6: Positions changed by mutagenesis
For CBR1 and CBR3 sequence alignment see Figure 4.

| **mutant** | **positions of CBR3 changed to correspond to CBR1** | **source and form of the fragment** |
|---|---|---|
| CBR3wt | none | provided by Yasser El-Hawari as undigested PCR product |
| K106Q | 106 | |
| SUMU | 142,143, 230, 236-244, 270 | |
| 97VA | 97, 98 | |
| SOE | 236-244 | provided by Yasser El-Hawari incorporated into pET-15b(+) vector |
| SOE P230W | 230, 236-244 | |
| Cys143Ser | 143 | constructed in this thesis |
| | **positions of CBR1 changed to Ser** | |
| CBR1wt | none | provided by Claudia Staab incorporated into pET-28b(+) vector |
| Cys226Ser | 226 | constructed in this thesis |
| Cys227Ser | 227 | |

Table 7**:** Composition of digesting reaction mixture

| **Component** | **Volume** |
|---|---|
| BSA (1 mg/ml) | 2 µl |
| NEB buffer 1 (10x) | 2 µl |
| DNA fragment | 5 µl |
| $H_2O$ | 9 µl |
| *Kpn*I (10 U/µl) | 1 µl |
| *Xho*I (20 U/µl) | 1 µl |
| Total volume | 20 µl |

### 5.1.7 Purification of DNA fragments and pET-28b(+) vector

Purification of digested fragments was carried out according to the QIAEX II Protocol. The QIAEX II Gel Extraction Kit is designed for purification and concentrating DNA fragments from 40 bp to 50 kb from aqueous solutions with no demand for using phenol extraction or ethanol precipitation. Enzymes such as restriction endonucleases, polymerases, phosphatases, as well as dNTPs and salts are removed. 60 µl of Buffer QX1 was added to 20 µl of samples and the colour of the mixtures turned yellow. QIAEX II solution was mixed by vortexing for 30 sec and 10 µl was added to the samples. The mixtures were incubated 10 min at room temperature while mixing every 2 minutes to keep QIAEX II in suspension. After that, the samples were centrifuged for 30 sec at (max) 10.000 x g and the supernatants removed. The pellets were washed twice with 500 µl of Buffer PE and air-dried for 15 min. DNA was eluted by 20 µl of 10 mM Tris, pH 8.5, vortexed shortly and incubated for 5 min at room temperature. Pure DNA was obtained by centrifuging the sample for 30 sec at (max) 10.000 x g. The supernatants contained the desired pure DNA.

Digested pET-28b(+) vector was purified via preparative agarose gel electrophoresis and the Qiagen gel extraction kit, as described under “Gel extraction and purification of DNA”. The Concentration of all samples was measured by the GeneQuant II UV spectrophotometer.

### 5.1.8 DNA Ligation

During DNA ligation, two linear DNA molecules are joined together by creating a covalent bond from the 3' hydroxyl of one nucleotide and the 5' phosphate of the other. This reaction is catalysed by a DNA ligase. T4 DNA ligase from the T4 bacteriophage is the most common used DNA ligase for molecular biology techniques.

A ligation reaction requires:

- two or more fragments of DNA
- a buffer containing ATP
- T4 DNA ligase

The Rapid DNA Ligation kit was used for ligation. Accurate amounts of digested and purified vector and fragments to be inserted were mixed. The recommended amount of the vector, which was also used in this thesis, is 50 – 100 ng per reaction. The ligation mixture contained 3 fold molar access of foreign DNA relative to the vector. 4 µl of 5 x rapid ligation buffer, $H_2O$ up to 9 µl and finally 1 µl of T4 DNA ligase were added into each tube. Mixtures were incubated overnight at 18°C.

### 5.1.9 Preparation of *E. coli* HB101 and BL21 strain competent cells

Considering the high hydrophilicity of the DNA molecule, the DNA is not able to pass through the bacterial cell membrane. The ability of a bacterial cell to take up extracellular DNA is called cell competence. Competence is distinguished into the natural competence and induced competence which arises during treating cells in laboratory cultures to make them permeable to DNA. In the present thesis, the calcium method was used to generate competent cells where a high calcium concentration creates small holes in the bacterial cell wall. Two *E. coli* strains were made competent, first, the *E. coli* HB101 strain, a non-expression host with resistance to streptomycin, which is suitable for routine cloning and second, the *E. coli* BL21 strain, an expression host for any gene, which is under control of a T7 promoter. The BL21 strain has no antibiotic resistance.

A starter culture of 2 ml LB medium was inoculated with a glycerol stock of HB101 or BL21 *E. coli* strains and incubated overnight in a shaker (200 rpm) at 37°C.

The next day, this culture was used to inoculate 250 ml sterile LB medium. The culture growth at 37°C and 200 rpm was observed to determine the mid-exponential growth phase, which is most suitable to make cells competent

When the optical density of the cell culture measured at 595 nm had reached about 0.4 – 0.5, the cultures were cooled on ice and centrifuged at 3.000 x g for 10 min at 4°C. The pellet was resuspended in 100 ml ice-cold sterile $CaCl_2$ solution (60 mM $CaCl_2$, 15 % glycerol, 10 mM PIPES, pH 7) and spun down at 3.000 x g for 10 min at 4°C. The resuspension and centrifugation step was repeated and the pellet was finally resuspended in 10 ml of ice-cold sterile $CaCl_2$ solution. The competent cells were aliquoted into prechilled tubes, snap-frozen in liquid nitrogen and stored at – 80°C.

### 5.1.10 Transformation

In the context of molecular biology, transformation is the genetic modification of a bacterium by the uptake and incorporation of exogenous DNA. Thus a foreign plasmid or a ligation product can be inserted into bacteria. The host cells will then replicate the foreign DNA along with their own. The condition is that the plasmid DNA that entered the cell must contain an origin of replication recognized by the host cell DNA polymerases. Plasmids used for transformation experiments usually also contain a gene conferring resistance to an antibiotic that the intended recipient bacterial strain is sensitive to. The selection of cells which have been transformed by the plasmid is then achieved by the ability to grow on media containing this antibiotic.

Transformation of plasmid DNA into $CaCl_2$-competent *E. coli* was performed using the heat shock method. 5 µl of ligation mixtures were added into 100 µl *E. coli* HB101 competent cells and the mixtures were incubated for 30 min on ice water. Subsequently the heat-shock step at 42°C for 90 sec in a heat block was carried out, directly followed by 3 min incubation on ice water. The heat-shock step causes depolarisation of the cell membrane treated with $CaCl_2$. The decreased membrane potential may reduce the negatively charged environment inside the cell and support the movement of negative DNA through the cell membrane. A subsequent cold-shock restores the membrane potential back to its original condition. After this, 500 µl of 37°C warm LB medium was added and the mixtures were incubated at 37°C under shaking for one hour and plated on agar plates containing kanamycin at a concentration of

25 µg/ml. The agar plates were left for approximately 30 min to soak up the medium and then incubated overnight with the bottom up at 37°C.

### 5.1.11 Picking colonies, culturing and PCR

An appropriate volume of LB medium with kanamycin (25 µg/ml, LB+KAN) was prepared. The clones grown were picked (2-3 colonies per construct) with a sterile tip and used for inoculating 500 µl of LB+KAN medium. These inoculated solutions served as precultures for later bigger cultures for plasmid preparation. The lids of the eppendorf tubes were perforated to allow for oxygenation and the cultures were incubated overnight at 37°C in a shaker. To check for the correct insertion of fragments into the vector during ligation, a PCR was run. As a template 1 µl from 500µl overnight precultures was taken. 1 µl of pET-15b(+) vector with incorporated CBR3 (provided by Yasser El-Hawari) sequence or 1 µl of CBR1 incorporated in pET-28b(+) (provided by Claudia Staab) were taken as a positive control. 5´- CBR3 and 3´- CBR3 fragments served as primers for CBR3 mutants, 5´- CBR1 and 3´- CBR1 primers were used for CBR1 mutants (for primer sequences see Table 8). The composition of the master mix for the reaction volume of 20 µl per reaction and PCR conditions were kept the same as listed in Tables 1 and 2.

Table 8: Sequences of primers used for PCR

| primer | sequence of the primer |
|---|---|
| 5´- CBR3 | ATGTGCTCCTGCAGCCGGGTG |
| 3´- CBR3 | CCAGTTTTGCACAACTTTGTC |
| 5´- CBR1 | ATGTCGTCCGGCATCCAT |
| 3´- CBR1 | TCACCACTGTTCAACTCTCTTCTC |

### 5.1.12 Plasmid preparation

Plasmids were purified according to the QIAGEN Plasmid Midi Protocol. 100 ml LB + KAN was inoculated with 100 µl of overnight precultures and cells were grown overnight at 37°C under shaking. After that, the bacterial cells were harvested by centrifugation at 6.000 x g for 15 min at 4°C. The pellets were resuspended in 4 ml Buffer P1. 4 ml of Buffer P2 were added; the solutions were mixed and incubated 5 min at room temperature. In the next step 4 ml of prechilled Buffer P3 were added followed by 15 min incubation and centrifugation at 20.000 x g for 30 min at 4°C. Supernatants containing plasmid DNA were removed promptly, centrifuged again at 20.000 x g for 15 min at 4°C and applied to the QIAGEN-tips 100 previously equilibrated with 4 ml of Buffer QBT. The QIAGEN-tips were washed with 2 x 10 ml of Buffer QC. DNA was eluted with 5 ml Buffer QF, precipitated by 3.5 ml of room temperature isopropanol and subsequently centrifuged at 15.000 x g for 30 min at 4°C. DNA pellets were washed with 2 ml of room temperature 70 % ethanol and centrifuged again at 15.000 x g for 10 min at 4°C. Supernatants were removed and the pellets were air-dried for 10 min. Finally the DNA was redissolved in 100 µl of elution buffer (10 mM Tris-HCl, pH 8.5). Concentrations of samples were measured by the GeneQuant II UV spectrophotometer.

### 5.1.13 Rolling circle amplification

The TempliPhi™ DNA Sequencing Template Amplification Kit, which was used in this assay, has been developed specifically to prepare templates for DNA sequencing. The TempliPhi method utilizes bacteriophage ϕ29 DNA isothermal polymerase enzyme to exponentially synthesize multiple copies of circular molecules of DNA templates by rolling circle amplification (RCA) (Nelson, Cai et al. 2002). In RCA, a circle of DNA, random hexamer primers and a polymerase enzyme catalyst converts dNTPs into DNA molecule. Unlike other amplification procedures, RCA produces an amplified product that remains linked to the DNA primer (Nallur, Luo et al. 2001). The proofreading activity of ϕ29 DNA polymerase ensures high fidelity of DNA replication. Using this amplification method (Figure 8), picogram amounts of sample are sufficient to obtain microgram quantities of product. Depending on the source of starting material, amplification is completed in 4–18 hours at 30˚C with no need for thermal cycling. The

synthesised DNA can be used directly for sequencing reactions without any need for further purification.

TempliPhi Kit components including sample buffer and reaction buffer were thawed on ice. Volume aliquots corresponding to 1 pg to 10 ng of DNA were added into the tubes containing 5 µl of sample buffer. Samples were denatured at 95°C for 3 min and then cooled to room temperature. The TempliPhi premix was prepared from 5 µl of reaction buffer and 0.2 µl of enzyme mix for each TempliPhi reaction. This premix contains all components necessary to generate the nonspecific amplification product, and must be kept on ice. 5 µl of TempliPhi premix were added to each cooled denatured sample and mixtures were incubate at 30°C for 5-18 hours. The enzyme was heat-inactivated at 65°C for 10 min and cooled to 4°C after.

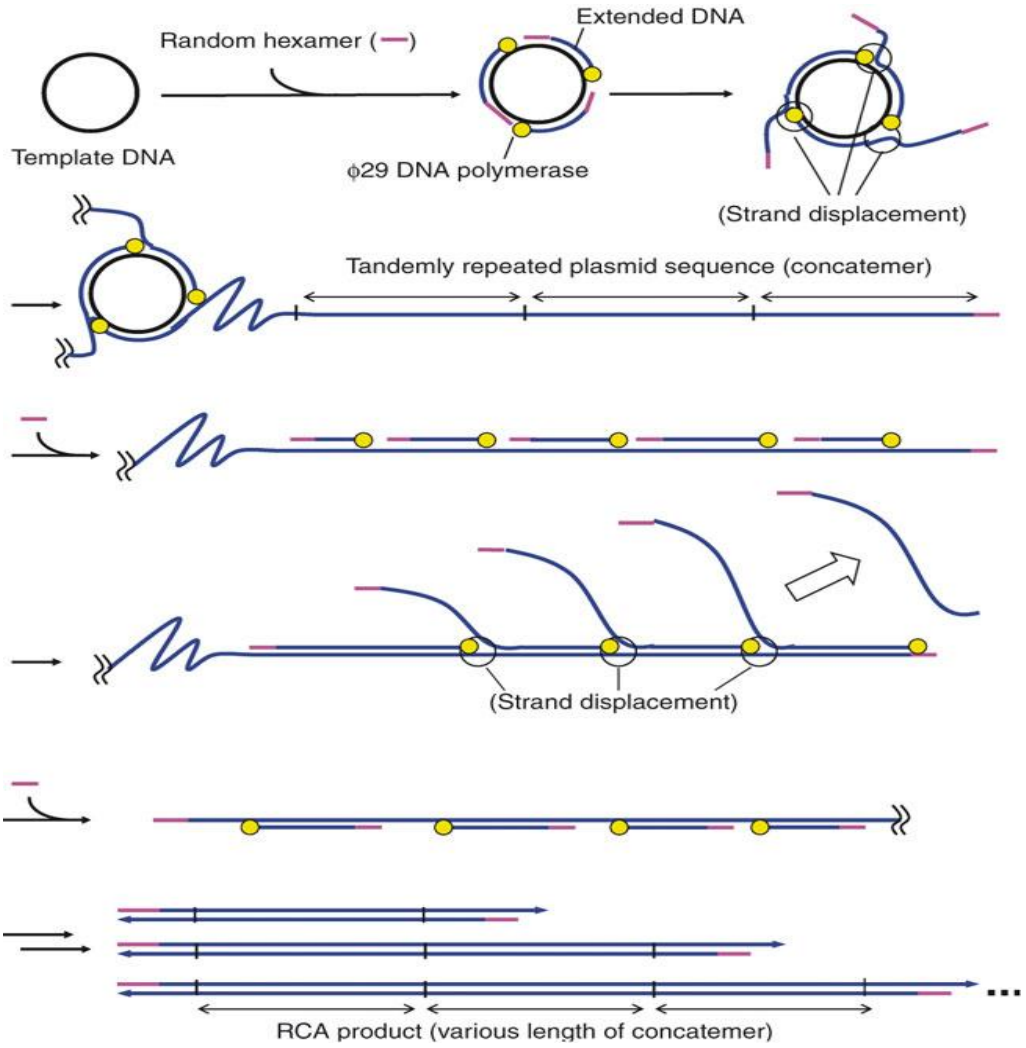


Figure 8: Mechanism of rolling circle amplification
(Fujii, Kitaoka et al. 2006)

### 5.1.14 Sequencing

The plasmid DNA synthesised by RCA was sequenced by the "Institute of Clinical Molecular Biology (ICMB)" in the "University Medical Centre Schleswig-Holstein" or "Eurofins MWG Operon". pLIC forward primer and pLIC reverse primer (see Table 9 for sequences) were used for initiating the reading reaction. The obtained sequences were checked against the known sequences from databases with the "Finch TV" programme (Geospiza). Sequence alignments were made using the bioinformatic tools “Nucleic Acid Sequence Massager” and “ClustalW”. If the complete identity with the corresponding sequence from databases was confirmed, it was used for further experiments.

Table 9: Sequences of primers used for sequencing

| primer | sequence of the primer |
|---|---|
| pLIC forward | TGTGAGCGGATAACAATTCC |
| pLIC reverse | AGCAGCCAACTCAGCTTCC |

## 5.2 Overexpression and purification of proteins

### 5.2.1 Overexpression

To overexpress protein in high quantity the lac operon induction method in combination with the pET vector expression system (Novagen) was used. The protein coding sequences were cloned into pET-15b(+) or a slightly modified pET-28b(+) vector which both exhibit the lac operon upstream of the multiple cloning site. In the absence of lactose, a repressor binds to the operator, inhibiting RNA polymerase from transcribing the genes that are under the control of the lac operon. When the inducer, lactose or an analogue, is added, it binds to the repressor and changes the repressor's 3D structure so the repressor is released from the operator and the transcription can start. In the pET vector system, the gene of interest is under the control of a T7 RNA polymerase promoter. When activated, *e.g.* by IPTG, the cells start to synthesise T7 RNA polymerase and the transcription of desired gene proceeds rapidly, followed by protein translation. Both the T7 promoter and the T7 polymerase do not occur naturally

in any procaryotic organism. Most of the pET expression vectors also encode N-terminal 6xHis fusion tags which can be used for further protein purification by immobilized metal affinity chromatography.

The pET-28b(+) and the pET-15b(+) vector expression constructs were transformed into *E. coli* BL21 strain. Because of the different plasmid-coded antibiotic resistances, for pET-28b(+) vector kanamycin-containing (25 µg/ml) agar plates, for pET-15b(+) vector ampicillin-containing (100 µg/ml) agar plates, were used as a culture medium. Clones from the transformation were picked for an inoculation of 5 ml of LB medium containing kanamycin (25 µg/ml) or ampicillin (100 µg/ml). The preparatory cultures were incubated overnight at 37°C in a shaker. These cultures were transferred into 200 ml of prewarmed LB medium containing kanamycin or ampicillin, again at the concentrations mentioned above. For the overexpression an optical density measured at 595 nm of nearly 0.6 is required, therefore the culture was incubated at 37°C until this OD was reached. At this moment 400 µl 0.5 M IPTG were added. The cultures were grown for additional 4.5 hours. After that, the cell cultures were harvested by centrifugation at 6.000 x g for 15 min at 4°C, the supernatant was decanted and the pellets were frozen at -20°C until the next day.

### 5.2.2 Cell lysis

The pellets were thawed 15 min on ice and resuspended in 10 ml of 10 mM imidazol buffer (see Table 10). For breaking the bacterial cell walls 10 mg of hen egg white lysozyme was added and the suspension incubated for 30 min on ice. Lysozyme acts by catalyzing the hydrolysis of 1,4-β-linkages in peptidoglycans and chitodextrins in the bacteria cell wall.

Efficient extraction is dependent on disrupting protein interactions to release proteins bound in macromolecular assemblies. Disruption of the cells by sonication was used here. Sonication is the process of converting an electrical signal into a physical vibration. In the solution, this powerful vibration evocates rupture of cells and disintegration of molecules. Since a huge amount of heat is produced, sonication must be performed on ice. Each sample was sonicated on ice 6 times for 10 s at 200 W. After sonication the samples were ultracentrifuged at 100.000 x g for 60 min at 4°C. The resulting supernatants were used for the following purification.

Table 10 : Composition of 10 mM imidazol buffer

| component | concentration | amount |
|---|---|---|
| $NaH_2PO_4$ . $H_2O$ | 20 mM | 2.76 g |
| NaCl | 500 mM | 29.22 g |
| Imidazol | 10 mM | 0.68 g |
| Glycerol 87 % | 10 % | 115 ml |
| $H_2O$ | | *ad* 1.000 ml |

### 5.2.3 Protein purification

Protein purification was achieved by fast protein liquid chromatography (FPLC) using 1 ml Ni-NTA (nickel-nitrilotriacetic acid) affinity. It is based on the high-affinity binding of six consecutive histidine residues (the 6xHis tag) to immobilised nickel ions that allows purification of tagged proteins. Elution was achieved by competition with increasing concentration of imidazol buffer (see Table 11), which binds to Ni-NTA and displaces the tagged protein. An imidazol gradient from 10 - 500 mM in 30 min with a flow rate of 1.1 ml per minute was used. The protein peak was monitored at 280 nm and the peak fraction, eluted approximately at 30 mM imidazol, was collected.

Table 11: Composition of 500 mM imidazol buffer

| component | concentration | amount |
|---|---|---|
| $NaH_2PO_4$ . $H_2O$ | 20 mM | 2.76 g |
| NaCl | 500 mM | 29.22 g |
| Imidazol | 500 mM | 34.04 g |
| Glycerol 85 % | 10 % | 115 ml |
| $H_2O$ | | *ad* 1000 ml |

### 5.2.4 Desalting and buffer exchange

To eliminate all unwanted ions and rebuffer the samples, the GE Healthcare PD-10 Desalting columns containing Sephadex™ G-25 Medium for group separation of high (Mr > 5.000) from low (Mr < 1.000) molecular weight substances, were used. First the columns were equilibrated with approximately 25 ml elution buffer (0.2 M potassium phosphate buffer, pH 7.4 in this case, see Table 12). After that, 2.5 ml of the samples were applied to the column. Finally, the protein was eluted with 3.5 ml of elution buffer.

Table 12: Composition of 1 M potassium phosphate buffer stock solution adjusted to pH 7.4
The solution was prepared from 500 ml of the basic solution and an aliquot of the acid solution needed to achieve pH 7.4.

| | component | amount/volume | pH |
|---|---|---|---|
| acid | 1 M $KH_2PO_4$ | 68.5 g/500 ml | ca 4.2 |
| base | 1 M $K_2HPO_4$ . $3H_2O$ | 114.1 g/500 ml | ca 9.3 |

### 5.2.5 Bradford method for determination of protein concentration

The so-called Bradford assay is based on the observation that the absorbance maximum for an acidic solution of the dye Coomassie Brilliant Blue G-250 shifts from 465 nm to 595 nm when the dye binds to protein residues (Bradford 1976). A series of standard solutions is prepared from a set of protein solutions with known concentrations. The standard values obtained are then used to construct a standard curve to which the sample values measured are compared and the unknown concentrations are determined. As standards six bovine serum albumin (BSA) serial diluted solutions ranging from 0.1 to 1.3 mg/ml (1.25; 1; 0.63; 0.5; 0.31; 0.16) were used.

5 µl of the standard solutions, the blank (0.2 M potassium phosphate buffer, pH 7.4) and the samples were pipetted into a 96-well-plate. To each well 250 µl of Bradford Reagent was added and incubated 5 min at room temperature. The measurement was done at 595 nm with the Tecan spectrophotometer.

### 5.2.6 SDS polyacrylamide gel electrophoresis

Sodium dodecyl sulphate (SDS) polyacrylamide gel electrophoresis (PAGE) is a technique used to separate proteins according to their size. The protein mobility in an electric field is a function of the polypeptide chain length or molecular weight. SDS, an anionic detergent, is used in SDS-PAGE to denature proteins to their primary linearised structure. To break disulphide bond linkages DTT is used. Hence, the protein retention time in the gel solely depends on the molecular mass and is not affected by the proteins' native three-dimensional structures or intrinsic charges. The NuPAGE® Bis-Tris Electrophoresis System was used. It is a neutral pH, discontinuous SDS-PAGE where the neutral pH environment ensures maximum stability of both proteins and gel matrix. Precast gels with a separating gel gradient of 4 – 12 % acrylamide concentration was used. Samples to be run on SDS-PAGE, containing about 2-5 µg of recombinant protein, were heated in the 1x NuPAGE® LDS Sample Buffer at 95°C for 3 min before loading. The Page Ruler ™ Prestained Protein Marker was taken to estimate protein size. Both inner and outer electrophoresis chamber were filled with 1x NuPAGE® SDS Running Buffer. When reducing conditions were required, 500 µl NuPAGE® Antioxidant were added into the inner chamber. The gel was run on constant voltage 200 V for 35 min. 0.02 % Coomassie dissolved in 10 % acetic acid solution was used to stain protein bands. The gel was left in the staining solution from 6 hours to overnight with gentle agitation. After that, the gel was destained in 10 % acetic acid until the background was transparent.

## 5.3 Preparation of GSNO according to Hart

GSNO was prepared according to Hart 1985 by incubating equimolar quantities of glutathione and sodium nitrite in acidified water on ice (Hart 1985). First a 2 N HCl stock solution was prepared by mixing 16.5 ml 37 % HCl with 83.5 ml $H_2O$. 2.5 ml of this solution was added to 5.5 ml $H_2O$ and in this solution 1.54 g (5 mmol) of glutathione was dissolved on ice until an ice-cold clear solution was achieved. In the next step 0.345 g (5 mmol) of $NaNO_2$ was added to this solution, which turned bright red immediately. After 40 min of stirring at 4°C in the cold room the solution was treated with 10 ml of ice-cold acetone and stirred for further 10 min. After the addition of acetone a pale-red precipitation appeared immediately. The precipitate was filtered

off and subsequently rinsed with 5 ml ice-cold water, 3 ml ice-cold acetone and dried overnight in the speedvac. The pink GSNO powder was stored frozen at -20°C. The GSNO purity was checked by measuring absorbance of a presumed 10 mM solution, prepared from 0.017 g of the GSNO dissolved in 5 ml of $H_2O$, at 340 nm. GSNO stock solutions were freshly prepared before each experiment and their concentrations were determined spectrophotometrically by absorbance at 340 nm, using the extinction coefficient 840 $M^{-1}$ $cm^{-1}$.

## 5.4 Kinetics

Catalytic properties were determined by measuring the decrease in absorbance at 340 nm. Both NADPH and GSNO absorb at 340 nm and cause change in absorbance due to the enzymatic reaction which is influenced by both substrate consumption and coenzyme utilization (Jensen, Belka et al. 1998). The initial rates were calculated from the absorbance decrease using an additive extinction coefficient of GSNO and NADPH. The extinction coefficient measured at 340 nm is 6.220 $M^{-1}$ $cm^{-1}$ for NADPH and 840 $M^{-1}$ $cm^{-1}$ for GSNO. Thus the additive extinction coefficient is 7.060 $M^{-1}$ $cm^{-1}$. The reaction velocity v was calculated in mol/mg . min, the amount of NADPH consumed in the reaction by 1 mg of enzyme per 1 min, using the equation below. The results were evaluated using Graph Pad Prism.

$$v = \frac{slope \,.\, (-1)}{E_{1M\ 1cm}^{NADPH} \cdot \frac{V_{enzym}}{V_{reaction\ volume}}\ c_{enzym} \,.\, 1000}$$

Equation 1: The reaction velocity v in mol/mg . min, calculated as the amount of NADPH consumed in the reaction by 1 mg of enzyme per 1 min

| | |
|---|---|
| v | reaction velocity in mol/mg . min |
| slope | change in absorbance per minute |
| $E_{1M\ 1cm}^{NADPH}$ | additive extinction coefficient of NADPH and GSNO |
| $V_{enzyme}$ | volume of enzyme |
| $V_{reaction\ volume}$ | reaction volume |
| $c_{enzyme}$ | concentration of enzyme in mg/ml |

A reaction mixture of total volume 1 ml (see Table 13) consisted of varying concentrations of GSNO ranging from 25 µM to 600 µM (minimum of 10 different concentrations) as substrate, 0.1 mM NADPH (50 µl of 2 mM stock solution per

reaction), 1 mM DTPA (diethylene triamine pentaacetic acid, 100 µl of 10 mM stock solution per reaction), 0.1 M potassium phosphate buffer pH 7.4 (500 µl of 0.2 mM stock solution, see Table 12) and enzyme dissolved in potassium phosphate buffer pH 7.4. GSNO and NADPH were prepared fresh before each assay and kept on ice. The exact concentration of the GSNO stock solution was determined spectrophotometrically before each series of measurements using the extinction coefficient of 840 $M^{-1}$ $cm^{-1}$. GSNO was protected from light by wrapping into aluminum foil. A concentration- and time-dependent stability test of GSNO was done. DTPA served as a metal chelator preventing GSNO decomposition in case of the presence of contaminating metal ions. Initial reaction velocities were measured at least three times for each substrate concentration. The reaction temperature was held constant at 25°C. Generally, the concentration of the enzyme must be much lower than the concentration of the substrate. In this thesis, a volume of enzyme solution, corresponding to 1 µg of protein (33 nM), was used per reaction. This volume was added to an appropriate volume of the reaction mixture resulting in 1 ml of total volume. A reference cuvette contained the reaction solution with potassium phosphate buffer pH 7.4 instead of the enzyme.

Table 13: Reaction conditions kept during all kinetic measurements

| reaction conditions | stock solution | amount of stock solution used per reaction (µl) |
|---|---|---|
| 0.1 M potassium phosphate buffer | 0.2 M potassium phosphate buffer | 500 |
| 1 mM DTPA | 10 mM DTPA | 100 |
| 0.1 mM NADPH | 2 mM NADPH prepared fresh each time | 50 |
| varying GSNO | 5 mM GSNO prepared fresh each time | varying |
| [E] << [S] | | corresponding to 1 µg of protein |
| | $H_2O$ | *ad* 1 ml |

To determine the kinetic constants, the GraphPad Prism equation for substrate inhibition was used to fit the values measured.

$$y = \frac{V_{max} \,.\, x}{K_m \,+\, x \,.\left(1 + \frac{x}{K_i}\right)}$$

Equation 2: The reaction rate calculated using the GraphPad Prism equation for substrate inhibition

| | |
|---|---|
| y | reaction rate (mol/mg . min) |
| x | the substrate concentration (µM) |
| $V_{max}$ | the maximum enzyme velocity (mol/mg . min) |
| $K_m$ | the Michaelis-Menten constant, corresponding to the substrate concentration of ½ $V_{max}$ (µM) |
| $K_i$ | the dissociation constant for substrate binding where two substrates can bind to an enzyme (µM) |

From the values obtained from GraphPad Prism, the $k_{cat}$ constant, determining the number of molecules of the substrate converted by an enzyme per minute and the $k_{cat}/K_m$ constant, determining the enzyme efficiency, were calculated.

$$k_{cat} = \frac{V_{max}}{c_{enzyme}\,(mol/l)} \quad (min^{-1})$$

Equation 3: The $k_{cat}$ constant calculation
$K_{cat}$ defines the number of substrate molecule each enzyme site converts to product per minute.

To calculate the molar enzyme concentration used in the equation for $k_{cat}$ determination the following equation was used.

$$c_{enzyme}(mol/l) = \frac{c_{enzyme}\,(mg/ml)}{M}$$

Equation 4: The molar enzyme concentration calculation based upon mass-volume percentage

M indicates the molecular weight including the coding sequence plus additional tag, in Da, which corresponds to the unit g/mol. The molecular weights of all mutants were obtained from the amino acid sequences using "the ExPASy - Prot Param" internet tool.

Table 14: The molecular weights of all mutants expressed from the modified pET-28b(+)vector

| mutant | molecular weight of the CDS + tag (Da) |
|---|---|
| CBR1wt | 32.633 |
| CBR3wt | 32.955 |
| K106Q | 32.954 |
| SUMU | 32.861 |
| 97VA | 32.923 |
| C143S | 32.938 |
| SOE | 32.879 |
| SOE P230W | 32.969 |

## 5.5 Concentrating CBR1

For performing the Saville-Griess assay, a higher concentration of the protein solution was needed. The Amicon® Ultra-4 centrifugal filter device was used to concentrate the samples. The device design incorporates the Millipore Ultracel® low binding membrane, which enables sample recoveries from dilute solutions. These samples can be quickly ultrafiltered, allowing fast separation of solutes from low molecular weight compounds. Up to 4 ml sample was added into the Amicon Ultra filter unit and centrifuged at 7.500 x g until the solution was concentrated ca. 7 times. After that, the exact protein concentration was measured using the Bradford method as described before.

## 5.6 Saville-Griess assay

The Saville-Griess (SG) assay is a method to quantify S-nitrosothiols. The NO-group is cleaved selectively from RS-NO by $Hg^{2+}$ or $Cu^{2+}$ ions. In the Saville reaction, first, due to the affinity of the metal ion to sulphur, a reversible complex between the S-nitrosothiol and the metal ion is formed. This coordination complex weakens the S-N bond which is now susceptible to the nucleophilic attack of water molecules. This attack then yields an equivalent of nitrous acid (Saville 1958). First, the nitrous acid is protonated

$$HONO + H^+ \leftrightarrow NO^+ + H_2O$$

and the originated reactive nitrosonium ion is used in the formation of an azo dye from sulphanilamide and N-1-naphthylethylenediamine (see Figure 9). The azo dye which has developed in this reaction is detected spectrophotometrically at 540 nm by means of a colour reaction (Griess 1879). In this work $Cu^{2+}$ ions were used, which provide the same result as $Hg^{2+}$ ions, but are less toxic. The sensitivity is extremely high, for as little as 2 x $10^{-8}$ g equivalents of a thiol in 1 ml of solution can be determined (Saville 1958).

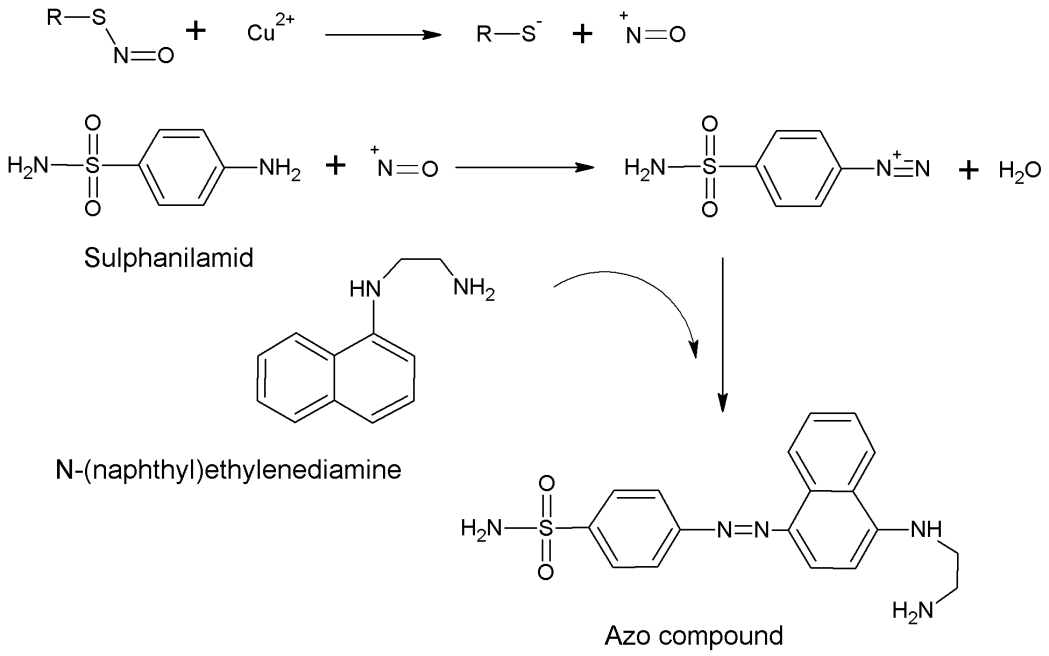


Figure 9: Formation of the azo dye in the Saville-Griess reaction

A CBR1 solution at a concentration of at least 2 mg/ml was incubated in 2 mM GSNO for 2 hours at room temperature. The total reaction volume was up to 2.5 ml at most. As controls solutions without GSNO and CBR1, respectively, were used. After incubating all solutions including the controls were rebuffered via PD10 desalting columns. A mixture of 615 µl of 1.3 % sulphanilamide, 80 µl of N-(naphthyl)ethylenediamine, 80 µl of 25 mM $CuCl_2$ and 25 µl of sample or standard solution (800 µl total volume) was pipetted into eppendorf tubes. For the blank $H_2O$ was used instead of $CuCl_2$. The mixtures were incubated for 15 min at room temperature and the optical density at 540 nm was measured. The standard curve was constructed from 10 GSNO standard solutions of the concentrations 0, 10, 20, 40, 60, 80, 100, 150, 200, 250 µM. All standard solutions were measured in duplicates. The

samples and both controls without GSNO or CBR1 were measured in triplicates. Two independent measurements were done.

In addition to the Saville-Griess assay the enzymatic activity with 100 µM GSNO was determined with all samples (as described under "Kinetics").

## 5.7 Treatment with dithiothreitol (DTT) and ascorbic acid

To assess the mechanism behind the apparent deactivation of CBR1 by incubation with GSNO (see results) 1.5 ml of the CBR1 and CBR3 solutions at a concentration of ca. 1mg/ml were treated with DTT and ascorbic acid. DTT is a strong reducing agent often used for reduction of disulphide bonds in proteins. Ascorbic acid has a capability to specifically reduce S-nitrosothiols releasing glutathione and oxidised products of NO (Kashiba-Iwatsuki, Yamaguchi et al. 1996).

1.5 ml of the sample (c = ca. 1 mg/ml) was incubated with 30 mM (CBR1 and CBR3) or 100 mM DTT (CBR3), and 10 mM ascorbic acid at room temperature for 2 hours. For more details see Table 15. After incubation enzyme activity with 100 µM GSNO was determined.

Table 15: Treatment of 1.5 ml protein, c = ca 1 mg/ml with DTT and ascorbic acid

| **sample volume 1.5 ml and concentration ca. 1 mg/ml** | **reaction conditions** | **stock solution** | **volume of the stock solution (ml)** | **volume of water (ml)** |
|---|---|---|---|---|
| CBR1 incubated with GSNO in SG | 10 mM ascorbic acid | 50 mM ascorbic acid | 0.5 | 0.5 |
| CBR1 incubated with GSNO in SG | 30 mM DTT | 100 mM DTT | 0.75 | 0.25 |
| CBR3 | 10 mM ascorbic acid | 50 mM ascorbic acid | 0.5 | 0.5 |
| CBR3 | 30 mM DTT | 100 mM DTT | 0.75 | 0.25 |
| CBR3 | 100 mM DTT | 500 mM DTT | 0.5 | 0.5 |

## 5.8 GSNO concentration-dependent inactivation of CBR1

To assess GSNO concentration dependency of the evident inactivation 125 µl of CBR1 at the concentration of about 1 mg/ml was incubated with different concentrations of GSNO ranging from 0 - 2 mM (0; 0.05; 0.1; 0.25; 0.5; 0.75; 1; 1.35; 1.7; 2 mM) for two hours at room temperature. The total reaction volume was 250 µl. The incubated enzyme was rebuffered via PD 10 desalting columns and concentrated via Amicon® Ultra-4 centrifugal filter device to the volume of ca. 0.5 ml. The protein concentration of all samples was measured using the Bradford method (described above) and the enzyme activity with 100 µM GSNO was determined.

## 5.9 DTT concentration-dependent reactivation of GSNO-treated CBR1

As inactivation of CBR1 had been confirmed in the previous assay, attempts were made to reactivate the enzyme by treatment with DTT. CBR1 was incubated with 2 mM GSNO for two hours at room temperature. To avoid spontaneous reactions between GSNO and DTT, the incubated enzyme was rebuffered and concentrated as mentioned above. After that, the inactivated enzyme was subjected to incubation with varying concentrations of DTT (0, 10, 20, 30, 50, 75, 100 mM in 250 µl total reaction volume) for 2 hours at room temperature, again followed by rebuffering and concentrating. The enzyme activity with 100 µM GSNO was determined before and after inactivation with GSNO as well as after treatment with DTT.

## 5.10 His-tag cleavage using the TEV cleavage site of modified pET-28b(+) vector

As mentioned in Methods, for cloning the slightly modified (by Yasser El-Hawari) pET-28b(+) vector was used (see appendix). The modifications consist in the introduction of more restriction endonuclease sites and the incorporation of a TEV (tobacco etch virus) cleavage region (ENLYLQG in our sequence, ENLYFQG in sequences used in literature). This specific TEV cleavage site allows for cleavage of the 6xHis-tag from the purified recombinant protein by the TEV protease enzyme. Together with thrombin, factor IX and enterokinase proteases, the TEV protease is the most

common enzyme used for His-tag removal which is essential in cases, when obtaining the protein in its natural condition without any additional tags *e.g.* for crystallisation or the cases when the His tag interferes with the enzyme activity is required. The advantage of the TEV protease is higher specificity in comparison to other proteases, which can digest the target protein in some cases (Kwon, Choi et al. 2005). Also a broad temperature range, including desired low temperatures (4-37°C) can be used for the TEV cleavage reaction (Polayes, Goldstein et al. 1994). However, the TEV cleavage efficiency is influenced both by the substrate and the tag and the ideal temperatures and enzyme concentration should be tested for every protein (Polayes, Goldstein et al. 1994).

The TEV cleavage conditions for CBR3 were investigated. The assay reaction mixture of total volume 110 µl consisted of 50 µl of CBR3 as a substrate (c = 1 µg/µl) in 100 mM Tris-Cl (pH 8), 1 mM DTT, and 5 µl of the TEV protease (c = 1 µg/µl) kindly provided by Prof. Dr. Axel J. Scheidig (Zoologisches Institut, Zentrum für Biochemie und Molekularbiologie Christian-Albrechts-Universität zu Kiel), together with the CFP-TEV-GFP protein which exhibits a TEV cleavage site. 2 µl of this CFP-TEV-GFP protein (c = 10 µg/µl) were used as a substrate for the positive cleavage control. In addition to substrate the control reaction mixture of a total volume 20 µl contained 2 µl of TEV protease; other conditions were kept the same as explained above. As negative control, a reaction mixture of total volume 105 µl without TEV protease and containing 50 µl of CBR3 was prepared. The mixtures were incubated at room temperature (RT) for 6 hours. Additionally, the temperature of 4°C for CBR3 was used (see Table 16 for the composition of all reaction mixtures).

Table 16: Composition of reaction mixtures used for TEV cleavage
The reactions were incubated for 6 hours; the conditions of all reactions were 100 mM Tris-Cl (pH 8) and 1 mM DTT.
c (CBR3) = 1 µg/µl, c (CFP-TEV-GFP) = 10 µg/µl, c (TEV protease) = 1 µg/µl

| substrate | volume of substrate (µl) | volume of TEV protease (µl) | incubation temperature | total reaction volume (µl) |
|---|---|---|---|---|
| CBR3 | 50 | 5 | RT | 110 |
| CBR3 | 50 | 5 | 4°C | 110 |
| CBR3 as a negative control | 50 | 0 | RT | 105 |
| CFP-TEV-GFP as a positive control | 2 | 2 | RT | 20 |

## 5.11 Confirmation of the TEV cleavage

To confirm the effective TEV cleavage the samples were purified via the QIAexpress Kit based on the Ni-NTA affinity principle. 20 µl of 50 % nickel slurry were added to the samples followed by incubation at 4°C for 30 min under gentle mixing. To pellet the resin the samples were centrifuged for 10 s at 15.000 x g at room temperature. The supernatants were transferred to a fresh tube. In the next step 35 µl of 500 mM imidazol buffer (see Table 11) were added and incubated 15 min to elute the bound protein and then centrifuged for 10 s at 15.000 x g at room temperature. The elution and centrifugation step was repeated and both supernatants were collected in one tube.

To analyze the successful TEV cleavage the supernatants from both steps were loaded on an SDS-PAGE gel as described in “SDS polyacrylamide gel electrophoresis“ chapter. The proteins with cleaved His-tag are not able to bind to nickel containing resin and should be found in the first collected fraction.

# 6 RESULTS AND DISCUSSION

Despite 72 % identity at the amino acid level in the sequence alignment of CBR1 and CBR3 (see Figure 4), these two enzymes exhibit high differences in substrate specificity. In the present thesis we focused on GSNO as a substrate for CBR1 (Bateman, Rauh et al. 2008). We tried to investigate the residues responsible for this property by changing some residues of CBR3 to correspond to CBR1. After that, we determined kinetic properties of the mutants and investigated the observed enzyme inhibition.

## 6.1 Selection of the residues to be changed

The GSH-binding site in CBR1 has been described by Bateman, Rauh et al. 2008. Bateman´s group had previously managed to crystallise CBR1 with its inhibitor OH-PP (hydroxy-1-*tert*-butyl-3-phenyl-1H-pyrazolo[3,4-d]pyrimidin-4-amine) and NADP (Tanaka, Bateman et al. 2005). For the structure determination of the CBR1*GSH complex they introduced GSH into the CBR1*OH-PP*NADP crystals using soaking experiments. The structure analysis confirmed the GSH bound in the CBR1 complex with OH-PP and NADP which allowed for characterisation of the GSH binding site (Bateman, Rauh et al. 2008).

Inspired by the results of this structure analysis, some residues were selected for directed mutagenesis in CBR3 to correspond to CBR1. Bateman *et al.* described only one side chain interaction between GSH and CBR1, namely the interaction between the α-amine of GSH and glutamine at the position 106 in the sequence. Thus we decided to change this position in CBR3, a lysine, to glutamine. Furthermore, the residues 97Ser and 98Asp of CBR3 were mutated to 97Val and 98Ala found in CBR1. These residues were chosen because Bateman *et al*. had found out, that the glutamyl carboxylate of GSH is anchored to the 97Val NH group (Bateman, Rauh et al. 2008). The other mutant, called SUMU in this thesis, includes more residues changed. El-Hawari, Favia et al, (2009) have described a relatively big influence of the changed residues in this mutant for catalytic activity with isatin and 9,10-phenanthrenequinone as substrates (for the positions changed see Table 6). Also two other mutants, SOE and SOE P230W, were described by the mentioned authors (El-Hawari, Favia et al. 2009). All three

variants include the change in the sequence at the positions 236-244, which is one of the few regions revealing low sequence similarity in an alignment of CBR1 and CBR3 (see Figure 4). Moreover the Trp230 of CBR1, is, as mentioned in the theoretical part, one of the two amino acids coded by a triplet differing in all three bases and, moreover, is located close to the cofactor in the three-dimensional structure. Finally, the last residue changed in the CBR3 sequence was Cys143 changed to Ser. This change was done in order to break a putative disulphide bond between the Cys at the position 226 or 227 and the Cys143. More details about this change will be discussed later. The changed positions of all mutants are shown in Figure 10.

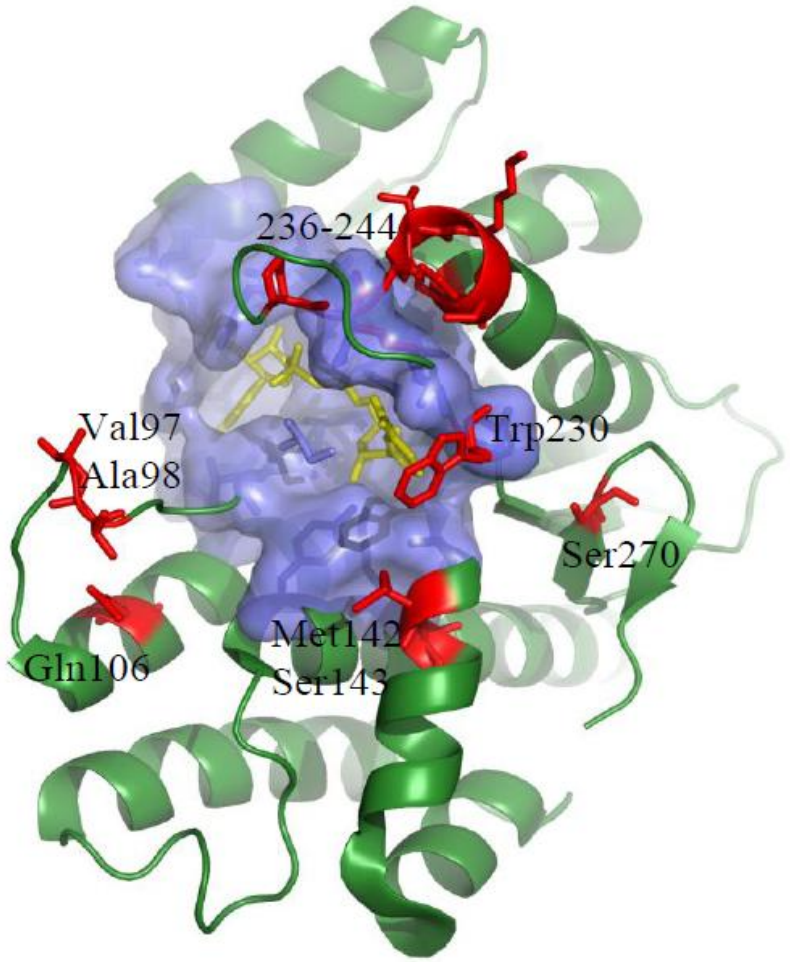


Figure 10: The crystal structure of CBR3 with the changed residues created in PyMOL
The changed residues are shown in red, the NADP cofactor in yellow, in blue is displayed the surface of amino acids surrounding the cofactor at a distance of 5 Ångström (1 Ångström = $10^{-10}$m)

## 6.2 Cloning, overexpression and protein purification

The insertion of the coding sequences for all CBR3 variants (wt, K106Q, 97VA and SUMU) into the pET-28b(+) vector was confirmed by loading the PCR samples from the reaction after ligation and transformation (see chapter 5.1.11) on the agarose gel. The primers used are mentioned in Table 9. The expected size 834 bp agreed well with the location on the gel for all samples. As a positive control the CBR3 coding sequence inserted into the pET-15b(+) vector was used for the PCR reaction.

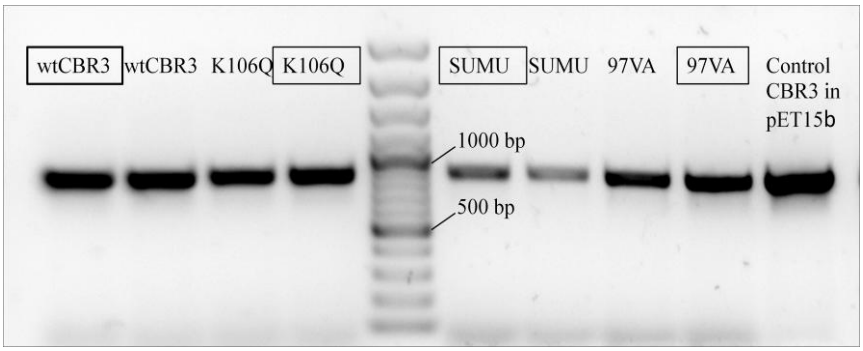


Figure 11: Confirmation of the incorporation of the fragments into the pET-28b(+) vector

The samples framed in Figure 11 were selected for sequencing. However, the sequencing reaction failed in three of four samples sent, probably because of some residual ethanol from the purification to which the sequencing reaction is very sensitive. From then on rolling circle amplification (RCA) was performed to avoid this ethanol contamination. After that, the sequencing reactions were successful and all sequences were confirmed to be correct, using the web-based sequence analysis tools "Nucleic Acid Sequence Massager" and "ClustalW".

During $Ni^{2+}$-affinity-based purification of the His-tagged CBR3 variants, the main protein peak fraction monitored at 280 nm during elution with imidazol was collected. An example of the protein elution is shown in Figure 12. First a minor peak, probably corresponding to some unspecifically bound fraction, appeared followed by the desired protein peak. Except for the 97VA variant, the protein peak looked the same in all variants and all the purifications. The 97VA variant peak was significantly lower, but the reason for this difference was not elucidated.

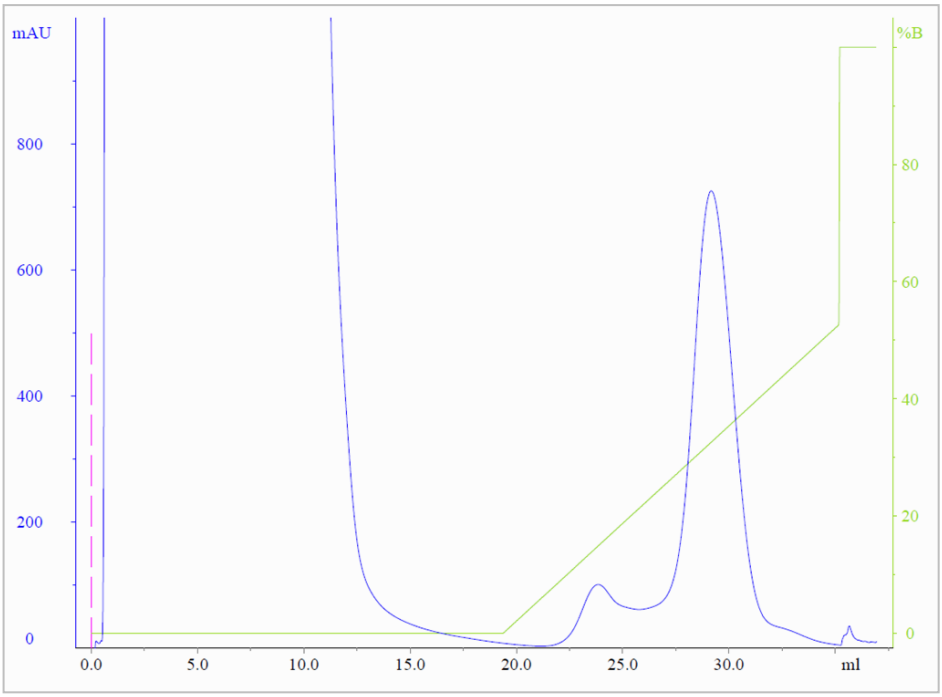


Figure 12: A representative chromatogram of Ni-NTA-based protein purification, here of the SOE mutant.
The blue line indicates absorbance at 280 nm, the green line shows the increasing concentration of imidazol during elution.

After rebuffering to 0.1 M potassium phosphate buffer pH 7.4, the concentration of the proteins was measured using the Bradford method (Bradford 1976). An example of the protein standard curve to which the samples were compared is shown in Figure 13.

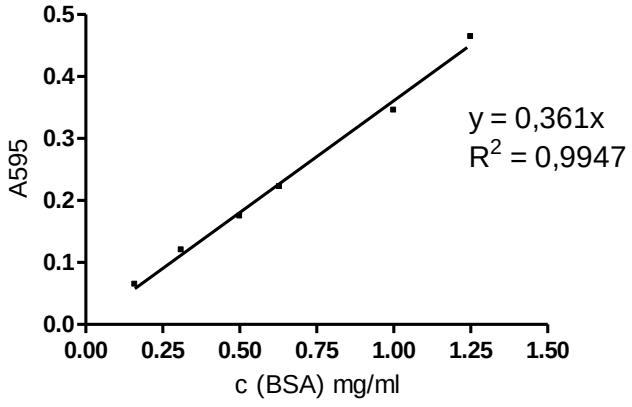


Figure 13: A typical BSA standard curve used for determination of protein concentration

The purity of the proteins was confirmed by SDS-polyacrylamide gel electrophoresis (SDS-PAGE) followed by Coomassie staining of the gel. To check and compare the purification process some samples were loaded both before and after purification (approximately 3 µg of pure protein were loaded). After purification all proteins showed pure single bands. Surprisingly, the location of the 97VA mutant band on the gel was higher than the other bands, indicating a higher molecular weight (Figure 14). Also during purification, the fraction peak of this mutant was much lower in comparison to the other mutants, but the reason for these differences was not clarified.

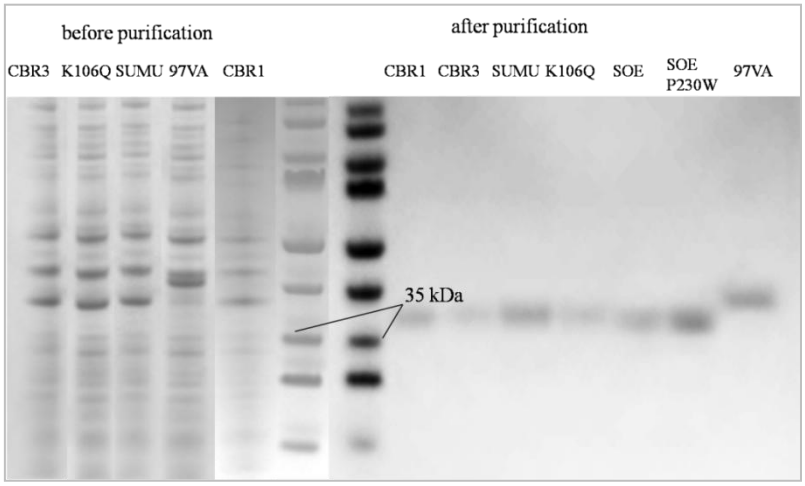


Figure 14: The confirmation of purity of the proteins on the SDS gel stained by Coomassie Samples on the left show not purified fraction after the ultracentrifugation step.

## 6.3 GSNO stability proof

First, GSNO, prepared according to Hart (Hart 1985), was checked for its purity by measurement of a presumed 10 mM solution at 340 nm. This solution was diluted 10 times and the absorbance value of 0.832 was measured. This corresponds to a concentration of 9.9 mM of the undiluted solution and almost 100 % purity. Generally, S-NOs are very unstable substances and are decomposed very quickly. Although GSNO is more stable in comparison to other S-NOs (Singh, Wishnok et al. 1996), a time- and concentration-dependent stability test was done to eliminate any doubts of the substrate interactions in kinetics. As GSNO is a well water-soluble substance, high concentration solutions can be achieved. A set of solutions of GSNO concentrations ranging from 50 – 1.500 µM (9 concentrations) was prepared and the absorbance at 340 nm was measured. A linear dependence was observed, confirming that GSNO is stable at high concentrations (Figure 15).

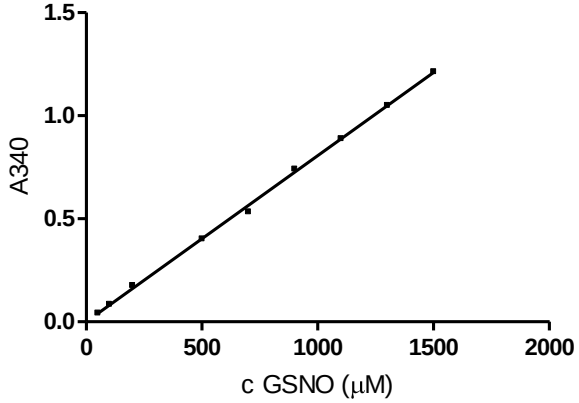


Figure 15: Concentration-dependent GSNO stability proof

In the next step, a time-dependent stability test was performed. The UV spectrum from 200-800 nm of 5 mM GSNO solution was recorded for 2 hours. No changes in absorbance were observed within this time (results not shown).

## 6.4 Kinetic properties of the constructs

The catalytic properties of the successfully overexpressed and purified proteins were determined with GSNO as a substrate. Of all variants, only 3 mutants and CBR1wt showed activity, namely the already mentioned CBR1, SUMU, SOE and SOE P230W. The other mutants including CBR3wt, K106Q and 97VA were inactive towards GSNO. The data from two independent experiments, where initial velocities for each substrate concentration was measured in triplicates, are shown. All the resulting data are summarized in Table 17.

**CBR1** kinetic number 1

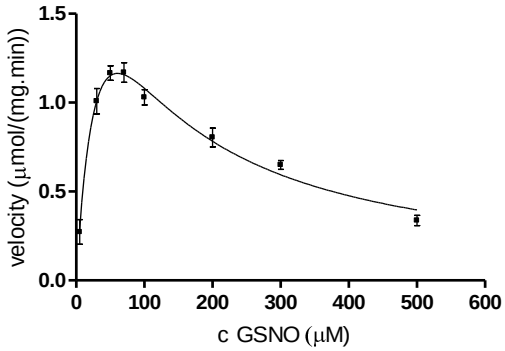


Vmax = 3.0 µmol/(mg.min)
Km = 47 µM
kcat = 97 min-1
kcat/Km = 2.1 (µM.min)-1
Ki = 78 µM

Standard errors
Vmax = 0.63 µmol/(mg.min)
Km = 16.7 µM
Ki = 23.57 µM

**CBR1** kinetic number 2

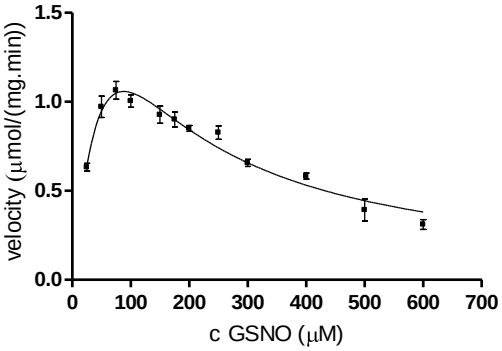


Vmax = 3.7 µmol/(mg.min)
Km = 112 µM
kcat = 122 min-1
kcat/km = 1.1 (µM.min)-1
Ki = 69 µM

Standard errors
Vmax = 1.03 µmol/(mg.min)
Km = 42.83 µM
Ki = 24.09 µM

**SUMU** kinetic number1

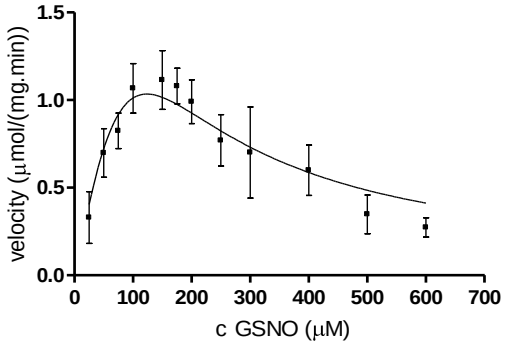


$V_{max}$ = 87.5 µmol/(mg.min)
$K_m$ = 5167 µM
$k_{cat}$ = 2876 $min^{-1}$
$k_{cat}/k_m$ = 0.56 $(\mu M.min)^{-1}$
$K_i$ = 3 µM

Standard errors
$V_{max}$ = 1438 µmol/(mg.min)
$K_m$ = 85831 µM
$K_i$ = 50.03 µM

**SUMU** kinetic number 2

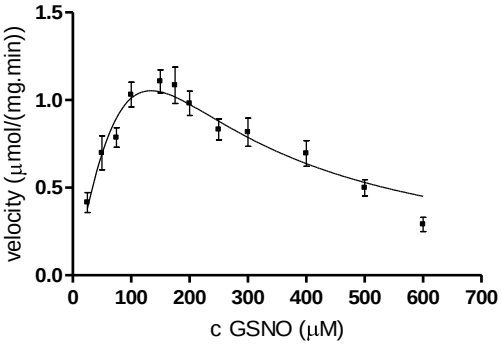


$V_{max}$ = 127 µmol/(mg.min)
$K_m$ = 8000 µM
$k_{cat}$ = 4167 $min^{-1}$
$k_{cat}/k_m$ = 0.52 $(\mu M.min)^{-1}$
$K_i$ = 2.2 µM

Standard errors
$V_{max}$ = 2336 µmol/(mg.min)
$K_m$ = 148531 µM
$K_i$ = 43.84 µM

**SOE** kinetic number1

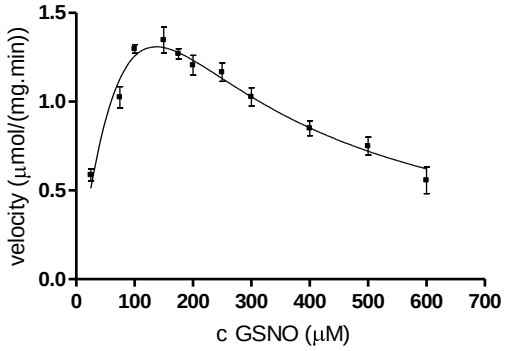


$V_{max}$ = 8.7 µmol/(mg.min)
$K_m$ = 387µM
$k_{cat}$ = 286 $min^{-1}$
$k_{cat}/k_m$ = 0.74 $(\mu M.min)^{-1}$
$K_i$ = 48.5 µM

Standard errors
$V_{max}$ = 5.4 µmol/(mg.min)
$K_m$ = 282.5 µM
$K_i$ = 34.1 µM

**SOE** kinetic number 2

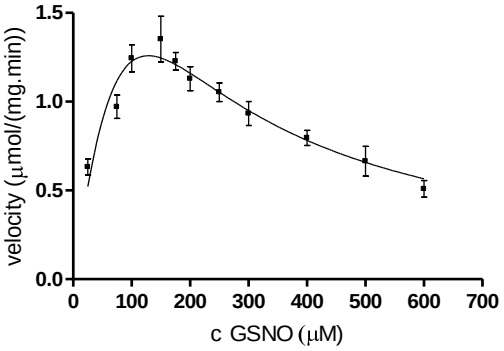


$V_{max}$ = 8.3 µmol/(mg.min)
$K_m$ = 360 µM
$k_{cat}$ = 273 $min^{-1}$
$k_{cat}/k_m$ = 0.75 $(\mu M.min)^{-1}$
$K_i$ = 46 µM

Standard errors
$V_{max}$ = 7.0 µmol/ µM (mg.min)
$K_m$ = 355.2 µM
$K_i$ = 44.6 µM

**SOE P230W** kinetic number 1

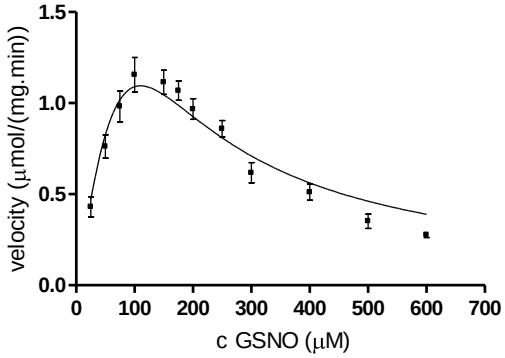


$V_{max}$ = 357 µmol/(mg.min)
$K_m$ = 17887 µM
$k_{cat}$ = 11756 $min^{-1}$
$k_{cat}/k_m$ = 0.66 $(\mu M.min)^{-1}$
$K_i$ = 0.68 µM

Standard errors
$V_{max}$ = 16219 µmol/(mg.min)
$K_m$ = 816036 µM
$K_i$ = 32.41 µM

**SOE P230W** kinetic number 2

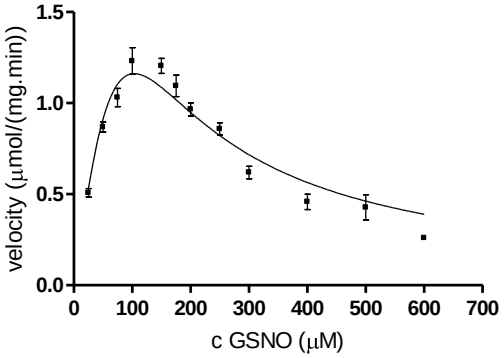


$V_{max}$ = 379 µmol/(mg.min)
$K_m$ = 16834 µM
$k_{cat}$ = 12508 $min^{-1}$
$k_{cat}/k_m$ = 0.74 $(\mu M.min)^{-1}$
$K_i$ = 0.64 µM

Standard errors
$V_{max}$ = 15056 µmol/(mg.min)
$K_m$ = 669911 µM
$K_i$ = 26.29 µM

Table 17: Comparison of kinetic parameters for the mutants with detected activity towards GSNO
The model of substrate inhibition was used for data evaluation. $R^2$ is a measure of the goodness of the fit.

| | **Measurement number 1** | | | | | **Standard errors** | | |
|---|---|---|---|---|---|---|---|---|
| | $K_m$ (μM) | $k_{cat}$ ($min^{-1}$) | $k_{cat}/K_m$ ($(\mu M.min)^{-1}$) | $K_i$ (μM) | $R^2$ | $V_{max}$ (μmol/ (mg.min)) | $K_m$ (μM) | $K_i$ (μM) |
| CBR1 | 47 | 97 | 2.1 | 78 | 0.94 | 0.63 | 16.7 | 23.57 |
| SUMU | 5167 | 2876 | 0.56 | 3 | 0.78 | 1438 | 85831 | 50.03 |
| SOE | 387 | 286 | 0.74 | 48.5 | 0.90 | 5.4 | 282.5 | 34.1 |
| SOE P230W | 17887 | 11756 | 0.66 | 0.68 | 0.87 | 16219 | 816036 | 32.41 |

| | **Measurement number 2** | | | | | **Standard errors** | | |
|---|---|---|---|---|---|---|---|---|
| | $K_m$ (μM) | $k_{cat}$ ($min^{-1}$) | $k_{cat}/K_m$ ($(\mu M.min)^{-1}$) | $K_i$ (μM) | $R^2$ | $V_{max}$ (μmol/ (mg.min)) | $K_m$ (μM) | $K_i$ (μM) |
| CBR1 | 112 | 122 | 1.1 | 69 | 0.91 | 1.03 | 42.83 | 24.09 |
| SUMU | 8000 | 4167 | 0.52 | 2.2 | 0.80 | 2336 | 148531 | 43.84 |
| SOE | 360 | 273 | 0.75 | 46 | 0.82 | 7.0 | 355.2 | 44.6 |
| SOE P230W | 16834 | 12508 | 0.74 | 0.64 | 0.90 | 15056 | 669911 | 26.29 |

In all variants that showed activity, enzyme inhibition starting at a substrate concentration of about 100 μM was observed. The reason for this inhibition was investigated and will be explained later; first the kinetic parameters of the mutants will be discussed. To compare and determine the kinetic constants, non-linear regression analysis in GraphPad Prism was performed, using the model of substrate inhibition, explained in more detail in the Material and methods section. The calculated standard errors obtained with this model were very high in two cases (SUMU and SOE P230W). Either more precise data are needed to obtain a better fit or the model chosen for the calculation is incorrect. Also the $R^2$ values, describing the quality of the fit, where a value of 1 signifies perfect agreement between the data and the regression curve, indicate that the model of substrate inhibition does not fit our data perfectly. Product inhibition may give a similar result, but this scenario is very unlikely as initial values were measured where the concentration of formed product is very low. However, $R^2$

values from 0.8 to 0.95 may be sufficiently well to compare and discuss the kinetic parameters.

### 6.4.1 CBR1 kinetics

Bateman *et al* reported GSNO as an ideal CBR1 substrate. In our experiments, wild-type CBR1 showed the highest $k_{cat}/K_m$ constant (2.1; 1.1 $(\mu M.min)^{-1}$) and the lowest $K_m$ (47; 112 μM) from all the mutants, which means, that among all variants, CBR1 wt reduces GSNO with the highest efficiency. The comparison of our results and the kinetic constants reported by Bateman *et al*. reveals considerable differences. This can be explained by the fact that this group did not mention any substrate inhibition and thus used the unmodified Michaelis-Menten equation to calculate the kinetic constants. The highest GSNO concentration used in their work was 151 μM. Thus it is possible that only classical Michaelis-Menten kinetics was observed, as we observed the strongest inhibition at concentrations higher than that.

### 6.4.2 Kinetics of the other mutants

Of all prepared CBR3 variants activity was observed in three cases. The mutant called SOE showed the best activity as it reduced GSNO with a $K_m$ of about 400 μM and a $k_{cat}/K_m$-value of about 0.5 $(\mu M.min)^{-1}$. The SOE mutant comprises the mutations at positions 236-244, which showed to be sufficient to activate the CBR3 enzyme for GSNO conversion, as CBR3 wt is inactive towards GSNO. Anyway, the enzyme efficiency never reaches the one of CBR1 wt, indicating that, for GSNO conversion, more residues are important. The addition of the mutation at the position 230 (Pro230Trp) resulting in the SOE P230W mutant increased the $K_m$ and $k_{cat}$ values ca 45 times, the ratio of $k_{cat}/K_m$ and thus the enzyme efficiency was still comparable to the SOE mutant. The lowest, $k_{cat}/K_m$ values were obtained with the SUMU mutant.

Considering that the activity was found only in the constructs comprising the mutation at the positions 236-244, this area, or a part of it, appears to be important for the GSNO activity, although the individual residues responsible for the activity were not identified. The $k_{cat}/K_m$-values of the mutants and the CBR1 wild-type did not vary much and were still comparable. Neither exchanging lysine 106 of CBR3 to glutamine or the

mutations at the 97/98 positions discussed in chapter number 6.1 were sufficient to activate CBR3 towards GSNO.

El-Hawari *et al.* investigated the kinetic properties of the SUMU, SOE and SOE P230W mutants towards isatin and 9,1-phenanthrenequinone as the substrates. This group reported the best enzyme efficiency for the SUMU mutant, followed by the SOE P230W and the SOE mutant (El-Hawari, Favia et al. 2009). The differences in the enzyme efficiency of the three mutants, demonstrated by the $k_{cat}/K_m$ constant, were quite big as can be seen in the Table 18, the SUMU mutant showed even higher efficiency than the CBR1 wt. In comparison, the $k_{cat}/K_m$ values obtained with the GSNO substrate were comparable for the three mutants and reached approximately 30-40 % of the CBR1 wt activity.

Table 18: The kinetic constants for the SOE, SOE P230W and SUMU mutants reported by El-Hawari et al (2009)

| | Isatin | | 9,10-phenanthrenequinone | |
|---|---|---|---|---|
| | $K_m$ (μM) | $k_{cat}/K_m$ ((μM.min)$^{-1}$) | $K_m$ (μM) | $k_{cat}/K_m$ ((μM.min)$^{-1}$) |
| CBR1 wt | 7.8 | 13.5 | 35.4 | 8.9 |
| SOE | 1600 | 0.24 | > 78 | 0.54 |
| SOE P230W | 47 | 5.3 | 56.4 | 5.7 |
| SUMU | 22.5 | 18.9 | 4.3 | 107.9 |

### 6.4.3 Investigation of the inactivity of CBR3 towards GSNO

The obvious inactivation of CBR1 and all other active mutants at higher GSNO concentration led us to the idea that S-nitrosylation or S-glutathionylation of cysteines 226 and/or 227 may be responsible for this inhibiting effect. This would agree with work by Tinguely and Wermuth (1999) in which they identified Cys227 as the only CBR1 cysteine residue involved in the glutathione binding process. The crystal structure of CBR3 (pdb-code 2HRB) suggests a disulphide bond between Cys227 and Cys143. We hypothesized that the presence or absence of this theoretical disulphide bond can play a role in the activity of the enzyme.

To investigate the case where the disulphide bond would be needed for the activity we overexpressed the CBR3 enzyme in the *E.coli* Origami strain, which favours

the generation of disulphide bonds. But the overexpression in Origami cells did not influence the activity and the CBR3 enzyme was still inactive towards GSNO as a substrate.

Considering the opposite theory, where the need of the breakage of the already created disulphide bond is necessary, we incubated CBR3 with 30 mM and 100 mM DTT. Furthermore, CBR3 was overexpressed and purified under reducing conditions with all the buffers used containing 1 mM DTT. None of these treatments, however, made CBR3 active towards GSNO.

To investigate the possibility of inactivation of CBR3 by this putative disulphide bond by yet another approach, we mutated the cysteine at position 143 to serine. During the mutagenesis and cloning the PCR fragment size was checked on an agarose gel (see Figure 16) and after that the correct mutant sequence was confirmed.

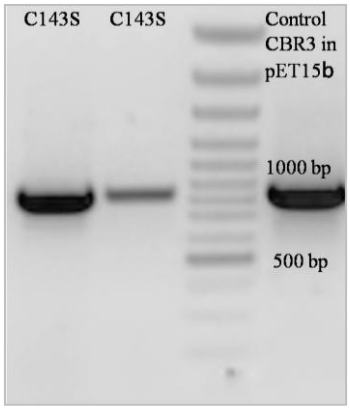


Figure 16: The Cys143Ser fragment size confirmation on the PCR gel

The purified protein was loaded on an SDS-PAGE gel to check the purity (Figure 17).

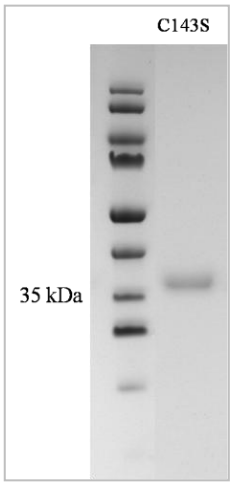


Figure 17: The C143S variant purified protein (Coomassie stain)

However, this CBR3 variant did not display activity towards GSNO either. Hence, presence or absence of the putative disulphide bond between the cysteines at the positions 226 or 227 and 143 is not responsible for the differences in activity between CBR1 and CBR3 towards GSNO as a substrate.

To exclude the possible cysteine modification by S-nitrosylation which can be created in the cells during overexpression, purified CBR3 was incubated in 10 mM ascorbic acid, which would specifically reduce the S-N bonds. Also this experiment did not affect the enzyme's inactivity towards GSNO.

## 6.5 The cause of the enzyme inhibition

To investigate the reason for inactivation of CBR1 at higher GSNO concentrations we considered two possible modifications caused by GSNO, which could inactivate the enzyme. Both of them are common protein modifications and play key roles in metabolism and enzyme regulation *in vivo*. The first possible modification is S-nitrosylation, the second S-glutathionylation; both are described in the theoretical part.

### 6.5.1 Assessment of the mechanism behind inactivation by GSNO

The possible S-nitrosylation of the proteins was checked by performing the Saville-Griess assay (Griess 1879; Saville 1958). The standard curve constructed using GSNO solutions of known concentrations is shown in Figure 18. All measurements were done in duplicates.

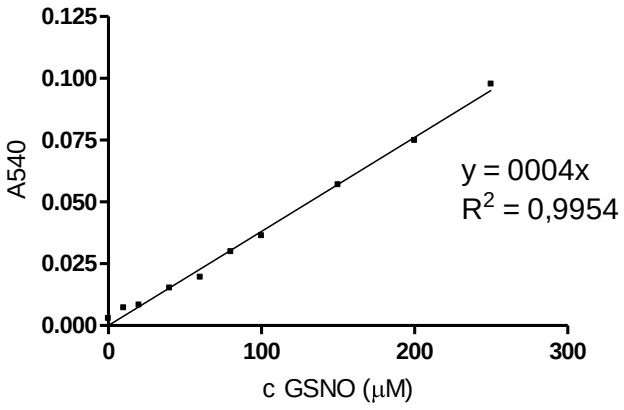


Figure 18: Saville-Griess assay standard curve measured in duplicates

The absorbance values measured with CBR1 incubated with GSNO as a sample and the CBR1 wt as a control were similar. The measurement did not show any significant increase in absorbance of the sample measured at 540 nm in comparison to the controls, signifying no S-nitrosylation. The results from two independent measurements are shown in Table 19.

Table 19: The results obtained by the Saville-Griess assay

| **measurement number** | **sample** | **A540** | **A540 average + standard deviation** |
|---|---|---|---|
| 1 | GSNO | 0.0249<br>0.0342<br>0.0226 | 0.0272 ± 0.0050 |
| | CBR1 | 0.0443<br>0.0416<br>0.0453 | 0.0437 ± 0.0016 |
| | CBR1 + GSNO | 0.0225<br>0.0444<br>0.0619 | 0.0429 ± 0.0161 |
| 2 | GSNO | 0.0343<br>0.0281<br>0.0256 | 0.0293 ± 0.0036 |
| | CBR1 | 0.0347<br>0.0456<br>0.0325 | 0.0376 ± 0.0057 |
| | CBR1 + GSNO | 0.0462<br>0.0494<br>0.0573 | 0.0510 ± 0.0047 |

Nevertheless, the activity measurement of the sample and the control from the Saville-Griess assay measured with 100 μM GSNO as substrate confirmed that CBR1 is really inactivated. The activity of the protein incubated with GSNO was ca 20-fold decreased in comparison to the CBR1 wt used as a control, see Table 20.

Table 20: The inactivation of CBR1 caused by GSNO

| | **Enzyme activity** $\Delta A_{340}$/min*mg of protein |
|---|---|
| CBR1 wt | 0.830 |
| CBR1 incubated with GSNO | 0.048 |

The first indication for S-glutathionylation as the reason behind the enzyme inhibition was that CBR1, which had been inactivated by treatment with GSNO, recovered activity after treatment with DTT (30 mM). The resulting activity was ca. 3 times higher than in the case of the inactivated enzyme, although it did not reach the original CBR1 wt activity (see Table 21).

Finally, also incubation of the GSNO-inactivated protein with ascorbic acid as a reducing agent was performed. As mentioned in "Material and methods", the ascorbic acid has an ability to reduce specifically the S-N bonds of the S-nitrosothiols. This assay did not rescue the enzyme's activity, which was yet another indication that S-nitrosylation is not the cause of the inactivation.

Table 21: The apparent reactivation of the inactivated CBR1 wt caused by the treatment with DTT

| | **Enzyme activity** $\Delta A_{340}$/min*mg of protein |
|---|---|
| CBR1 wt | 0.830 |
| inactivated CBR1 incubated with GSNO | 0.048 |
| inactivated CBR1 treated with DTT | 0.150 |
| inactivated CBR1 treated with ascorbic acid | 0.059 |

This strongly suggests disulphide bonds as the underlying cause of inactivation of CBR1. Next, to study this in more detail, the dose-dependency of inactivation by GSNO as well as of reactivation by DTT was investigated.

### 6.5.2 In- and reactivation of CBR1 by GSNO and DTT

To study the dose-dependency of CBR1 inactivation, the enzyme was treated with different GSNO concentrations for 2 h at room temperature, followed by assessment of enzyme activity. This resulted in the GSNO concentration-dependent inactivation shown in Figure 19. The y-axis defines the enzyme activity, expressed as change in absorbance at 340 nm (slope, $\Delta A$) caused by one milligram of protein per minute. Figure 19 shows an obvious decrease in enzyme activity with increasing GSNO concentrations. The parallel CBR1 wt activity measurement showed activities around 1.8 per milligram of protein per minute and excluded any interferences of the enzyme

stability within the incubation. The experiment was repeated and the results were confirmed (data not shown).

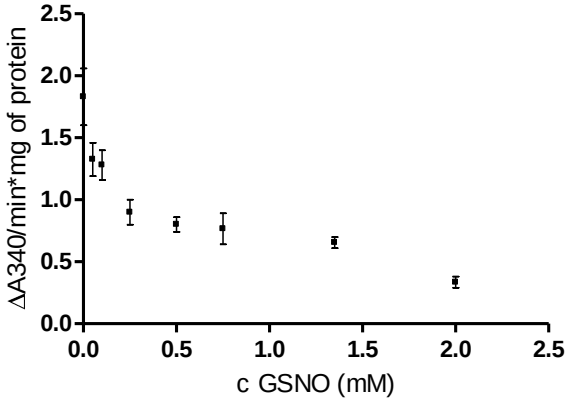


| c (GSNO) [mM] | $\Delta A_{340}$/min*mg of protein (2 measurements) | |
|---|---|---|
| 0 | 1.60 | 2.06 |
| 0.05 | 1.46 | 1.19 |
| 0.1 | 1.40 | 1.16 |
| 0.25 | 1.00 | 0.80 |
| 0.5 | 0.74 | 0.86 |
| 0.75 | 0.64 | 0.89 |
| 1.35 | 0.70 | 0.61 |
| 2 | 0.29 | 0.38 |

Figure 19: The GSNO concentration-dependent inactivation of CBR1
CBR1 was incubated 2 h with different concentrations of GSNO, rebuffered and concentrated. Next, enzyme activity with 100 μM GSNO was measured. The loss of activity is clearly GSNO concentration-dependent.

Also the DTT concentration-dependency of reactivation was assessed. Here, CBR1 first inactivated with 2 mM GSNO was treated with different concentrations of DTT. DTT caused disulphide bond reduction and reactivated the enzyme, which is shown in Figure 20. Also this experiment was repeated and comparable values were measured in both assays (data not shown).

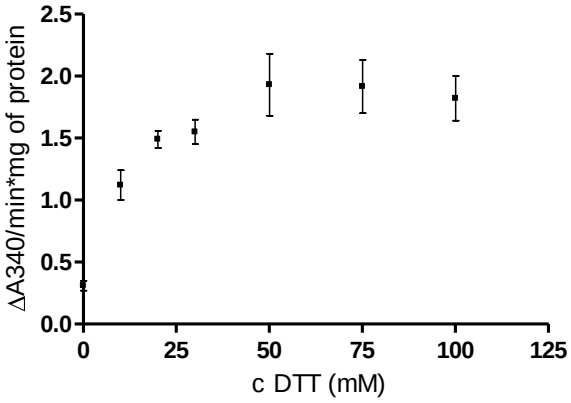


| c (DTT) [mM] | $\Delta A_{340}$/min*mg of protein (2 measurements) | |
|---|---|---|
| 0 | 0.35 | 0.27 |
| 10 | 1.05 | 1.24 |
| 20 | 2.27 | 0.71 |
| 30 | 1.65 | 1.45 |
| 50 | 2.18 | 1.68 |
| 75 | 1.70 | 2.13 |
| 100 | 1.64 | 2.00 |

Figure 20: The DTT concentration dependent reactivation of CBR1
The CBR1 inactivated by the incubation with 2 mM GSNO (2 hours) was reactivated with treating the inactivated CBR1 with different DTT concentrations for 2 hours. After rebuffering and concentrating the enzyme the activity was detected again with 100 μM GSNO.

The two latest experiments confirmed that the enzyme inactivation observed in the kinetic measurements is most likely caused by S-glutathionylation. However, to confirm the S-glutathionylation to 100 %, the modification should be verified by mass spectrometry. The GSNO concentration-dependent enzyme inactivation starts at low GSNO concentrations and the first part of the curve is very steep, which implies that the enzyme is sensitive to relatively low GSNO concentrations. As physiological GSNO concentrations can be as high as 1-10 μM (Gaston, Carver et al. 2003), this indicates a possible physiological role for S-glutathionylation of CBR1 triggered by GSNO.

During reactivation of CBR1 by DTT, maximal CBR1 activity was achieved at a concentration of about 50 mM DTT and stayed stable at higher DTT concentrations up to 100 mM. This reactivation restored CBR1 activity to 100 % of its original activity. However, the role of this modification *in vivo* needs to be investigated in more detail. One possibility to test is, if S-glutathionylation and inactivation of CBR1 is equally caused by the oxidised form of glutathione, GSSG. This would suggest that CBR1 is inactivated during oxidative stress.

### 6.5.3 The position determination of the S-glutathionylated cysteine

The CBR1 amino acid sequence comprises 5 cysteines at positions 26, 122, 150, 226 and 227. Tinguely and Wermuth (1999) mutated all these cysteines to alanines to investigate the involvement of the cysteines in the glutathione binding. Only the Cys227Ala mutant showed a role in glutathione binding. To assess if this cysteine, or Cys 226, are responsible for the inhibition that was revealed in the kinetics, Cys 226 and 227 were changed to Ser by site-directed mutagenesis. The double digested SOE fragments with the desired mutations were cloned into the modified pET-28b(+) vector. However, the sequencing results showed that almost all of the first half of the sequence was missing. The solution of this problem was clarified; unfortunately the CBR1 sequence displayed a restriction site for *Kpn*I which was used for cloning. Therefore the first part of the sequence prior to the *Kpn*I site was cut out (see Figure 21). The restriction sites for *Kpn*I are displayed in yellow; the coding sequence is in bold. More details about the modified vector can be seen in the appendix.

ATGGGCAGCAGCCATCATCATCATCACGAGAACCTGTATCTGCAGGGTACC
CCCGGGATGTCGTCCGGCATCCATGTAGCGCTGGTGACTGGAGGCAACAAGGG
CATCGGCTTGGCCATCGTGCGCGACCTGTGCCGGCTGTTCTCGGGGGACGT
GGTGCTCACGGCGCGGGACGTGACGCGGGGCCAGGCGGCCGTACAGCAGC
TGCAGGCGGAGGGCCTGAGCCCGCGCTTCCACCAGCTGGACATCGACGATC
TGCAGAGCATCCGCGCCCTGCGCGACTTCCTGCGCAAGGAGTACGGGGGCC
TGGACGTGCTGGTCAACAACGCGGGCATCGCCTTCAAGGTTGCTGATCCCAC
ACCCTTTCATATTCAAGCTGAAGTGACGATGAAAACAAATTTCTTTGGTACC
CGAGATGTGTGCACAGAATTACTCCCTCTAATAAAACCCCAAGGGAGAGTGG
TGAACGTATCTAGCATCATGAGCGTCAGAGCCCTTAAAAGCTGCAGCCCAGA
GCTGCAGCAGAAGTTCCGCAGTGAGACCATCACTGAGGAGGAGCTGGTGGG
GCTCATGAACAAGTTTGTGGAGGATACAAAGAAGGGAGTGCACCAGAAGGA
GGGCTGGCCCAGCAGCGCATACGGGGTGACGAAGATTGGCGTCACCGTTCT
GTCCAGGATCCACGCCAGGAAACTGAGTGAGCAGAGGAAAGGGGACAAGAT
CCTCCTGAATGCCTGCTGCCCAGGGTGGGTGAGAACTGACATGGCGGGACC
CAAGGCCACCAAGAGCCCAGAAGAAGGTGCAGAGACCCCTGTGTACTTGGC
CCTTTTGCCCCCAGATGCTGAGGGTCCCCATGGACAATTTGTTTCAGAGAAG
AGAGTTGAACAGTGGTGAGGATCCGAATTCGAGCTCCGTCGACAAGCTTGCGGC
CGCACTCGAGCACCACCACCACCACTGA

Figure 21: The CBR1 sequence with the *Kpn*I restriction site in the middle of the enzyme highlighted

Despite the digestion of the CBR1 coding sequence, it could be seen, that the mutations are implemented correctly as the mutations are located in the second part of the enzyme. The modified pET-28b(+) provides a possibility of using another restriction enzyme, namely *Xma*I, instead of *Kpn*I to clone the fragments into the pET-28b(+) vector. But because of lack of time this was not done and will be a task for the future continuators of the project.

## 6.6 The His-tag cleavage

The His-tag cleavage was done in order to achieve the protein without any additional tags, which is necessary *e.g.* for protein crystallisation, which is one of the future tasks of the project. Moreover, some cases are known where the C- or N-terminal His-tag influences the enzyme activity (Ledent, Duez et al. 1997; Sayari, Mosbah et al. 2007). The temperatures chosen for the His-tag cleavage were room temperature and 4°C. The TEV protease used in this assay, has been shown to work at a

wide temperature range (4°C – 37°C) (Polayes, Goldstein et al. 1994). To assure the enzyme stability, we did not use 37°C but stuck to the above mentioned temperatures.

The His-tag cleavage was confirmed by loading the samples and the control (explained in the chapters 5.10. and 5.11) on an SDS gel (Figure 22).

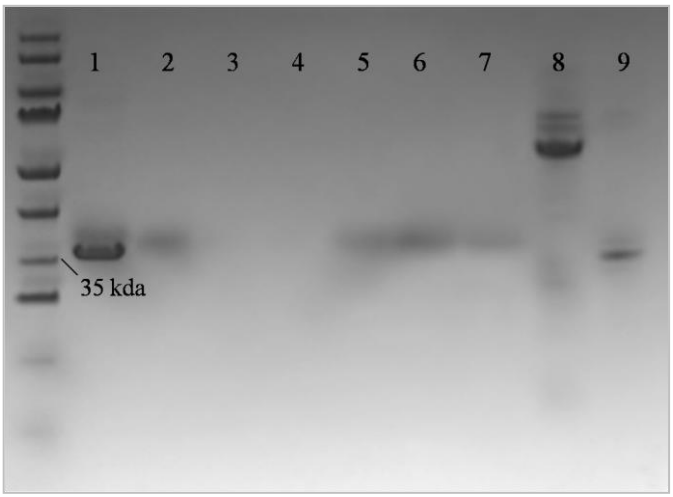


Figure 22: The confirmation of the His-tag cleavage

lane 1: TEV protease + CBR3
lane 2: The unbound protein fraction incubated at room temperature (step 1 in chapter 5.10. and 5.11)
lane 3: The unbound protein fraction incubated at 4°C (step 1 in chapter 5.10. and 5.11)
lane 4: The unbound fraction of uncleaved CBR3 as control
lane 5: The nickel-resin bound fraction incubated at room temperature (step 2 in chapter 5.10. and 5.11)
lane 6: The nickel-resin bound fraction incubated at 4°C (step 2 in chapter 5.10. and 5.11)
lane 7: The nickel-resin bound fraction of uncleaved CBR3 as control
lane 8: The CFP-TEV-GFP positive control - not digested
lane 9: The CFP-TEV-GFP positive control – digested

The His-tag cleavage, shown in Figure 22, was proven by treating the samples with the nickel-containing slurry, which is able to bind only the His-tagged protein. Thus the cleaved protein is not able to bind to the resin and will be found in the first fraction (step 1), the protein which was not cleaved and still contains the His-tag will bind to the resin and will be found in the second fraction after imidazol elution (step 2). The cleavage was successful just in the case of incubation at room temperature (sample 2, lane 2 and lane 5), where the band can be seen in the first unbound protein fraction, as well as in the eluted fraction, signifying that the cleavage was not 100 % and some uncleaved protein was bound to the resin. The digestion at 4°C did not work at all and the protein band could be found in the elution fraction, which is shown on the gel in sample 6. The sample 3 and 7 stands for the control CBR3 (without TEV cleavage)

correctly found in the fraction eluted by imidazol. Number 8 shows the control protein with the TEV cleavage region incorporated in the middle, which was cleaved by TEV protease at room temperature as shown in sample 9.

The result that only the room temperature cleavage worked showed that the cleavage conditions need to be investigated more thoroughly, especially the temperature, the TEV protease amount and the incubation time. All these factors together with the protein structure influence the cleavage efficiency and are specific for each protein.

## 6.7 The physiological relevance of the results obtained

### 6.7.1 S-glutathionylation and its protective role in oxidative stress

Many authors have described the S-glutathionylation as a response to oxidative stress and a link between oxidative stress and protein alteration (Cotgreave and Gerdes 1998). To protect the cell against reactive oxygen species the reversibility of the S-glutathionylation is important and was described in a number of cell types (Schuppe-Koistinen, Gerdes et al. 1994; Seres, Ravichandran et al. 1996). This modification may protect proteins from irreversible oxidation leading to damaged malfunctioning proteins associated with many diseases (Casadei, Persichini et al. 2008). Examples of proteins affected by S-glutathionylation during oxidative stress are creatine kinase, actin, glycogen phosphorylase b, glyceraldehyde-3-phosphate dehydrogenase (GADPH) or HIV-protease.

### 6.7.2 Other enzymes inhibited by GSNO-mediated S-glutathionylation in relation to CBR1

Protein inhibition caused by GSNO-mediated S-glutathionylation is described for some enzymes, *e.g.* the inhibition of glyceraldehyde-3-phosphate dehydrogenase, an $NAD^+$-dependent enzyme involved in glycolysis and gluconeogenesis is specifically caused by GSNO (Mohr, Hallak et al. 1999). The levels of the S-glutathionylated GADPH protein are increased during exposure to oxidative stress and GADPH was identified as the major S-glutathionylated protein in endothelial cells during the

hydrogen peroxide exposition. After removal of the oxidant the enzyme activity was recovered (Schuppe-Koistinen, Moldeus et al. 1994).

Another enzyme inhibited by GSNO-mediated S-glutathionylation is aldose reductase (AKR1B1), converting short- and medium-chain aldehydes to their corresponding alcohols. It is an NADPH-dependent stress related protein and participates in glucose metabolism and osmoregulation. The S-glutathionylated inactive form of the enzyme is formed by the GSNO from exogenously delivered NO and GSH. In contrast, endogenously generated NO causes S-nitrosylation which activates the enzyme. Thus the NO donor can either increase or decrease the enzyme activity (Baba, Wetzelberger et al. 2009).

Thioredoxin (Trx), an enzyme with a wide range of functions *e.g.* in apoptosis, as antioxidant or regulator of transcription factors also can undergo S-glutathionylation resulting in the inactivation of the protein, especially under conditions of oxidative stress (Casagrande, Bonetto et al. 2002). Interestingly, Trx has the ability to break the S-N bond in the GSNO molecule, thus Trx is inhibited by its own substrate as in the case of CBR1. Trx can furthermore autoactivate itself by deglutathionylation (Casagrande, Bonetto et al. 2002). For CBR1 this ability was not investigated.

The physiological relevance of the discovery that CBR1 is inhibited by GSNO at higher concentration needs to be investigated. The major question is, does the S-glutathionylation observed *in vitro* take place *in vivo*? Physiological GSNO levels are 1-10 μM (Gaston, Carver et al. 2003); here, however, the effect of concentrations below 50 μM was not assessed. Nevertheless, when GSNO concentration-dependent inactivation of CBR1 was assessed, inhibition was evident from the lowest GSNO concentration which suggests that *in vivo* S-glutathionylation of CBR1 is possible. Here another question arises. Would the oxidised form of GSH, GSSG, be able to S-glutathionylate CBR1? And if yes, will the modification be reversible or not? This will be the tasks for the future project continuators to investigate.

The physiological significance of CBR1 S-glutathionylation may lie in the protection of the enzyme from irreversible damage during oxidative stress by the formation of a reversible mixed-disulphide as mentioned above and CBR1 would be inactivated by oxidative stress. During oxidative stress, the level of NO, which is needed for GSNO formation, is increased. Another question worth addressing might be

whether the redox state of the cell determined by the ratio of [GSH]/[GSSG] may influence enzyme activation/inactivation via GSNO formation from GSH and NO.

## 6.8 The role of CBR1 in GSNO metabolism and the redox state of the cell

The fact, that CBR1 metabolises GSNO was unknown until 2008, when Bateman *et al* detected the ability of CBR1 to metabolise GSNO. Before discovering this, only ADH3, already mentioned in the theoretical part, was known to regulate endogenous levels of GSNO by reduction using NADH as a cofactor and thus regulating the dynamic equilibrium between GSNO and S-nitrosylated proteins (Jensen, Belka et al. 1998; Liu, Hausladen et al. 2001; Staab, Hellgren et al. 2008). Cofactor requirement often reflects the role of enzymes in the normal redox state of the cell. In contrast to NADPH-dependent CBR1, ADH3 requires NADH as the cofactor. The redox state of the cell is determined by the ratio of these two cofactors and its reduced/oxidised forms. In the cell environment the $NADPH/NADP^+$ ratio is about 100 while the $NADH/NAD^+$ form is about 1/700, which shows the different functions of these two cofactors (Ido 2007; Ying 2008). Hence, as ADH3 requires NADH for GSNO reduction, which is scarce in the cell, CBR1 might play a more important role in physiological GSNO reduction as it uses the much more available cofactor NADPH.

## 6.9 Possible effects of the S-glutathionylation of CBR1 on the quinone-reducing activity

CBR1 is able to metabolise a wide spectrum of endogenous and exogenous substrates, namely prostaglandins, steroids, lipid aldehydes, aromatic aldehydes and ketones, quinones and NNK. The quinone reducing activity enables to reduce quinone-containing substances and thus to excrete them. The docking experiments done by El-Hawari *et al* showed the H-bond interaction of the quinone substrate and the tyrosine 194 of the enzyme. This H-bond was situated between the Trp230 and Met 142 in the catalytic cleft. Moreover this author group highlighted the importance of the Trp 230 (El-Hawari, Favia et al. 2009).

To investigate if S-glutathionylation of CBR1 would affect CBR1-mediated quinone reduction, it can be speculated that, considering that Cys 227 (or Cys 226) is

the most promising candidate for S-glutathionylation, the enzyme activity may not be affected as, until now, there are no references of those cysteines and its role in CBR1-mediated quinone reduction. But first of all the Cys residue, responsible for the enzyme inactivation, must be determined.

## 6.10 Summary of the results

In the present thesis some residues of CBR3 were changed to correspond to CBR1 by site-directed mutagenesis. After the successful cloning of the fragments, comprising the desired changes in the sequence, the catalytic properties of the wild type of both CBR1 and CBR3 enzymes together with the mutants were investigated. It was found out that wild-type CBR3 was inactive *in vitro* towards GSNO as a substrate. The CBR3 mutants comprising changes at the positions 236-244 (SUMU, SOE and SOE P230W) were able to metabolise GSNO although the activity did not achieve the CBR1 wild type´s values. The $K_m$ of the mutants varied widely, but the $k_{cat}/K_m$ values of the mutants were comparable and about 3 times lower than those of the CBR1 wild type.

Next it was discovered, that at GSNO concentrations higher than 100 μM CBR1 together with the CBR3 mutants were inhibited. Further experiments put forward S-glutathionylation as the most probable inactivating modification. First S-nitrosylation was excluded performing the Saville-Griess assay and after that S-glutathionylation was indicated by the DTT-caused reactivation of the enzyme. The inactivation was shown to be GSNO concentration-dependent as well as the reactivation by DTT, which resulted in an activity increase up to 100 % of activity of the untreated enzyme.

The next aim of the thesis was to detect the cysteine responsible for the inactivation of CBR1. Unfortunately these experiments were not finished and will be the task for the future project continuators.

# 7 APPENDIX

## 7.1 The pET-28b(+) modified vector

The pET-28b(+) vector modified by Yasser El-Hawari containing TEV cleavage site and HisTag

BglII PstI KpnI XmaI BamHI other restriction sites XhoI
bold underlined: start and stop codon
bold dotted: HisTag
**bold**: TEV cleavage site (Literature: ENLYFQG, our: ENLYLQG)
underlined: coding sequence

AGATCTCGATCCCGCGAAATTAATACGACTCACTATAGGGGAATTGTGAGC
GGATAACAATTCCCCTCTAGAAATAATTTTGTTTAACTTTAAGAAGGAGATA
TACCATGGGCAGCAGCCATCATCATCATCATCAC**GAGAACCTGTATCTGCA**
**GGGT**ACCCCCGGGATG ... coding sequence ... TGAGGATCCGAATTCGAGCTCC
GTCGACAAGCTTGCGGCCGCACTCGAGCACCACCACCACCACCACTGA

## 7.2 The sequences of the mutants

### CBR1 (in the pET-28b(+) vector)

ATGGGCAGCAGCCATCATCATCATCATCACGAGAACCTGTATCTGCAGGGTACCCCCGGG
ATGTCGTCCGGCATCCATGTAGCGCTGGTGACTGGAGGCAACAAGGGCATCGGCTTGGCCAT
CGTGCGCGACCTGTGCCGGCTGTTCTCGGGGGACGTGGTGCTCACGGCGCGGGACGTGACGC
GGGGCCAGGCGGCCGTACAGCAGCTGCAGGCGGAGGGCCTGAGCCCGCGCTTCCACCAGCT
GGACATCGACGATCTGCAGAGCATCCGCGCCCTGCGCGACTTCCTGCGCAAGGAGTACGGG
GGCCTGGACGTGCTGGTCAACAACGCGGGCATCGCCTTCAAGGTTGCTGATCCCACACCCTT
TCATATTCAAGCTGAAGTGACGATGAAAACAAATTTCTTTGGTACCCGAGATGTGTGCACAG
AATTACTCCCTCTAATAAAACCCCAAGGGAGAGTGGTGAACGTATCTAGCATCATGAGCGTC
AGAGCCCTTAAAAGCTGCAGCCCAGAGCTGCAGCAGAAGTTCCGCAGTGAGACCATCACTG
AGGAGGAGCTGGTGGGGCTCATGAACAAGTTTGTGGAGGATACAAAGAAGGGAGTGCACCA
GAAGGAGGGCTGGCCCAGCAGCGCATACGGGGTGACGAAGATTGGCGTCACCGTTCTGTCC
AGGATCCACGCCAGGAAACTGAGTGAGCAGAGGAAAGGGGACAAGATCCTCCTGAATGCCT
GCTGCCCAGGGTGGGTGAGAACTGACATGGCGGGACCCAAGGCCACCAAGAGCCCAGAAG
AAGGTGCAGAGACCCCTGTGTACTTGGCCCTTTTGCCCCCAGATGCTGAGGGTCCCCATGGA
CAATTTGTTTCAGAGAAGAGAGTTGAACAGTGGTGA

**CBR3 (in the pET-28b(+) vector)**

ATGGGCAGCAGCCATCATCATCATCATCACGAGAACCTGTATCTGCAGGGTACC
ATGTCGTCCTGCAGCCGCGTGGCGCTGGTGACCGGGGCCAACAGGGGCATCGGCTTGGCCAT
CGCGCGCGAACTGTGCCGACAGTTCTCTGGGGATGTGGTGCTCACCGCGCGGGACGTGGCGC
GGGGCCAGGCGGCCGTGCAGCAGCTGCAGGCGGAGGGCCTGAGCCCGCGCTTCCACCAACT
GGACATCGACGACTTGCAGAGCATCCGCGCCCTGCGCGACTTCCTGCGCAAGGAGTACGGG
GGGCTCAATGTACTGGTCAACAACGCGGCCGTCGCCTTCAAGAGTGATGATCCAATGCCCTT
TGACATTAAAGCTGAGATGACACTGAAGACAAATTTTTTTGCCACTAGAAACATGTGCAACG
AGTTACTGCCGATAATGAAACCTCATGGGAGAGTGGTGAATATCAGTAGTTTGCAGTGTTTA
AGGGCTTTTGAAAACTGCAGTGAAGATCTGCAGGAAAGGTTCCACAGTGAGACACTCACAG
AAGGAGACCTGGTGGATCTCATGAAAAAGTTTGTGGAGGACACAAAAAATGAGGTGCATGA
GAGGGAAGGCTGGCCCAACTCACCTTATGGGGTGTCCAAGTTGGGGGTCACAGTCTTATCGA
GGATCCTGGCCAGGCGTCTGGATGAGAAGAGGAAAGCTGACAGGATTCTGGTGAATGCGTG
CTGCCCAGGACCAGTGAAGACAGACATGGATGGGAAAGACAGCATCAGGACTGTGGAGGA
GGGGGCTGAGACCCCTGTCTACTTGGCCCTCTTGCCTCCAGATGCCACTGAGCCACAAGGCC
AGTTGGTCCATGACAAAGTTGTGCAAAACTGGTAA

**K106Q (in the pET-28b(+) vector)**

ATGGGCAGCAGCCATCATCATCATCATCACGAGAACCTGTATCTGCAGGGTACC
ATGTCGTCCTGCAGCCGCGTGGCGCTGGTGACCGGGGCCAACAGGGGCATCGGCTTGGCCAT
CGCGCGCGAACTGTGCCGACAGTTCTCTGGGGATGTGGTGCTCACCGCGCGGGACGTGGCGC
GGGGCCAGGCGGCCGTGCAGCAGCTGCAGGCGGAGGGCCTGAGCCCGCGCTTCCACCAACT
GGACATCGACGACTTGCAGAGCATCCGCGCCCTGCGCGACTTCCTGCGCAAGGAGTACGGG
GGGCTCAATGTACTGGTCAACAACGCGGCCGTCGCCTTCAAGAGTGATGATCCAATGCCCTT
TGACATTCAGGCTGAGATGACACTGAAGACAAATTTTTTTGCCACTAGAAACATGTGCAACG
AGTTACTGCCGATAATGAAACCTCATGGGAGAGTGGTGAATATCAGTAGTTTGCAGTGTTTA
AGGGCTTTTGAAAACTGCAGTGAAGATCTGCAGGAAAGGTTCCACAGTGAGACACTCACAG
AAGGAGACCTGGTGGATCTCATGAAAAAGTTTGTGGAGGACACAAAAAATGAGGTGCATGA
GAGGGAAGGCTGGCCCAACTCACCTTATGGGGTGTCCAAGTTGGGGGTCACAGTCTTATCGA
GGATCCTGGCCAGGCGTCTGGATGAGAAGAGGAAAGCTGACAGGATTCTGGTGAATGCGTG
CTGCCCAGGACCAGTGAAGACAGACATGGATGGGAAAGACAGCATCAGGACTGTGGAGGA
GGGGGCTGAGACCCCTGTCTACTTGGCCCTCTTGCCTCCAGATGCCACTGAGCCACAAGGCC
AGTTGGTCCATGACAAAGTTGTGCAAAACTGGTAA

**SUMU (in the pET-28b(+) vector)**

ATGGGCAGCAGCCATCATCATCATCATCACGAGAACCTGTATCTGCAGGGTACC
ATGTCGTCCTGCAGCCGCGTGGCGCTGGTGACCGGGGCCAACAGGGGCATCGGCTTGGCCAT
CGCGCGCGAACTGTGCCGACAGTTCTCTGGGGATGTGGTGCTCACCGCGCGGGACGTGGCGC
GGGGCCAGGCGGCCGTGCAGCAGCTGCAGGCGGAGGGCCTGAGCCCGCGCTTCCACCAACT
GGACATCGACGACTTGCAGAGCATCCGCGCCCTGCGCGACTTCCTGCGCAAGGAGTACGGG
GGGCTCAATGTACTGGTCAACAACGCGGCCGTCGCCTTCAAGAGTGATGATCCAATGCCCTT
TGACATTAAAGCTGAGATGACACTGAAGACAAATTTTTTTGCCACTAGAAACATGTGCAACG
AGTTACTGCCGATAATGAAACCTCATGGGAGAGTGGTGAATATCAGTAGTTTGATGAGCTTA
AGGGCGTTTGAAAACTGCAGTGAAGATCTGCAGGAAAGGTTCCACAGTGAGACACTCACAG
AAGGAGACCTGGTGGATCTCATGAAAAAGTTTGTGGAGGACACAAAAAATGAGGTGCATGA
GAGGGAAGGCTGGCCCAACTCACCTTATGGGGTGTCCAAGTTGGGGGTCACAGTCTTATCGA
GGATCCTGGCCAGGCGTCTGGATGAGAAGAGGAAAGCTGACAGGATTCTGGTGAATGCGTG
CTGCCCAGGATGGGTGAAGACAGACATGGCGGGACCCAAGGCCACCAAGAGCCCAGAGGA
GGGGGCTGAGACCCCTGTCTACTTGGCCCTCTTGCCTCCAGATGCCACTGAGCCACAAGGCC
AGTTGAACAGTGACAAAGTTGTGCAAAACTGGTAA

**97VA (in the pET-28b(+) vector)**

ATGGGCAGCAGCCATCATCATCATCATCACGAGAACCTGTATCTGCAGGGTACC
ATGTCGTCCTGCAGCCGCGTGGCGCTGGTGACCGGGGCCAACAGGGGCATCGGCTTGGCCAT
CGCGCGCGAACTGTGCCGACAGTTCTCTGGGGATGTGGTGCTCACCGCGCGGGACGTGGCGC
GGGGCCAGGCGGCCGTGCAGCAGCTGCAGGCGGAGGGCCTGAGCCCGCGCTTCCACCAACT
GGACATCGACGACTTGCAGAGCATCCGCGCCCTGCGCGACTTCCTGCGCAAGGAGTACGGG
GGGCTCAATGTACTGGTCAACAACGCGGCCGTCGCCTTCAAGGTTGCTGATCCAATGCCCTT
TGACATTAAAGCTGAGATGACACTGAAGACAAATTTTTTTGCCACTAGAAACATGTGCAACG
AGTTACTGCCGATAATGAAACCTCATGGGAGAGTGGTGAATATCAGTAGTTTGCAGTGTTTA
AGGGCTTTTGAAAACTGCAGTGAAGATCTGCAGGAAAGGTTCCACAGTGAGACACTCACAG
AAGGAGACCTGGTGGATCTCATGAAAAAGTTTGTGGAGGACACAAAAAATGAGGTGCATGA
GAGGGAAGGCTGGCCCAACTCACCTTATGGGGTGTCCAAGTTGGGGGTCACAGTCTTATCGA
GGATCCTGGCCAGGCGTCTGGATGAGAAGAGGAAAGCTGACAGGATTCTGGTGAATGCGTG
CTGCCCAGGACCAGTGAAGACAGACATGGATGGGAAAGACAGCATCAGGACTGTGGAGGA
GGGGGCTGAGACCCCTGTCTACTTGGCCCTCTTGCCTCCAGATGCCACTGAGCCACAAGGCC
AGTTGGTCCATGACAAAGTTGTGCAAAACTGGTAA

**C143S (in the pET-28b(+) vector)**

ATGGGCAGCAGCCATCATCATCATCATCACGAGAACCTGTATCTGCAGGGTACC
ATGTCGTCCTGCAGCCGCGTGGCGCTGGTGACCGGGGCCAACAGGGGCATCGGCTTGGCCAT
CGCGCGCGAACTGTGCCGACAGTTCTCTGGGGATGTGGTGCTCACCGCGCGGGACGTGGCGC
GGGGCCAGGCGGCCGTGCAGCAGCTGCAGGCGGAGGGCCTGAGCCCGCGCTTCCACCAACT
GGACATCGACGACTTGCAGAGCATCCGCGCCCTGCGCGACTTCCTGCGCAAGGAGTACGGG
GGGCTCAATGTACTGGTCAACAACGCGGCCGTCGCCTTCAAGAGTGATGATCCAATGCCCTT
TGACATTAAAGCTGAGATGACACTGAAGACAAATTTTTTTGCCACTAGAAACATGTGCAACG
AGTTACTGCCGATAATGAAACCTCATGGGAGAGTGGTGAATATCAGTAGTTTGCAGTCTTTA
AGGGCTTTTGAAAACTGCAGTGAAGATCTGCAGGAAAGGTTCCACAGTGAGACACTCACAG
AAGGAGACCTGGTGGATCTCATGAAAAAGTTTGTGGAGGACACAAAAAATGAGGTGCATGA
GAGGGAAGGCTGGCCCAACTCACCTTATGGGGTGTCCAAGTTGGGGGTCACAGTCTTATCGA
GGATCCTGGCCAGGCGTCTGGATGAGAAGAGGAAAGCTGACAGGATTCTGGTGAATGCGTG
CTGCCCAGGACCAGTGAAGACAGACATGGATGGGAAAGACAGCATCAGGACTGTGGAGGA
GGGGGCTGAGACCCCTGTCTACTTGGCCCTCTTGCCTCCAGATGCCACTGAGCCACAAGGCC
AGTTGGTCCATGACAAAGTTGTGCAAAACTGGTAA

**SOE (in the pET-15b(+) vector)**

ATGGGCAGCAGCCATCATCATCATCATCACAGCAGCGGCCTGGTGCCGCGCGGCAGCCAT
ATGTCGTCCTGCAGCCGCGTGGCGCTGGTGACCGGGGCCAACAGGGGCATCGGCTTGGCCAT
CGCGCGCGAACTGTGCCGACAGTTCTCTGGGGATGTGGTGCTCACCGCGCGGGACGTGGCGC
GGGGCCAGGCGGCCGTGCAGCAGCTGCAGGCGGAGGGCCTGAGCCCGCGCTTCCACCAACT
GGACATCGACGACTTGCAGAGCATCCGCGCCCTGCGCGACTTCCTGCGCAAGGAGTACGGG
GGGCTCAATGTACTGGTCAACAACGCGGCCGTCGCCTTCAAGAGTGATGATCCAATGCCCTT
TGACATTAAAGCTGAGATGACACTGAAGACAAATTTTTTTGCCACTAGAAACATGTGCAACG
AGTTACTGCCGATAATGAAACCTCATGGGAGAGTGGTGAATATCAGTAGTTTGCAGTGTTTA
AGGGCGTTTGAAAACTGCAGTGAAGATCTGCAGGAAAGGTTCCACAGTGAGACACTCACAG
AAGGAGACCTGGTGGATCTCATGAAAAAGTTTGTGGAGGACACAAAAAATGAGGTGCATGA
GAGGGAAGGCTGGCCCAACTCACCTTATGGGGTGTCCAAGTTGGGGGTCACAGTCTTATCGA
GGATCCTGGCCAGGCGTCTGGATGAGAAGAGGAAAGCTGACAGGATTCTGGTGAATGCGTG
CTGCCCAGGACCAGTGAAGACAGACATGGCGGGACCCAAGGCCACCAAGAGCCCAGAGGA
GGGGGCTGAGACCCCTGTCTACTTGGCCCTCTTGCCTCCAGATGCCACTGAGCCACAAGGCC
AGTTGGTCCATGACAAAGTTGTGCAAAACTGGTAA

**SOEP230W (in the pET-15b(+) vector)**

ATGGGCAGCAGCCATCATCATCATCATCACAGCAGCGGCCTGGTGCCGCGCGGCAGCCAT
ATGTCGTCCTGCAGCCGCGTGGCGCTGGTGACCGGGGCCAACAGGGGCATCGGCTTGGCCAT
CGCGCGCGAACTGTGCCGACAGTTCTCTGGGGATGTGGTGCTCACCGCGCGGGACGTGGCGC
GGGGCCAGGCGGCCGTGCAGCAGCTGCAGGCGGAGGGCCTGAGCCCGCGCTTCCACCAACT
GGACATCGACGACTTGCAGAGCATCCGCGCCCTGCGCGACTTCCTGCGCAAGGAGTACGGG
GGGCTCAACGTACTGGTCAACAACGCGGCCGTCGCCTTCAAGAGTGATGATCCAATGCCCTT
TGACATTAAAGCTGAGATGACACTGAAGACAAATTTTTTTGCCACTAGAAACATGTGCAACG
AGTTACTGCCGATAATGAAACCTCATGGGAGAGTGGTGAATATCAGTAGTTTGCAGTGTTTA
AGGGCTTTTGAAAACTGCAGTGAAGATCTGCAGGAAAGGTTCCACAGTGAGACACTCACAG
AAGGAGACCTGGTGGATCTCATGAAAAAGTTTGTGGAGGACACAAAAAATGAGGTGCATGA
GAGGGAAGGCTGGCCCAACTCACCTTATGGGGTGTCCAAGTTGGGGGTCACGGTCTTATCGA
GGATCCTGGCCAGGCGTCTGGATGAGAAGAGGAAAGCTGACAGGATTCTGGTGAATGCGTG
CTGCCCAGGATGGGTGAAGACAGACATGGCGGGACCCAAGGCCACCAAGAGCCCAGAGGA
GGGGGCTGAGACCCCTGTCTACTTGGCCCTCTTGCCTCCAGATGCCACTGAGCCACAAGGCC
AGTTGGTCCATGACAAAGTTGTGCAAAACTGGTAA

## 7.3 The 100 bp DNA ladder

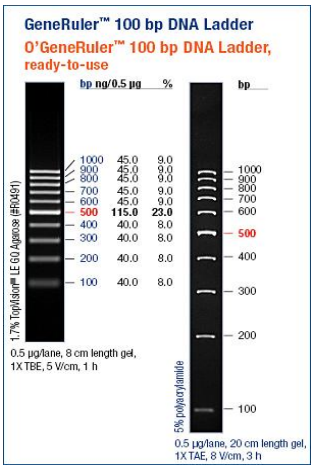


## 7.4 The protein molecular weight marker

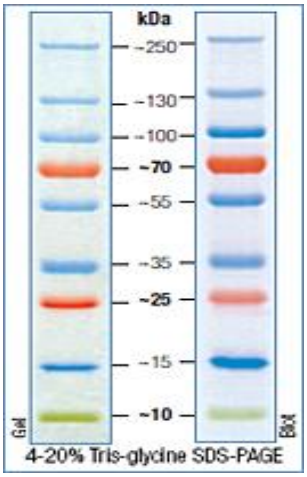

# LIST OF TABLES

# LIST OF FIGURES

# LIST OF EQUATIONS



# LIST OF ABBREVIATIONS

| | |
|---|---|
| AKR | aldo-keto reductase |
| ATP | adenosine triphosphate |
| bp | basepair |
| BSA | bovine serum albumin |
| CBR1 | carbonyl reductase 1 |
| CBR3 | carbonyl reductase 3 |
| CBR4 | carbonyl reductase 4 |
| cGMP | cyclic guanosine monophosphate |
| CR | carbonyl reducing enzyme |
| DNA | deoxyribonucleic acid |
| dNTPs | deoxynucleotide triphosphates |
| DTPA | diethylenetriaminepentaacetic acid |
| DTT | dithiothreitol |
| *E. coli* | Escherichia coli |
| EDTA | ethylenediaminetetraacetic acid |
| eNOS | endothelial NOS |
| ER | endoplasmic reticulum |
| FPLC | fast protein liquid chromatography |
| GSH | glutathione |
| GADPH | glyceraldehyde-3-phosphate dehydrogenase |
| GSNO | S-nitrosoglutathione |
| GSNOR | S-nitrosoglutathione reductase |
| GSSG | oxidased form of glutathione |
| $H_2O_2$ | hydrogen peroxide |

| | |
|---|---|
| hCBR1,3 | human CBR1, CBR3 |
| HCl | hydrochloric acid |
| iNOS | inducible NOS |
| IPTG | isopropyl-D-1-thiogalactopyranoside |
| kDa | kilodalton |
| LB meduim | Luria-Bertani Medium |
| $M_r$ | relative molecular mass |
| NaCl | sodium chloride |
| $NAD^+$/NADH | nicotinamide adenine dinucleotide (oxidised/reduced) |
| $NADP^+$/NADPH | nicotinamide adenine dinucleotide phosphate (oxidised/reduced) |
| NEB | New England Biolabs |
| Ni-NTA | nickel-nitrilotriacetic acid |
| NKK | 4-(methylnitrosamino)- 1-(3-pyridyl)-1-butanone |
| nNOS | neuronal NOS |
| NO | nitric oxide |
| NOS | nitric oxide synthase |
| NOS1, 2, 3 | nitric oxide synthase1, 2, 3 |
| $NO_x$ | oxides of nitrogen |
| $O_2$ | oxygen |
| ODx | optical density at x nm |
| PCR | polymerase chain reaction |
| PDI | protein didsulfide isomerase |
| PGE1 | prostaglandin E1 |
| PGE2 | prostaglandin E2 |
| PGF2α | prostaglandin F2 α |
| QR | quinone reductase |
| RCA | rolling circle amplification |
| RCC | reactive carbonyl compound |
| rpm | revolutions per minute |
| RT | room temperature |
| SDR | short-chain dehydrogenase/reductase |
| SDS | sodium dodecyl sulfate |
| SDS-PAGE | SDS polyacrylamide gel electrophoresis |

| | |
|---|---|
| SG | Saville-Griess assay |
| SNO | S-nitrosothiols |
| SOD | superoxide dismutase |
| SOE | splice overlap extension |
| TAE | tris-acetate-EDTA |
| TEV | tobacco etch virus |
| Tris | tris(hydroxymethyl)aminomethane |
| Trx | thioredoxin |
| TrxR | thioredoxin reductase |
| UV/VIS | utraviolet/visible spectroscopy |
| v | reaction velocity |
| wt | wild type |

## Amino acid letter code

| Amino acid | Three letter code | One letter code |
|---|---|---|
| Alanine | Ala | A |
| Arginine | Arg | R |
| Asparagine | Asn | N |
| Aspartic acid | Asp | D |
| Cysteine | Cys | C |
| Glutamine | Gln | Q |
| Glutamic acid | Glu | E |
| Glycine | Gly | G |
| Histidine | His | H |
| Isoleucine | Ile | I |
| Leucine | Leu | L |
| Lysine | Lys | K |
| Methionine | Met | M |
| Phenylalanine | Phe | F |
| Proline | Pro | P |
| Serine | Ser | S |
| Threonine | Thr | T |
| Tryptophan | Trp | W |
| Tyrosine | Tyr | Y |
| Valine | Val | V |

# ACKNOWLEDGEMENTS

First of all, I would like to deeply thank Dr. Claudia Staab for guiding me, spending her time, sharing her ideas and providing detailed comments and advices. Thank you for your friendly approach, patience, willingness and help at any time. Also, I am grateful to Dr. Hans-Jörg Martin for his useful and helpful assistance in any situation.

Next I want to thank Prof. Dr. Edmund Maser and Prof. Ing. Vladimír Wsól, Ph.D. for giving me the opportunity to do the diploma thesis at the Department of Toxicology and Pharmacology in Kiel.

Third, I would like to express my gratitude to Dr. Yasser El-Hawari who laid the foundations of the project and helped me to continue it. I also thank you for discussing all encountered problems and for giving useful ideas and suggestions. I also want to thank to Michael Kisiela for his computer help and assistance.

Next I thank all the people working at the institute for being so kind to me and making a friendly working environment.

The last and big thanks belong to my family, for their help, support and love.

# BIBLIOGRAPHY


Atalla, A. and E. Maser (2001). "Characterization of enzymes participating in carbonyl reduction of 4-methylnitrosamino-1-(3-pyridyl)-1-butanone (NNK) in human placenta." Chem Biol Interact **130-132**(1-3): 737-48.

Baba, S. P., K. Wetzelberger, et al. (2009). "Posttranslational glutathiolation of aldose reductase (AKR1B1): a possible mechanism of protein recovery from S-nitrosylation." Chem Biol Interact **178**(1-3): 250-8.

Barski, O. A., S. M. Tipparaju, et al. (2008). "The aldo-keto reductase superfamily and its role in drug metabolism and detoxification." Drug Metab Rev **40**(4): 553-624.

Bateman, R. L., D. Rauh, et al. (2008). "Human carbonyl reductase 1 is an S-nitrosoglutathione reductase." The Journal of biological chemistry **283**(51): 35756-62.

Benhar, M., M. T. Forrester, et al. (2008). "Regulated protein denitrosylation by cytosolic and mitochondrial thioredoxins." Science **320**(5879): 1050-4.

Benhar, M., M. T. Forrester, et al. (2009). "Protein denitrosylation: enzymatic mechanisms and cellular functions." Nat Rev Mol Cell Biol **10**(10): 721-32.

Botella, J. A., J. K. Ulschmid, et al. (2004). "The Drosophila carbonyl reductase sniffer prevents oxidative stress-induced neurodegeneration." Current Biology **14**(9): 782-6.

Bradford, M. M. (1976). "A rapid and sensitive method for the quantitation of microgram quantities of protein utilizing the principle of protein-dye binding." Anal Biochem **72**: 248-54.

Bray, J. E., B. D. Marsden, et al. (2009). "The human short-chain dehydrogenase/reductase (SDR) superfamily: a bioinformatics summary." Chemico-Biological Interactions **178**(1-3): 99-109.

Carbone, D. L., J. A. Doorn, et al. (2004). "4-Hydroxynonenal regulates 26S proteasomal degradation of alcohol dehydrogenase." Free Radical Biology and Medicine **37**(9): 1430-9.

Casadei, M., T. Persichini, et al. (2008). "S-glutathionylation of metallothioneins by nitrosative/oxidative stress." Exp Gerontol **43**(5): 415-22.

Casagrande, S., V. Bonetto, et al. (2002). "Glutathionylation of human thioredoxin: a possible crosstalk between the glutathione and thioredoxin systems." Proc Natl Acad Sci U S A **99**(15): 9745-9.

Castellano, I., M. R. Ruocco, et al. (2008). "Glutathionylation of the iron superoxide dismutase from the psychrophilic eubacterium Pseudoalteromonas haloplanktis." Biochim Biophys Acta **1784**(5): 816-26.

Cotgreave, I. A. and R. G. Gerdes (1998). "Recent trends in glutathione biochemistry--glutathione-protein interactions: a molecular link between oxidative stress and cell proliferation?" Biochem Biophys Res Commun **242**(1): 1-9.

de Belder, A. J., R. MacAllister, et al. (1994). "Effects of S-nitroso-glutathione in the human forearm circulation: evidence for selective inhibition of platelet activation." Cardiovasc Res **28**(5): 691-4.

Duax, W. L., D. Ghosh, et al. (2000). "Steroid dehydrogenase structures, mechanism of action, and disease." Vitam HormVitamins and hormones **58**: 121-48.

Duester, G., J. Farres, et al. (1999). "Recommended nomenclature for the vertebrate alcohol dehydrogenase gene family." Biochem Pharmacol **58**(3): 389-95.

El-Hawari, Y., A. D. Favia, et al. (2009). "Analysis of the substrate-binding site of human carbonyl reductases CBR1 and CBR3 by site-directed mutagenesis." Chem Biol Interact **178**(1-3): 234-41.

Endo, S., T. Matsunaga, et al. (2008). "Human carbonyl reductase 4 is a mitochondrial NADPH-dependent quinone reductase." Biochem Biophys Res Commun **377**(4): 1326-30.

Finckh, C., A. Atalla, et al. (2001). "Expression and NNK reducing activities of carbonyl reductase and 11beta-hydroxysteroid dehydrogenase type 1 in human lung." Chemico-biological interactions **130-132**(1-3): 761-73.

Forrest, G. L. and B. Gonzalez (2000). "Carbonyl reductase." Chemico-biological interactions **129**(1-2): 21-40.

Francis, S. H. and J. D. Corbin (1999). "Cyclic nucleotide-dependent protein kinases: intracellular receptors for cAMP and cGMP action." Crit Rev Clin Lab Sci **36**(4): 275-328.

Fujii, R., M. Kitaoka, et al. (2006). "Error-prone rolling circle amplification: the simplest random mutagenesis protocol." Nat Protoc **1**(5): 2493-7.

Gaston, B., J. Reilly, et al. (1993). "Endogenous nitrogen oxides and bronchodilator S-nitrosothiols in human airways." Proc Natl Acad Sci U S A **90**(23): 10957-61.

Gaston, B., D. Singel, et al. (2006). "S-nitrosothiol signaling in respiratory biology." Am J Respir Crit Care Med **173**(11): 1186-93.

Gaston, B. M., J. Carver, et al. (2003). "S-nitrosylation signaling in cell biology." Mol Interv **3**(5): 253-63.

Giustarini, D., A. Milzani, et al. (2005). "S-nitrosation versus S-glutathionylation of protein sulfhydryl groups by S-nitrosoglutathione." Antioxid Redox Signal **7**(7-8): 930-9.

Griess, P. (1879). "Bemerkungen zu der abhandlung der H.H. Weselsky und Benedikt "Ueber einige azoverbindungen"." Chemische Berichte **12**: 426-428.

Grimm, C., E. Maser, et al. (2000). "The crystal structure of 3alpha -hydroxysteroid dehydrogenase/carbonyl reductase from Comamonas testosteroni shows a novel oligomerization pattern within the short chain dehydrogenase/reductase family." J Biol CheThe Journal of biological chemistry **275**(52): 41333-9.

Hart, T. W. (1985). "Some observations cocncerning the S-nitroso and S-phenylsulphonyl derivatives of L-cysteine and glutathione." Tetrahedron Letters **26**(16): 2013-2016.

Hess, D. T., A. Matsumoto, et al. (2005). "Protein S-nitrosylation: purview and parameters." Nat Rev Mol Cell Biol **6**(2): 150-66.

Ho, S. N., H. D. Hunt, et al. (1989). "Site-directed mutagenesis by overlap extension using the polymerase chain reaction." Gene **77**(1): 51-9.

Hoffmann, F. and E. Maser (2007). "Carbonyl reductases and pluripotent hydroxysteroid dehydrogenases of the short-chain dehydrogenase/reductase superfamily." Drug Metabolism Reviews **39**(1): 87-144.

Hogg, N., R. J. Singh, et al. (1996). "The role of glutathione in the transport and catabolism of nitric oxide." FEBS Lett **382**(3): 223-8.

Horton, R. M. (1995). "PCR-mediated recombination and mutagenesis. SOEing together tailor-made genes." Mol Biotechnol **3**(2): 93-9.

Horton, R. M. (1997). "In vitro recombination and mutagenesis of DNA. SOEing together tailor-made genes." Methods Mol Biol **67**: 141-9.

Hou, Y., Z. Guo, et al. (1996). "Seleno compounds and glutathione peroxidase catalyzed decomposition of S-nitrosothiols." Biochem Biophys Res Commun **228**(1): 88-93.

Chance, B., H. Sies, et al. (1979). "Hydroperoxide metabolism in mammalian organs." Physiol Rev **59**(3): 527-605.

Ido, Y. (2007). "Pyridine nucleotide redox abnormalities in diabetes." Antioxid Redox Signal **9**(7): 931-42.

Inoue, K., T. Akaike, et al. (1999). "Nitrosothiol formation catalyzed by ceruloplasmin. Implication for cytoprotective mechanism in vivo." J Biol Chem **274**(38): 27069-75.

Ismail, E., F. Al-Mulla, et al. (2000). "Carbonyl reductase: a novel metastasis-modulating function." Cancer Research **60**(5): 1173-6.

Jaffrey, S. R., H. Erdjument-Bromage, et al. (2001). "Protein S-nitrosylation: a physiological signal for neuronal nitric oxide." Nat Cell Biol **3**(2): 193-7.

Jensen, D. E., G. K. Belka, et al. (1998). "S-Nitrosoglutathione is a substrate for rat alcohol dehydrogenase class III isoenzyme." Biochem J **331 ( Pt 2)**: 659-68.

Jez, J. M., M. J. Bennett, et al. (1997). "Comparative anatomy of the aldo-keto reductase superfamily." Biochem J **326 ( Pt 3)**: 625-36.

Jörnvall, H., B. Persson, et al. (1995). "Short-chain dehydrogenases/reductases (SDR)." Biochemistry **34**(18): 6003-13.

Kallberg, Y., U. Oppermann, et al. (2002). "Short-chain dehydrogenases/reductases (SDRs)." Eur J Biochem **269**(18): 4409-17.

Kashiba-Iwatsuki, M., M. Yamaguchi, et al. (1996). "Role of ascorbic acid in the metabolism of S-nitroso-glutathione." FEBS Lett **389**(2): 149-52.

Kavanagh, K. L., H. Jornvall, et al. (2008). "Medium- and short-chain dehydrogenase/reductase gene and protein families : the SDR superfamily: functional and structural diversity within a family of metabolic and regulatory enzymes." Cell Mol Life Sci **65**(24): 3895-906.

Kelner, M. J., L. Estes, et al. (1997). "Heterologous expression of carbonyl reductase: demonstration of prostaglandin 9-ketoreductase activity and paraquat resistance." Life sciences **61**(23): 2317-22.

Kinnula, V. L., J. D. Crapo, et al. (1995). "Generation and disposal of reactive oxygen metabolites in the lung." Lab Invest **73**(1): 3-19.

Klatt, P. and S. Lamas (2000). "Regulation of protein function by S-glutathiolation in response to oxidative and nitrosative stress." Eur J Biochem **267**(16): 4928-44.

Lakhman, S. S., D. Ghosh, et al. (2005). "Functional significance of a natural allelic variant of human carbonyl reductase 3 (CBR3)." Drug Metabolism and Disposition **33**(2): 254-7.

Ledent, P., C. Duez, et al. (1997). "Unexpected influence of a C-terminal-fused His-tag on the processing of an enzyme and on the kinetic and folding parameters." FEBS Lett **413**(2): 194-6.

Lindermayr, C., G. Saalbach, et al. (2005). "Proteomic identification of S-nitrosylated proteins in Arabidopsis." Plant Physiol **137**(3): 921-30.

Liu, L., A. Hausladen, et al. (2001). "A metabolic enzyme for S-nitrosothiol conserved from bacteria to humans." Nature **410**(6827): 490-4.

Liu, L., Y. Yan, et al. (2004). "Essential roles of S-nitrosothiols in vascular homeostasis and endotoxic shock." Cell **116**(4): 617-28.

Marino, S. M. and V. N. Gladyshev (2009). "Structural analysis of cysteine S-nitrosylation: a modified acid-based motif and the emerging role of trans-nitrosylation." J Mol Biol **395**(4): 844-59.

Martinez-Ruiz, A. and S. Lamas (2007). "Signalling by NO-induced protein S-nitrosylation and S-glutathionylation: convergences and divergences." Cardiovasc Res **75**(2): 220-8.

Matsunaga, T., S. Shintani, et al. (2006). "Multiplicity of mammalian reductases for xenobiotic carbonyl compounds." Drug Metab Pharmacokinet **21**(1): 1-18.

Medvedev, A., O. Buneeva, et al. (2007). "Biological targets for isatin and its analogues: Implications for therapy." Biologics **1**(2): 151-62.

Mieyal, J. J., M. M. Gallogly, et al. (2008). "Molecular mechanisms and clinical implications of reversible protein S-glutathionylation." Antioxid Redox Signal **10**(11): 1941-88.

Miura, T., Y. Itoh, et al. (2009). "Investigation of the role of the amino acid residue at position 230 for catalysis in monomeric carbonyl reductase 3." Chem Biol Interact **178**(1-3): 211-4.

Miura, T., T. Nishinaka, et al. (2008). "Different functions between human monomeric carbonyl reductase 3 and carbonyl reductase 1." Mol Cell Biochem **315**(1-2): 113-21.

Mohr, S., H. Hallak, et al. (1999). "Nitric oxide-induced S-glutathionylation and inactivation of glyceraldehyde-3-phosphate dehydrogenase." J Biol Chem **274**(14): 9427-30.

Moro, M. A., V. M. Darley-Usmar, et al. (1994). "Paradoxical fate and biological action of peroxynitrite on human platelets." Proc Natl Acad Sci U S A **91**(14): 6702-6.

Nallur, G., C. Luo, et al. (2001). "Signal amplification by rolling circle amplification on DNA microarrays." Nucleic Acids Res **29**(23): E118.

Negre-Salvayre, A., C. Coatrieux, et al. (2008). "Advanced lipid peroxidation end products in oxidative damage to proteins. Potential role in diseases and therapeutic prospects for the inhibitors." British Journal of Pharmacology **153**(1): 6-20.

Nelson, J. R., Y. C. Cai, et al. (2002). "TempliPhi, phi29 DNA polymerase based rolling circle amplification of templates for DNA sequencing." Biotechniques **Suppl**: 44-7.

Nikitovic, D. and A. Holmgren (1996). "S-nitrosoglutathione is cleaved by the thioredoxin system with liberation of glutathione and redox regulating nitric oxide." J Biol Chem **271**(32): 19180-5.

Oppermann, U. (2007). "Carbonyl reductases: the complex relationships of mammalian carbonyl- and quinone-reducing enzymes and their role in physiology." Annu Rev Pharmacol Toxicol **47**: 293-322.

Oppermann, U. C. and E. Maser (2000). "Molecular and structural aspects of xenobiotic carbonyl metabolizing enzymes. Role of reductases and dehydrogenases in xenobiotic phase I reactions." Toxicology **144**(1-3): 71-81.

Perez-Mato, I., C. Castro, et al. (1999). "Methionine adenosyltransferase S-nitrosylation is regulated by the basic and acidic amino acids surrounding the target thiol." J Biol Chem **274**(24): 17075-9.

Persson, B., Y. Kallberg, et al. (2009). "The SDR (short-chain dehydrogenase/reductase and related enzymes) nomenclature initiative." Chemico-biological interactions **178**(1-3): 94-8.

Persson, B., Y. Kallberg, et al. (2003). "Coenzyme-based functional assignments of short-chain dehydrogenases/reductases (SDRs)." Chem Biol InteraChemico-biological interactions **143-144**: 271-8.

Pilka, E. S., F. H. Niesen, et al. (2009). "Structural basis for substrate specificity in human monomeric carbonyl reductases." PLoS One **4**(10): e7113.

Polayes, D. A., A. Goldstein, et al. (1994). "TEV protease, recombinant: A site-specific protease for efficient cleavage of affinity tags from expressed proteins." Focus **16**(1): 2-5.

Ris, M. M. and J. P. von Wartburg (1973). "Heterogeneity of NADPH-dependent aldehyde reductase from human and rat brain." Eur J Biochem **37**(1): 69-77.

Rosemond, M. J. and J. S. Walsh (2004). "Human carbonyl reduction pathways and a strategy for their study in vitro." Drug metabolism reviews **36**(2): 335-61.

Rusterucci, C., M. C. Espunya, et al. (2007). "S-nitrosoglutathione reductase affords protection against pathogens in Arabidopsis, both locally and systemically." Plant Physiol **143**(3): 1282-92.

Sandau, K. and B. Brune (1996). "The dual role of S-nitrosoglutathione (GSNO) during thymocyte apoptosis." Cell Signal **8**(3): 173-7.

Sausbier, M., R. Schubert, et al. (2000). "Mechanisms of NO/cGMP-dependent vasorelaxation." Circ Res **87**(9): 825-30.

Saville, B. (1958). "A Scheme for the colorimetric cetermination of microgram amounts of thiols." Analyst **83**: 670-672.

Sayari, A., H. Mosbah, et al. (2007). "The N-terminal His-tag affects the enantioselectivity of staphylococcal lipases: a monolayer study." J Colloid Interface Sci **313**(1): 261-7.

Seres, T., V. Ravichandran, et al. (1996). "Protein S-thiolation and dethiolation during the respiratory burst in human monocytes. A reversible post-translational modification with potential for buffering the effects of oxidant stress." J Immunol **156**(5): 1973-80.

Schade, S. Z., S. L. Early, et al. (1990). "Sequence analysis of bovine lens aldose reductase." The Journal of biological chemistry **265**(7): 3628-35.

Schmidt, M., M. Grey, et al. (1996). "A microbiological assay for the quantitative determination of glutathione." Biotechniques **21**(5): 881, 884-6.

Schuppe-Koistinen, I., R. Gerdes, et al. (1994). "Studies on the reversibility of protein S-thiolation in human endothelial cells." Arch Biochem Biophys **315**(2): 226-34.

Schuppe-Koistinen, I., P. Moldeus, et al. (1994). "S-thiolation of human endothelial cell glyceraldehyde-3-phosphate dehydrogenase after hydrogen peroxide treatment." Eur J Biochem **221**(3): 1033-7.

Singh, R. J., N. Hogg, et al. (1999). "Mechanism of superoxide dismutase/H(2)O(2)-mediated nitric oxide release from S-nitrosoglutathione--role of glutamate." Arch Biochem Biophys **372**(1): 8-15.

Singh, S. P., J. S. Wishnok, et al. (1996). "The chemistry of the S-nitrosoglutathione/glutathione system." Proc Natl Acad Sci U S A **93**(25): 14428-33.

Sliskovic, I., A. Raturi, et al. (2005). "Characterization of the S-denitrosation activity of protein disulfide isomerase." J Biol Chem **280**(10): 8733-41.

Smolenski, A., A. M. Burkhardt, et al. (1998). "Functional analysis of cGMP-dependent protein kinases I and II as mediators of NO/cGMP effects." Naunyn Schmiedebergs Arch Pharmacol **358**(1): 134-9.

Staab, C. A., M. Hellgren, et al. (2008). "Medium- and short-chain dehydrogenase/reductase gene and protein families : Dual functions of alcohol dehydrogenase 3: implications with focus on formaldehyde dehydrogenase and S-nitrosoglutathione reductase activities." Cell Mol Life Sci **65**(24): 3950-60.

Stamler, J. S., O. Jaraki, et al. (1992). "Nitric oxide circulates in mammalian plasma primarily as an S-nitroso adduct of serum albumin." Proc Natl Acad Sci U S A **89**(16): 7674-7.

Stamler, J. S., E. J. Toone, et al. (1997). "(S)NO signals: translocation, regulation, and a consensus motif." Neuron **18**(5): 691-6.

Stoyanovsky, D. A., Y. Y. Tyurina, et al. (2005). "Thioredoxin and lipoic acid catalyze the denitrosation of low molecular weight and protein S-nitrosothiols." J Am Chem Soc **127**(45): 15815-23.

Tanaka, M., R. Bateman, et al. (2005). "An unbiased cell morphology-based screen for new, biologically active small molecules." PLoS Biol **3**(5): e128.

Tanaka, N., T. Nonaka, et al. (1996). "Crystal structure of the ternary complex of mouse lung carbonyl reductase at 1.8 A resolution: the structural origin of coenzyme specificity in the short-chain dehydrogenase/reductase family." Structure **4**(1): 33-45.

Testa, B. and S. D. Kramer (2007). "The biochemistry of drug metabolism--an introduction: Part 2. Redox reactions and their enzymes." Chemistry and biodiversity **4**(3): 257-405.

Thomas, J. A., B. Poland, et al. (1995). "Protein sulfhydryls and their role in the antioxidant function of protein S-thiolation." Arch Biochem Biophys **319**(1): 1-9.

Tietze, F. (1969). "Enzymic method for quantitative determination of nanogram amounts of total and oxidized glutathione: applications to mammalian blood and other tissues." Anal Biochem **27**(3): 502-22.

Tinguely, J. N. and B. Wermuth (1999). "Identification of the reactive cysteine residue (Cys227) in human carbonyl reductase." European Journal of Biochemistry **260**(1): 9-14.

Trujillo, M., M. N. Alvarez, et al. (1998). "Xanthine oxidase-mediated decomposition of S-nitrosothiols." J Biol Chem **273**(14): 7828-34.

Usami, N., K. Kitahara, et al. (2001). "Characterization of a major form of human isatin reductase and the reduced metabolite." European journal of biochemistry **268**(22): 5755-63.

Vallejo, A. N., R. J. Pogulis, et al. (1994). "In vitro synthesis of novel genes: mutagenesis and recombination by PCR." PCR Methods Appl **4**(3): S123-30.

van der Vliet, A., P. A. Hoen, et al. (1998). "Formation of S-nitrosothiols via direct nucleophilic nitrosation of thiols by peroxynitrite with elimination of hydrogen peroxide." J Biol Chem **273**(46): 30255-62.

Watanabe, K., C. Sugawara, et al. (1998). "Mapping of a novel human carbonyl reductase, CBR3, and ribosomal pseudogenes to human chromosome 21q22.2." Genomics **52**(1): 95-100.

Wermuth, B. (1981). "Purification and properties of an NADPH-dependent carbonyl reductase from human brain. Relationship to prostaglandin 9-ketoreductase and xenobiotic ketone reductase." The Journal of biological chemistry **256**(3): 1206-13.

Wermuth, B., K. L. Platts, et al. (1986). "Carbonyl reductase provides the enzymatic basis of quinone detoxication in man." Biochem Pharmacol **35**(8): 1277-82.

Wilson, D. K., K. M. Bohren, et al. (1992). "An unlikely sugar substrate site in the 1.65 A structure of the human aldose reductase holoenzyme implicated in diabetic complications." Science **257**(5066): 81-4.

Wirth, H. and B. Wermuth (1992). "Immunohistochemical localization of carbonyl reductase in human tissues." The journal of histochemistry and cytochemistry **40**(12): 1857-63.

Wirth, H. P. and B. Wermuth (1985). "Immunohistochemical localisation of aldehyde and aldose reductase in human tissues." Progress in clinical and biological research **174**: 231-9.

Wu, H., I. Romieu, et al. (2007). "Genetic variation in S-nitrosoglutathione reductase (GSNOR) and childhood asthma." J Allergy Clin Immunol **120**(2): 322-8.

Ying, W. (2008). "NAD+/NADH and NADP+/NADPH in cellular functions and cell death: regulation and biological consequences." Antioxid Redox Signal **10**(2): 179-206.

Zeng, H., N. Y. Spencer, et al. (2001). "Metabolism of S-nitrosoglutathione by endothelial cells." Am J Physiol Heart Circ Physiol **281**(1): H432-9.